ฟิล์มวัสดุเชิงประกอบพอลิอิไมด์กับซิลิคอนไนไตรด์ที่นำความร้อนสูง

นางสาวขวัญจิตร พีรพรธรรม

วิทยานิพนธ์นี้เป็นส่วนหนึ่งของการศึกษาตามหลักสูตรปริญญาวิศวกรรมศาสตรมหาบัณฑิต

สาขาวิชาวิศวกรรมเคมี ภาควิชาวิศวกรรมเคมี

คณะวิศวกรรมศาสตร์ จุฬาลงกรณ์มหาวิทยาลัย

ปีการศึกษา 2554

HIGH THERMAL CONDUCTIVITY OF POLYIMIDE/SILICON NITRIDE COMPOSITE FILMS

Ms. Khwanjit Peeraporntam

A Thesis Submitted in Partial Fulfillment of the Requirements
for the Degree of Master of Engineering Program in Chemical Engineering
Department of Chemical Engineering
Faculty of Engineering
Chulalongkorn University
Academic Year 2011

Thesis Title	HIGH THERMAL CONDUCTIVITY OF POLYIMIDE/ SILICON NITRIDE COMPOSITE FILMS
By	Ms. Khwanjit Peeraporntam
Field of Study	Chemical Engineering
Thesis Advisor	Associate Professor ML. Supakanok Thongyai, Ph.D.

Accepted by the Faculty of Engineering, Chulalongkorn University in Partial Fulfillment of the Requirement for the Master's Degree

…….....Dean of the Faculty of Engineering

(Associate Professor Boonsom Lerdhirunwong, Dr.Ing.)

THESIS COMMITTEE

……Chairman

(Assistant Professor Anongnat Somwangthanaroj, Ph.D.)

……Thesis Advisor

(Associate Professor ML. Supakanok Thongyai, Ph.D.)

……Examiner

(Associate Professor Bunjerd Jongsomjit, Ph.D.)

……Examiner

(Assistant Professor Soorathep Kheawhom, Ph.D.)

……External Examiner

(Assistant Professor Sirirat Wacharawichanant, D.Eng.

ขวัญจิตร พีรพรธรรม : ฟิล์มวัสดุเชิงประกอบพอลิอิไมด์กับซิลิคอนไนไตรด์ที่นำความร้อนสูง(HIGH THERMAL CONDUCTIVITY OF POLYIMIDE/SILICON NITRIDE COMPOSITE FILMS) อ. ที่ปรึกษาวิทยานิพนธ์หลัก : รศ. ดร. มล. ศุภกนก ทองใหญ่ 97 หน้า.

จุดประสงค์ของงานวิจัยนี้คือศึกษาการเตรียมฟิล์มวัสดุเชิงประกอบพอลิอิไมด์กับซิลิคอนไนไตรด์ที่นำความร้อนสูงโดยใช้ซิลิคอนไนไตรด์เป็นสารเติมแต่ง ศึกษาผลของสารควบคู่ไซเลนและขนาดของซิลิคอนไนไตรด์ต่อสมบัติเชิงความร้อนและเชิงกลของฟิล์มวัสดุเชิงประกอบพอลิอิไมด์ สารควบคู่ไซเลน 3 ชนิด ที่ศึกษาผลของการปรับสภาพผิวซิลิคอนไนไตรด์ที่มีผลต่อฟิล์มวัสดุเชิงประกอบ สารควบคู่ ได้แก่ 3-อะมิโนโพรพิลไตรเอทอกซีไซเลน (เอพีทีเอส), 3-(2-อะมิโนเอทิลอะมิโน)โพรพิลไตรเมทอกซีไซเลน(เออีพีทีเอส) และ 3-[2-(2-อะมิโนเอทิลอะมิโน)เอทิลอะมิโน]โพรพิลไตรเมทอกซีไซเลน(เออีอีพีทีเอส) อนุภาคซิลิคอนไนไตรด์สามขนาดที่แตกต่างกันคือ ขนาดไมครอน, ขนาดซับไมครอน และ ขนาดนาโน ฟิล์มวัสดุเชิงประกอบพอลิอิไมด์ที่ถูกเติมด้วยซิลิคอนไนไตรด์ที่ถูกปรับสภาพผิวด้วยสารควบคู่ไซเลนมีคุณสมบัติเชิงกลดีกว่าฟิล์มวัสดุเชิงประกอบที่เติมด้วยซิลิคอนไนไตรด์ที่ไม่ถูกปรับสภาพผิว ฟิล์มวัสดุเชิงประกอบพอลิอิไมด์ที่ถูกเติมด้วยสารเติมแต่งซิลิคอนไนไตรด์ที่ถูกปรับสภาพผิวด้วยเอพีทีเอสแสดงค่าการนำความร้อนที่สูงกว่าฟิล์มวัสดุเชิงประกอบที่เติมด้วยซิลิคอนไนไตรด์ที่ปรับสภาพผิวด้วยเออีพีทีเอส, ไม่ถูกปรับสภาพผิวและเออีอีพีทีเอส ตามลำดับ ฟิล์มวัสดุเชิงประกอบที่เติมด้วยซิลิคอนไนไตรด์ขนาดนาโนแสดงค่าการนำความร้อนที่สูงกว่าขนาดอื่นที่อัตราส่วนของน้ำหนักเท่ากันซึ่งมากกว่าขนาดไม่ครอนสองเท่าและมากกว่าขนาดซับไมครอนหนึ่งเท่า การเติมซิลิคอนไนไตรด์ที่ผสมขนาดไมครอนกับซับไมครอน และขนาดซับไมครอนกับนาโนที่ความหนาแน่นของการอัดตัวสูงที่สูงเข้าไปในเมทริกซ์พอลิอิไมด์สามารถเพิ่มค่าการนำความร้อนได้สูงกว่าการเติมสารเติมแต่งซิลิคอนไนไตรด์ขนาดเดียว นอกจากนี้โมแบบจำลองของอาการิและยูโนสามารถทำนายการนำความร้อนทางการทดลองได้ดีกว่าแบบจำลองทางทฤษฎีแบบอื่น

ภาควิชา.....วิศวกรรมเคมี..... ลายมือชื่อนิสิต….....
สาขาวิชา.....วิศวกรรมเคมี..... ลายมือชื่อ อ.ที่ปรึกษาวิทยานิพนธ์หลัก.....
ปีการศึกษา...2554.....

5370403421: MAJOR CHEMICAL ENGINEERING
KEYWORDS: POLYIMIDE COMPOSITE FILMS / SILICON NIITRIDE FILLER/ SILANE COUPLING AGENT / THERMAL CONDUCTIVITY/ SURFACE MODIFICATION

KHWANJIT PEERAPORNTAM : HIGH THERMAL CONDUCTIVITY OF POLYIMIDE/SILICON NITRIDE COMPOSITE FILMS. ADVISOR: ASSOC. PROF.ML.SUPAKANOK THONGYAI, Ph.D., 97 pp.

This research aim was to investigate study the preparation of high thermal conductivity of polyimide composite films that using silicon nitride (Si_3N_4) as filler. The effect of the difference types of coupling agents and the amount of Si_3N_4 on the thermal and mechanical properties were studied. Three types of silane coupling agents were used for the investigation of the effects of Si_3N_4 surface modification on composite films. There were 3-minopropyltrimethoxysilane (APTS), 3-(2-aminoethylamino)propyltrimethoxymethylsilane (AEPDS) and 3-[2-(2-aminoethyl amino) ethylamino]propyltrimethoxysilane (AEEPTS). Three different sizes of Si_3N_4 particles are micron, submicron and nano sized. The PI filled modified Si_3N_4 fillers using silane coupling agent have better mechanical properties than that of untreated Si_3N_4 fillers. The PI composite films with APTS treated Si_3N_4 fillers showed higher thermal conductivity higher than that of AEPTS, untreated and AEEPTS, respectively. The composite films filled with nano sized Si_3N_4 shows higher thermal conductivity than other sizes at the same weight fraction that were more than two times of micron sized particle and about two times of submicron sized particle. The incorporation of hybrid micron-submicron and submicron-nano sized Si_3N_4 at the maximum packing density into polyimide matrix can give thermal conductivity higher than mono sizes of Si_3N_4 fillers regardless of the same weight ratio of Si_3N_4. In addition, Agari and Uno model can well predict the experimental thermal conductivity better than any other theoretical models.

Department : Chemical Engineering Student's Signature .....

Field of Study : Chemical Engineering Advisor's Signature .....

Academic Year : 2011

ACKNOWLEDGEMENTS

I would like to express my deeply gratitude to my advisor, Associate Professor Dr. ML. Supakanok Thongyai, Ph.D. to his continuous guidance, enormous number of invaluable discussions, helpful suggestions, warm encouragement and patience to correct my writing. I am grateful to Professor Suttichai Assabumrungrat, Ph.D., Assistant Professor Anongnat Somwangthanaroj, Ph.D., Associate Professor Bunjerd Jongsomjit Ph.D. and Assistant professor Sirirat Wacharawichanant, D.Eng. for serving as chairman and thesis committees, respectively, whose comments were constructively and especially helpful.

Sincere thanks are made to Mektec Manufacturing Corporation (Thailand) Ltd. for supporting the materials for synthesis polyimide and the characterize equipments, the financial support from the graduate school at Chulalongkorn University, and Department of Chemical Engineering ,Faculty of Engineering Chulalongkorn University.

Sincere thanks to all my friends and all members of the Center of Excellent on Catalysis & Catalytic Reaction Engineering, Department of Chemical Engineering, Chulalongkorn University for their assistance and friendly encouragement.

Finally, I would like to dedicate this thesis to my parents and my family, who generous supported and encouraged me through the year spent on this study.

CONTENTS

Page

Page

LIST OF TABLES

LIST OF FIGURES

Page

Page

Page

Page

CHAPTER I

INTRODUCTION

Polyimide (PI) is the high performance material due to its excellent thermal stability, high mechanical strength, good electrical properties, high radiation resistance, good solvent resistance and low dielectric constant [1]. Polyimides have widely application that been used as a standard electronic material for making circuit boards, interlayer dielectric films, aerospace, automotive and packaging industries. However, they exhibit intrinsic low thermal conductivities and fairly high thermal expansion coefficients, which can cause problems in heat dissipation and thermal fatigue failure in the electronic systems [2-3].

The dispersion of thermally conductive fillers in an insulating polymer matrix can increase thermal conductivity of that polymer and improve the heat dissipation problem. Popper ceramic fillers, such as aluminum nitride (AlN)[3-6], silicon nitride (Si_3N_4)[7], boron nitride (BN)[8-10], silicon carbide (SiC)[4, 10], alumina (Al_2O_3)[11] and silica (SiO_2) were used as the thermal conductive fillers included in a polymer matrix [8].

Recently, polymer composites were investigated by several researchers. In the case of polyimide, polyimide composites were filled with several ceramic fillers such as aluminum nitride (AlN) [3, 6], silver nano particle [2], carbon nano tube [12] and boron nitride (BN) [8]. The results indicated that ceramic fillers filled polyimide could improve thermal conductivity property of the composite. However, no one has investigated the silicon nitride filled polyimide film. In previous works with other polymers, they showed that silicon nitride (Si_3N_4) was the good alternative filler because of its high thermal conductivity (higher than 150 W/mK). Moreover, it has better mechanical and thermal properties than other ceramic fillers. Recent reports showed that Si_3N_4 has a relatively high thermally conductivity similar to that of aluminum nitride (AlN). However it has many stable properties, good insulation

properties, better erosion resistance and it was commercially available (even more commercially than boron nitride), also its low cost [13].

The performance of composites depends on the filler characteristics (particle size and shape), also depends on the dispersion and the adhesion between filler particles and polymer matrix. The improvement methods to good dispersion of inorganic fillers in polymer matrix can be done by various techniques, mechanical or chemical process. The application of mechanical processes are the dispersion of fillers in the polymer by high shear rates that help to avoiding agglomerations while the chemical process is the modification of the surface particles by silane coupling agents. Silanes are widely used as coupling agents because they have two reactive groups of different types (hydrolyzable group and nonhydrolyzable group). The hydrolyzable groups react with inorganic materials to form a chemical bond with inorganic surface, while the nonhydrolyzable groups react with organic materials. In addition to several types of silane coupling agents can be used for surface treatment to increase the compatibility between fillers and polymer matrix [11].

In this work, to study the preparation of polyimide/silicon nitride composite films in order to improve the thermal conductivity of polyimide composite films. Polyimide is prepared via two-step polymerization method of equimolar of 4,4'-oxydianiline (ODA) and pyromellitic dianhydride (PMDA). Three different sizes silicon nitride (Si_3N_4) used as ceramic filler and Si_3N_4 are surface modified with three kinds of silane coupling agent. Polyimide/silicon nitride composite films are characterized for thermal and mechanical properties to verify the properties improvement.

1.1 THE OBJECTIVE OF THIS THESIS

To prepare high thermal conductivity of polyimide composite films comprised silicon nitride as ceramic fillers.

To study the effect of particle size and the amount of silicon nitride on thermal conductivity, electrical properties and the mechanical properties of silicon nitride filled polyimide composite films.

To study the effect of surface modification by using the difference types of silane coupling agents on thermal conductivity and the mechanical properties of silicon nitride filled polyimide composite films.

1.2 THE SCOPE OF THIS THESIS

1. To synthesize poly(amic acid) from equimolar of 4,4'-oxydianiline (ODA) and pyromellitic dianhydride (PMDA) by using two-step polymerization method.
2. Three different sizes of silicon nitride particles were used as a ceramic filler in this study which were <10 μm, <1 μm and <50 nm.
3. Three different types of silane coupling agents were used for the investigation of effects of surface modification on thermal conductivity and mechanical properties of silicon nitride filled polyimide composite films. There are 3-aminopropyltrimethoxysilane (APTS), 3-(2-aminoethylamino) propyltrimethoxy silane (AEPDS) and 3-[2-(2- aminoethylamino) ethylamino] propyl-trimethoxysilane (AEEPTS)
4. To investigate various volume fractions of different sizes of silicon nitride that were added into polyimide matrix.
5. To characterize polyimide/silicon nitride composite films by using Laser flash, SEM, FT-IR, TEM, TGA, LCR meter and Tensile strength.

1.3 BENEFITS OF THE THESIS

1. To improve thermal conductivity of polyimide composite films when using as electronic packaging applications by using silicon nitride (Si_3N_4) as ceramic filler.

2. To compare the effect of type of coupling agent, size and the amount of modified Si_3N_4 on thermal conductivity of polyimide/silicon nitride composite films. In order to find the optimum ratio that gives the highest thermal conductivity.

CHAPTER II

THEORY

2.1 POLYIMIDE

Polyimides (PI) are a class of high performance polymers due to their high thermally stable [13] and polyimide is a polymer of imide containing monomers. Polyimides are synthesized from both aromatic dianhydrides and aliphatic and diamines. The structure of aromatic polyimides consists primarily of heterocyclic imide and aryl groups, which are linked sequentially by simple atoms or groups [13] as shown in Figure 2.1. The generic repeat unit can be shown as below.

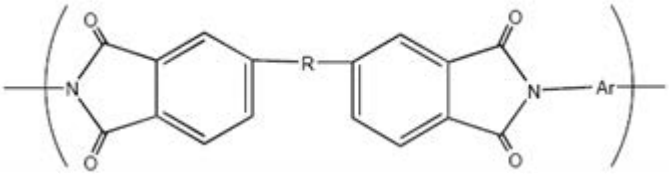

Figure 2.1 Aromatic Polyimide Repeat Unit

Polyimides have two forms. The first form of polyimide is a linear structure where the atoms of the imide group are part of a linear chain and the second form is a heterocyclic structure where the imide group is part of a cyclic unit in the polymer chain as shown in Figure 2.2.

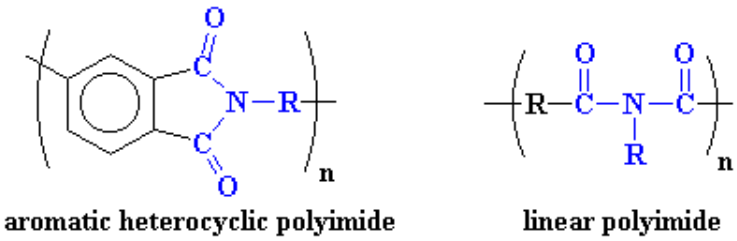

Figure 2.2 Two types of polyimides

As mentioned above, Polyimides are high performance polymers with their commercially importance in verities of applications because of their excellent thermal

stability, high mechanical strength and good dimensional stability. The famous applications of PIs in component such as microelectronic, aerospace, automotive and packaging industries is widely accepted with no other materials can rival.

2.2 PROPERTIES OF POLYIMIDE

2.2.1 Normal properties of polyimide

- Polyimide commercially available as uncured resins, polyimide solution stock, shaped in thin sheets, laminates and machined parts.
- Thermoplastic: very often called *pseudothermoplastic*
- Thermal conductivity 0.52 W/m.K [15]
- Crystalline, Semi-crystalline or Amorphorous polymer; Kapton Polyimide
- Density 1.42 g/cm^3
- Maximum Operating Temp 260 °C
- Flexural Modulus 2.48 GPa
- Tensile Strength more than 72 MPa
- Dielectric Strength 22 MV/m

2.2.2 Advantages and Disadvantages

Table 2.1: The advantages and disadvantages of polymide

Classification	Advantages	Disadvantages
Characteristic	●Molecular design suitable to need Purification ●Heat resistance and Low smoke emission ●Chemical resistance ●Low dielectric constant	● Expensive ●High moisture absorption and penetration ●Poor resistance to alkali and hydrolysis
Technological	● Elasticity, absorption of mechanical stress	

2.3 SYNTHESIS OF POLYIMIDES

A polyimide has two methods for synthesis that are one-step and two-step methods.

2.3.1 Two-Step Method Polymerization Via Poly(amic acid)s

In 1950's, the process about a soluble polymer precursor was pioneered by workers at Dupont and to this day, continues to be the primary route by which most polyimides are made.[15] In other words, the most common method of polyimide synthesis is the two-step poly(amic acid) process. The polyimide synthesis involves reaction of a dianhydride and a diamine at ambient conditions in a dipolar aprotic solvent, such as N,N-dimethylacetamide(DMAc), N-methylpyrrolidinone (NMP) or dimethylsulfoxide (DMSO) to form a soluble poly(amic acid).

The formation of the high molecular weight isomeric poly(amic acid) is completed within 24 hours or less than 24 hours, depended on monomer reactivity. The poly(amic acid) solution usually cast into film on a suitable substrate. Next step is the cyclodehydration reaction that is completed by heated poly(amic acid) film to elevated temperature (thermal), or incorporating a chemical dehydration agent (chemical).

This process generated the first commercial polyimide, Kapton™ by incorporating the monomer of pyromellitic dianhydride (PMDA) and 4,4'-oxydianiline (ODA) in a dipolar aprotic solvent and the process can be showed in Figure 2.3. Most polyimides are infusible and insoluble due to their rigid aromatic repeat unit and then usually need to be processed from the two steps route. In other case, the soluble poly(amic acid) intermediates are heated to elevated temperatures that generated the fully cyclized films by spin coat casting procedures.

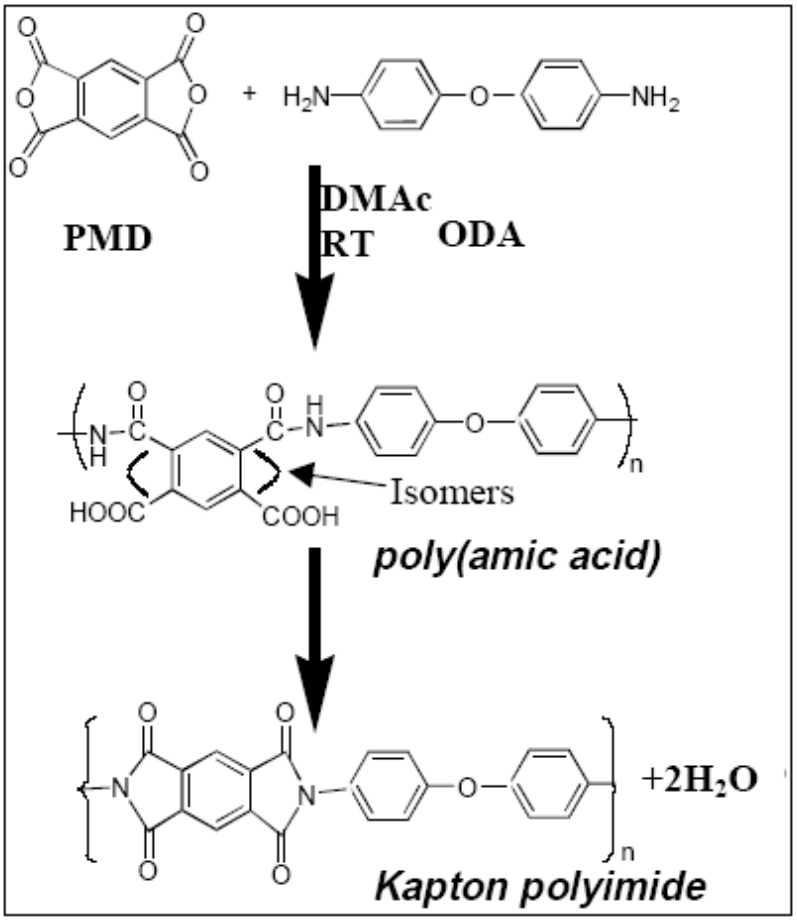

Figure 2.3 The reaction scheme for the preparation of Kapton^{TM} polyimide.[16]

2.3.2 One-Step Method Polymerization

Processing and handling poly(amic acid)s and then the development of soluble fully-cyclized polyimides become important[17] beside their difficulties. One step method of high-temperature solution polymerization can be employed for polyimides that are soluble in organic solvents at polymerization temperatures. The most common were used as solvents are benzonitrile, nitrobenzene, α-chloronaphthalene, *o*-dichlorobenzene, trichlorobenzenes, and phenolic solvents such as m-cresol and chlorophenols in addition to dipolar aprotic amide solvents and toluene is often used as a cosovent for removal of the condense water. The stoichiometric mixture of monomers was heated with a high boiling solvent or a mixture of solvents at 120-180 °C and then the imidization reaction is took place rapidly. The high-molecular-weight poly(amic acid) process is not necessary in this method, but imidization still proceeds via amic acid intermediate. The imidization proceeds rapidly and water was emitted due to the reaction and was distilled off continuously as an azeotrope along with the solvent at during polymerization. The amic acid undergoes imidization and polymerization proceeded via the amic acid route although the concentration of amic acid is very small at any time during the polymerization, because amic acid is unstable at high temperature and either rapidly imidizes, or reverts to amine and anhydride. Because water is formed as the result of the imide formation and some of the anhydride groups are rapidly hydrolyzed to o-dicarboxylic acid. The amic acid group rapidly converts to an imide or reverts back to amine and dianhydride. [16]

In this process, when the solution combined diamine, dianhydride, and a solvent and is heated at intermediate temperature of 30-100°C then a viscous solution is form. The composition of the product is mainly poly(amic acid). At this stage, phase separation is usually observed in nonpolar solvents such as chlorinated aromatic hydrocarbons. Moreover, the temperature rising to 120-160°C that a vigorous evolution of water occurs and the reaction mixture suddenly becomes homogeneous. At this stage the product is essentially a low molecular-weight polyimide having o-dicarboxy and amino end groups. Thereafter, a slow stepwise polycondensation takes place according to the reaction between the end groups.

Structures of polyimide

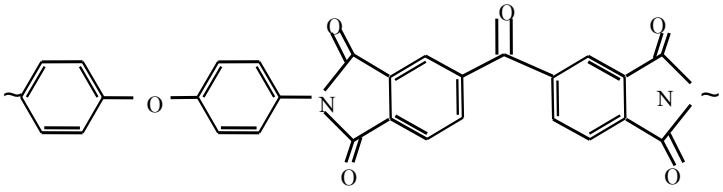

Figure 2.4 BTDA-ODA

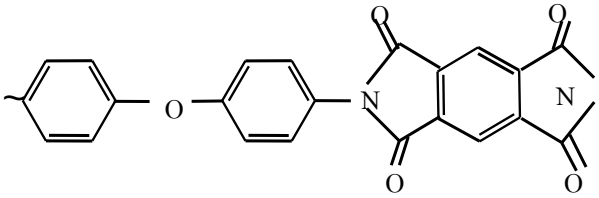

Figure 2.5 BTDA-MPDA

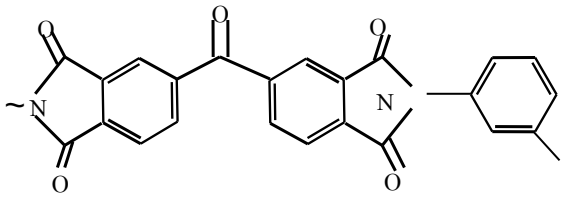

Figure 2.6 PMDA-ODA

Table 2.2: Commonly used diamine monomers

Dianhydride Structure	Name	Abbreviation
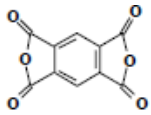	Pyromellitic dianhydride	PMDA
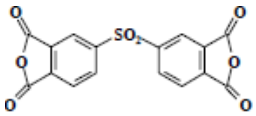	3,3',4,4'- Diphenylsulfone tetracarboxylic dianhydride	DSDA
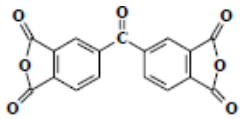	3,Y,4,4'-Benzophenonetetracarboxylic dianhydride	BTDA
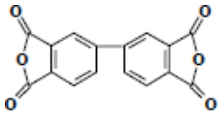	3,Y,4,4'-biphenyltetracarboxylie dianhydride	BPDA
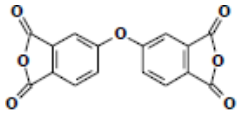	3,3',4,4'-oxydiphthalic anhydride	ODPA
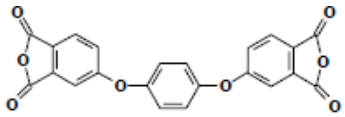	Hydroquinone diphthalic anhydride	HQDA
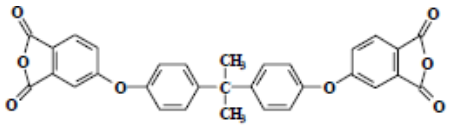	4,4'-Bisphenol A dianhydride	BPADA

Table 2.3: Commonly used diamine monomers

Diamine Structure	Name	Abbreviation
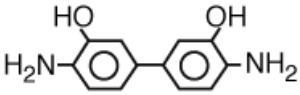	3,3'-Dihydroxy-4,4'-diamino-biphenyl	HAD
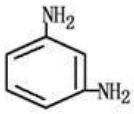	M-phenylene diamine	MPD
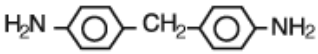	4,4'-Methylene dianiline	MDA
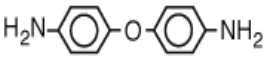	4,4'-Oxydianiline	ODA
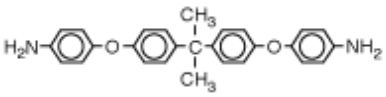	2,2-Bis [4-(4-aminophenoxy)phenyl] propane	BAPP
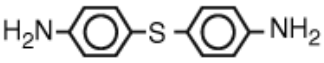	4,4'-Diaminodiphenyl sulfide	ASD
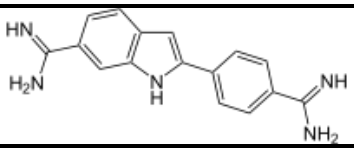	4',6-diamidino-2-phenylindole	DAPI

2.4 SILICON NITRIDE

Silicon nitride (Si_3N_4) is located in a class of IV nitrides group and is a one of the advanced engineering ceramics due to its high strength, high hardness, high toughness, excellent chemical resistance, excellent ware resistance, superior thermal shock, and thermal stability. Moreover Si_3N_4 exhibits unique properties comprising low density, low CTE and good electrical insulation. Typical property of Si_3N_4 was shown in Table 2.4.

Silicon nitride (Si_3N_4) can be synthesized from several different chemical reaction methods. The materials are pressed and sintered to produce a ceramic. The basic building unit of Si_3N_4 structure is the silicon-nitrogen tetrahedron form that is a silicon atom lies at the center of a tetrahedron, and four nitrogen atoms at each corner surrounding the silicon atom. Each silicon atom has four nitrogen atoms as nearest neighbors and each nitrogen atom has three silicon atoms as nearest neighbors as shown in Figure 2.7. Silicon nitride (Si_3N_4) structure is rather different from silicon dioxide and nitrogen atoms are arranged in tetrahedral around the silicon, as in silicon dioxide. Moreover, instead of flexible, Si-O-Si bond, the Si-N-Si is more rigid by nitrogen forming three bonds rather than two bonds as presented in silicon dioxide structure.

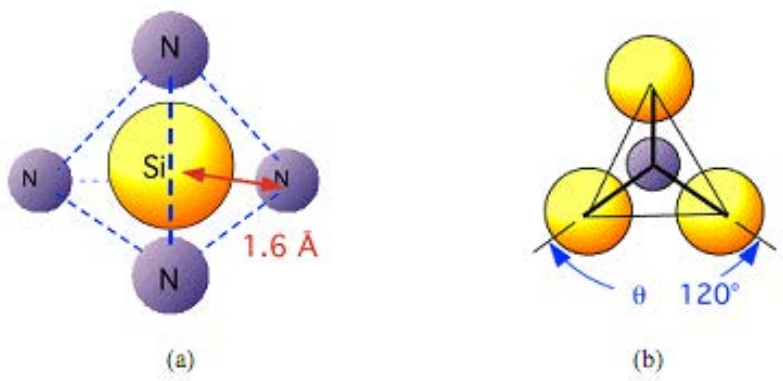

Figure 2.7 Structure of Si_3N_4 [19]

Table 2.4: Typical property of Si_3N_4 [18]

Properties	**Value**
Molecular weight (g/mol)	140.28
Density (g/cm^3)	3.44
Coefficient of thermal expansion (ppm/^{o}C)	4.4
Thermal conductivity (W/mK)	>150
Electrical resistivity (Ωcm)	$\geq 10^{13}$
Dielectric constant	8.3

2.5 SILANE COUPLING AGENTS

Silane coupling agents could be mightily bound between organic and inorganic materials. The general structure of a silane coupling agent is R-(CH_2)n-Si-X_3, as shown in Figure 2.8, where "X" is a hydrolyzable group typically alkoxy, acyloxy, halogen or amine and "R" being an a nonhydrolysable (organofunctional) group such as amino, epoxy and methacryloxy. The simple picture of the silane coupling mechanism as shown in Figure 2.9

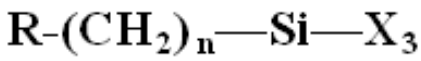

Figure 2.8 General structure of silane coupling agent

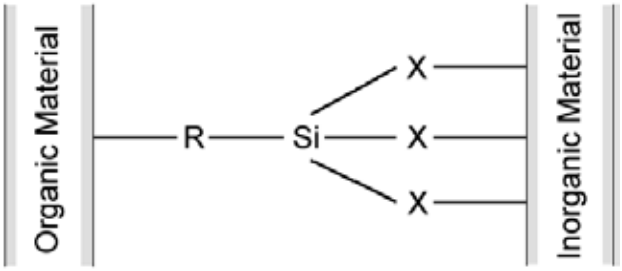

Figure 2.9 The simple picture of the silane coupling mechanism [20]

The hydrolysable group (X) of the silane molecule can be hydrolyzed that produces silanol group. Following hydrolysis, the reactive silanol group is formed a metal hydroxide or siloxane bond with the inorganic material which can be condensed with other silanol groups, for example forming siloxane linkages on the surface of ceramic fillers etc. The silanol group is a stable condensation which formed with other oxides such as those of aluminum, zirconium, tin, titanium, and nickel and its less stable bonds were formed with oxides of boron, iron, and carbon.

In addition, the silanol groups do not form stable bonds with alkali metal oxides and carbonates. In a part of the organofunctional group (R) that will react with the organic material to produce a covalent bond. As a result the organic material and the inorganic material are together tightly bound. Moreover, Silanes are materials used in a wide range of application including the adhesion characteristics of the substrates, used as a coupling agents, crosslink agents, dispersing agents and surface modifiers. [21, 23] Thus. silane coupling agent is one of a good choice for various applications.

The popular majority of surface treatment applications is the alkoxy groups of the trialkoxysilanes that are hydrolyzed to form silanol groups. The bond formation is possible to three routes and reaction of these silanes includes four steps and that as shown in Figure 2.10 and Figure 2.11, respectively.

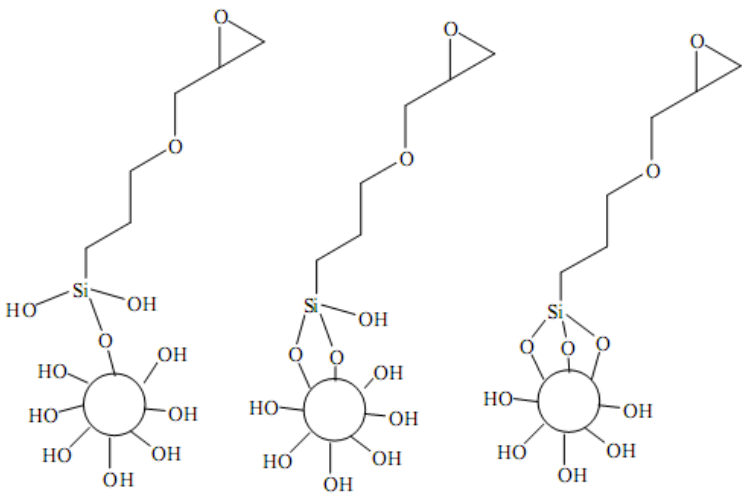

Figure 2.10 Three possible routes of bond formation in Glycidoxypropyl-trimethoxysilane (GPS) functionalized nanoparticles (NP) [24].

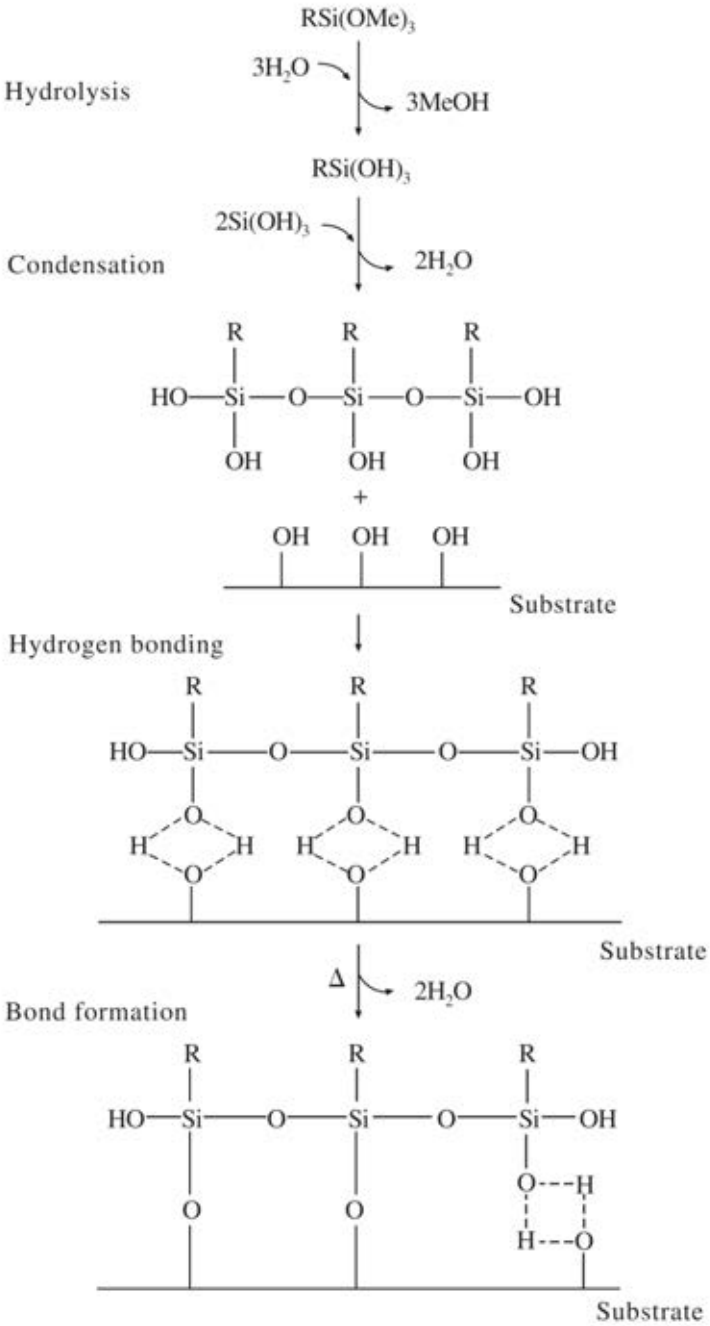

Figure 2.11 Hydrolytic deposition mechanisms of silane coupling agents [B. Arkles, CHEMTECH, 7, 766, 1977]

CHAPTER III

LITERATURE REVIEWS

X. LU et al. [11] have investigated the thermally conductive polymer composites that concentrated on polyurethane (PUR) composites filled with alumina (Al_2O_3) or carbon fibers (CF) of various volume fractions and the effects of filler sizes on their thermal conductivities. The two sizes of alumina (Al_2O_3) at the average diameter of 20 and 100 micron were selected. The carbon fibers (CF) sized 8 microns in diameter and length of 100 and 30 microns were used. Alumina (Al_2O_3) or carbon fibers (CF) each were added into polyurethane solution in chloroform as the solvent. The mixtures were cast to form films. The thermal conductivity of PUR/Al_2O_3 and PUR/CF films were increased with volume fraction of the fillers and the thermal conductivity of PUR/CF film was higher than PUR/Al_2O_3 composite. The thermal conductivity of 10% volume fraction PUR/CF film was around 10 $Wm^{-1}K^{-1}$, that was about 10 times higher than PUR/Al_2O_3 and 50 times higher than pure polyurethane, while their electrical conductivities were approximately below 10^{-8} Scm^{-1} that was in the appropriate range for electronic applications.

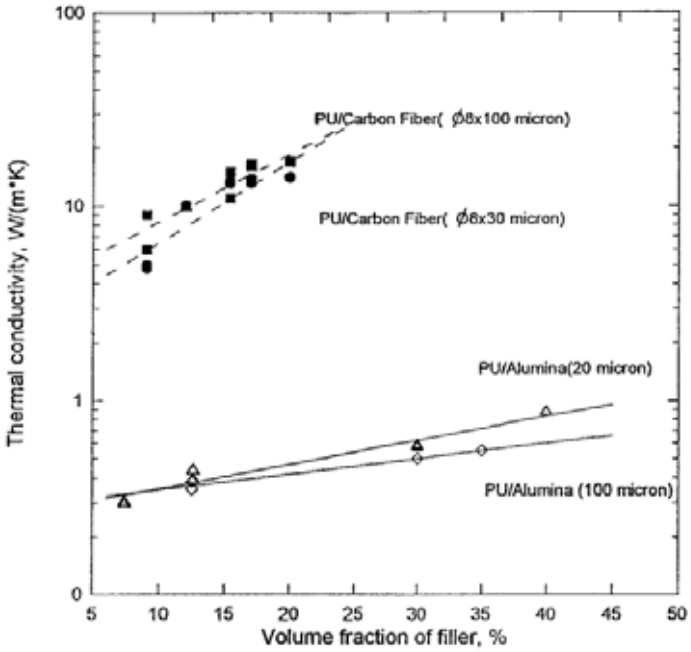

Figure 3.1 Schematic diagram of an apparatus used for measurement of the thermal conductivity of materials: (1) insulating material; (2) aluminum blocks; (3) cartridge heater; (4) cooling water; (5) sample.

Hatsuo Ishida et al. [9] have investigated a very high thermal conductivity polybenzoxazine composite filled with boron nitride. The polybenzoxazine used was a bisphenol-A-methy-lamine type. Bimodal size distribution hexagonal boron nitride with mean particle size of ca. 225 μm that has large aggregates of flake-like crystals was used as the fillers. The monomer powder was mixed with boron nitride at various desired volume fractions. The mixture was heated up to 80°C and further mixed by hand for 10 min to obtain the paste compound. The thermal conductivity measurement was investigated by Schroder's technique. The thermal conductivity of boron nitride-filled polybenzoxazine exhibited a very high thermal conductivity with stable mechanical strength. The highest thermal conductivity of 32.5 W/mK at the maximum boron nitride loading of 78.5% by volume was obtained, while its glass-transition temperature value of ca. 220 ^{o}C was obtained.

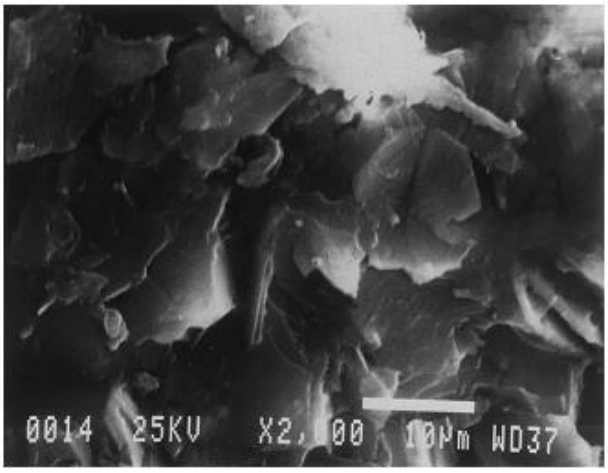

Figure 3.2 SEM micrograph of the fracture surface of 20 wt% of boron nitride flake in polybenzoxazine matrix.

Yunsheng Xu et al. [4] have investigated the thermally conducting aluminum nitride polymer-matrix composites. Polyvinylidene fluoride (PVDF) was used as the polymer with silane coupling agent for aluminum nitride surface treatment. The PVDF-matrix composites were fabricated by maximizing PVDF power (5μm size) and fillers. Aluminum nitride particles (115 μm), aluminum nitride whiskers and Silicon carbride whiskers were used as the fillers. Firstly, the PVDF-matrix composites were fabricated by mixing PVDF power (5μm size) and fillers in acetone.

Secondly, surface of aluminum nitrides powder were treated by two types of silane (Z-6040 or Z-6020). Finally, epoxy resin was mixed with curing agent in the weight ratio 100:13, added filler and mixed thoroughly. Composite was heated at 45°C and 10 MPa to complete polymerization. The results showed the increased in thermal conductivity when increasing filler volume fraction. Also, the highest thermal conductivity of 11.5 W/(m K) was obtained by using PVDF, AlN whiskers and AlN particles (7μm) when the total fillers volume fraction was 60% and the AlN particle ratio was 1:25.7. The addition of fillers to the polymer (either AlN or SiC) increased the dielectric constants, while SiC was greatly increased the dielectric constant.

Jiajun Wang et al. [3] reported the preparation and the properties of PMR-type polyimide composites with aluminum nitride powder as filler. The preparation consisted of three steps. Firstly, the mixture of three monomers; 4,4ı -methylene dianiline (MDA), ,4,4_-benzophenone tetracarboxylic acid BTDE and 5-norbornene-2,3-dicarboxylic acid (NE) was reacted to form imide prepolymer. Secondly, the imide prepolymer was mixed with AlN powders with average particle size of 2.0 μm. Finally, PI/AlN composite were molded by hot compression. The PMR-type PI composite specimens showed high thermal conductivity. The dielectric constant of PI/AlN composites varied from 2 to 4 for AlN volumes fraction from 0 to 62%, but the dielectric loss was lower than 0.003.

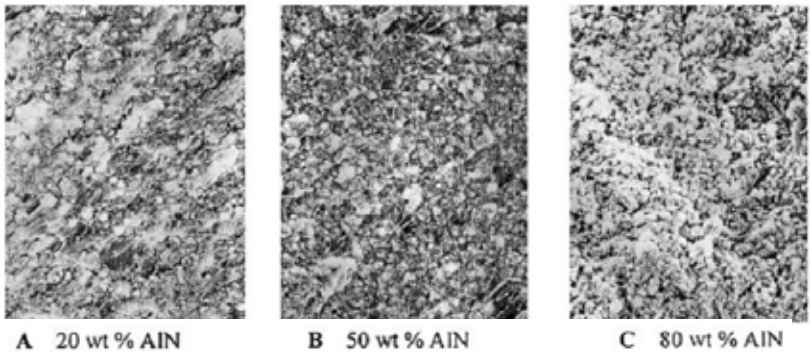

Figure 3.3 SEM micrographs of AlN/PI composite materials (x1k)

Zhi-Kang Xu et al. [6] have investigated Polyimide/aluminum nitride (AlN) composites. The polyimide/aluminum nitride (AlN) composites based on pyromellitic dianhydride (PMDA) and 4,4'-oxydianiline (ODA) were prepared by in situ polymerization. In this process, γ - glycidoxypropyltrimethoxysilane (GPTS) was

used as coupling agent. The composites were made by adding coupling agent treated AlN powder to the PMDA and ODA monomer solution. ASTM methods with Thermal – gravimetric analyses (TGA) were used for characterization of thermal properties, dielectric properties and surface and volume resistance of the obtained composites. It was found that the thermal stability and the thermal conductivity of the composite were increased, while the dielectric constant was increased slightly. The thermal conductivity and dielectric constant of the composite were greatly influenced after loading AlN and the coupling agent.

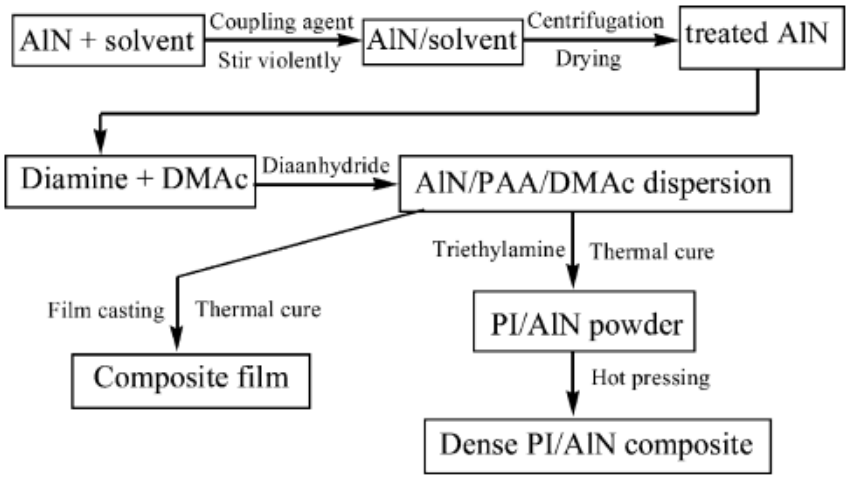

Figure 3.4 Schematic representation of the preparation process of the polyimide–AlN composite.

Geon-Woong Lee et al. [10] prepared polymer composite filled with hybrid filler in order to enhance thermal conductivity. Aluminum nitride (AlN), silicon carbide (SiC) whisker, boron nitride (BN) and wollastonite with different shapes and sizes were used as thermally conductive fillers. The composites contained various fillers at different amount of filler contents. The matrix was a powdered high density polyethylene (HDPE). Firstly, the surfaces of fillers were modified by titanate coupling agent. Finally, the fillers and HDPE were mixed at low filler content (10, 30 and 50 vol %) and high filler content (60 vol %). The polymer composites filled with hybrid filler could enhance thermal conductivity and also surface treatment of filler could increase thermal conductivity by reducing the CTE and minimizing the

interfacial phonon scattering. The composite containing the larger size particle improved thermal conductivity more than the smaller size particle.

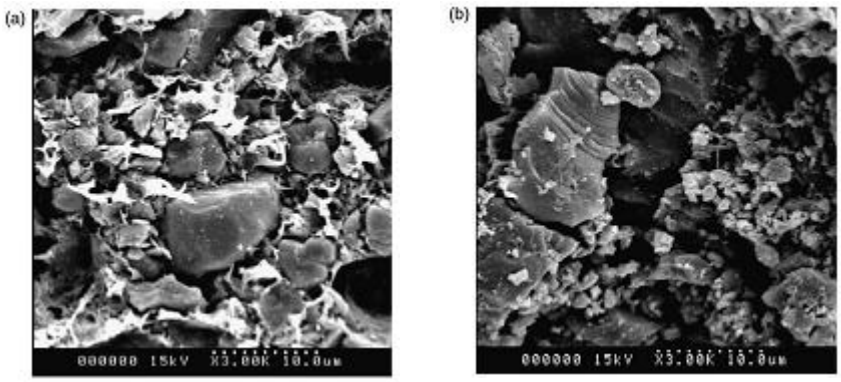

Figure 3.5 SEM images of the fracture surface of AlN(A-100)/HDPE composites containing (a) 60 vol%, (b) 75 vol% of AlN.

Shoichi Kume et al. [5] have investigated the high thermal conductivity AlN filler for polymer/ceramics composites. The experimental procedure consisted of three steps. The first step was the preparation of sintered AlN granules (mean granule size 79 μm) by dewaxed at 600°C. The dewaxed granules were placed in a BN crucible and sintered from 1600° to 1850°C. Secondly, measurement of the thermal properties of sintered AlN granules by a thermal microscope was implemented. The sintered AlN granules showed a very high thermal conductivity of 266±26 W (m.^{o} C)$^{-1}$. Finally, the polymer/ceramics composites were prepared by mixing polyimide resin with ceramic fillers that consisted of AlN granules and minute hexagonal boron nitride particles (h-BN). Laser flash device and FE-SEM were used for characterization the polymer composites. The polymer/ceramics composites showed the highest thermal conductivity of 9.3 W/(m.^{o}C)$^{-1}$ when consisted of 49 vol% AlN granules, 21 vol% h-BN powder and 30 vol% polyimide resins.

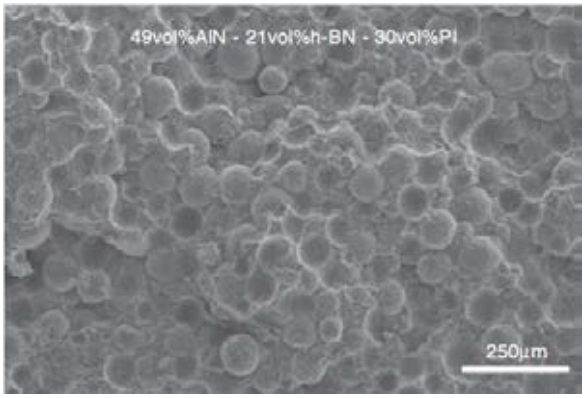

Figure 3.6 SEM photograph of fractured surfaces of polymer matrix composite filled with aluminum nitride (AlN) granules and minute hexagonal boron nitride particles (h-BN) particles.

Steve Lien-Chung Hsu et al. [8] prepared the thermally conductive polyimide composites film containing the hybrid filler of micro and nanosized BN. The preparation consisted of three steps. Firstly, the polyimide precursor base on pyromellitic dianhydride (PMDA) and 4,4′-diaminodiphenyl ether (4,4′-ODA) was synthesized. Secondly, Boron Nitride Fillers were modified with 3-mercaptopropionic acid (MPA). Finally, the thermal conductive PI/BN composites were prepared by homogeneously mixing the PMDA-ODA poly(amic acid) with surface modified mBN and nBN. The FTIR Spectrometer, Thermal – gravimetric analyses (TGA), Hot Disk Thermal Analyzer, scanning electron microscope (SEM), and the Thermal Mechanical Analyzer (TMA) used for characterization properties of the PI/BN composites. The thermal conductivity of the PI/BN composites films largely increased when both of the microsize and nanosize BN particles were added into the polyimide matrix, and also the glass transition temperatures of the polyimide composites were higher than the pure polyimide. The highest thermal conductivity of the PI/BN composite consisted of 30 wt % of BN fillers at the weight ratio of micro:nanosized equal to 7:3

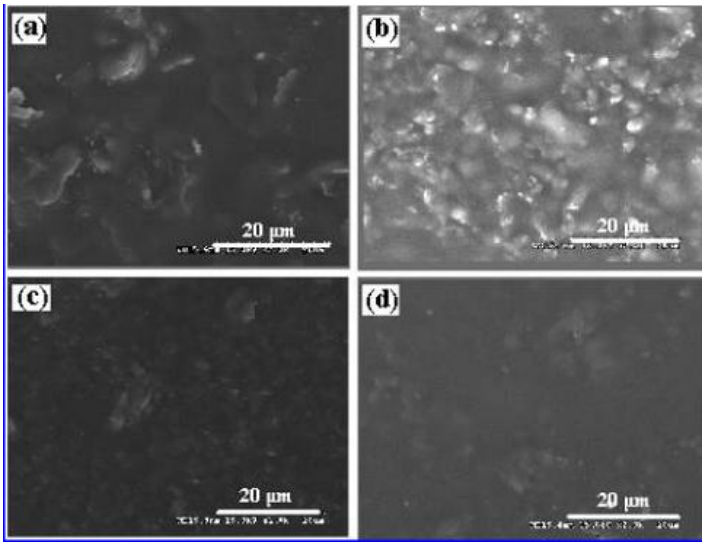

Figure 3.7 SEM micrographs of (a) polyimide/mBN30, (b) polyimide/7mBN30, (c) polyimide/3mBN, and (d) polyimide/nBN composite films.

Shinji Ando et al. [2] have investigated the method to enhance thermal diffusivity of vertical double percolation (VDP) structures in polyimide blend films containing silver nanoparticles. Polyimide precursors were prepared by addition polymerization of equimolar amounts of 3,3',4,4'-Biphenyltetracarboxylic dianhydride (BPDA) and diamines, 4,4'-Thiodianiline (SDA) or 2,2'-Bis(trifluoromethyl)-4,4'-diaminobiphenyl (TFDB) which BPDA-SDA as a sulfur-containing PI and BPDA-TFDB as a fluorine-containing PI. The poly (amic acid) (PAA) solutions were blended with $AgNO_3$ as a soluble precursor of Ag-NPs. The transparent PAA solutions were spin-coated onto a 4-inch silicon wafer and the films were thermally cured at the final condition of 300 ^{o}C for 1.5 h. The thickness of the PI film was 15-30 µm. As the main characterization of this study, the thermal conductivities of PI blend films were measured by temperature wave analysis (TWA). The results showed that the PI blend films exhibited higher the thermal diffusivity along the out-of-plane direction ($D_{\perp}$) values than the mono phase homo-PI films with homogeneously dispersed Ag-NPs. These results indicated the VDP structure has been developed for generating thermal conductivity of the PI blend films. So the VDP structure in the PI blend system was a pathway to enhance the thermal diffusivity of polymer dielectric materials.

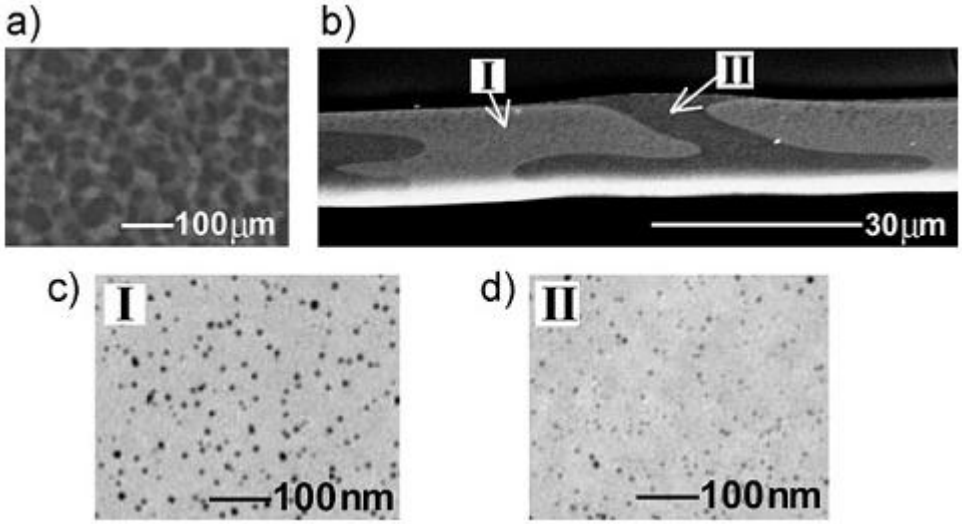

Figure 3.8 Morphology of the micro-phase-separated blend film of $SD_{70}/TF_{30}/Ag_{20}$. a) Surface image by optical microscope and b) cross-sectional SEM image by back scattered electron mode. Bright white line on the bottom of the film in b) is an SEM artifact. Cross-sectional TEM images of c) domain I (Ag-rich phase) and d) domain II (Ag-poor phase). Black dots correspond to Ag-NPs.

Robert S. Farr et al. [25] was investigated close packing density of polydisperse hard spheres. They propose an approximate solution to the problem of polydisperse packing density obtained by abstracting what to be essential features of the physics and geometry of packing. In this study, it correctly reproduces the exact solution for bidisperse spheres with infinite size ratio. This limit is given as following:

$$\psi_{\max} = \min\left(\frac{\phi_{\mathrm{RCP}}}{1 - w(1 - \phi_{\mathrm{RCP}})}, \frac{\phi_{\mathrm{RCP}}}{w}\right) \qquad (3.1)$$

where Ψ_{max} is the maximum packing fraction, ϕ_{RCP} is the maximum packing fraction for a monodisperse system, and w is the mass fraction of large spheres on the total particle volume, so $w = \phi_{large} (\phi_{large} + \phi_{small})$. For w value very close to the cusp, w= $1/(2- \phi_{RCP})$.

Table 3.1 Simulation results for the maximum packing fraction of bidisperse spheres, with diameters *D*1 and *D*2. The mass fraction present in the large spheres is given by $w = \phi_{large} (\phi_{large} + \phi_{small})$

w	$D_2/D_1=0.5$	$D_2/D_1=0.3$	$D_2/D_1=0.2$	$D_2/D_1=0.1$
0	0.6435	0.6435	0.6435	0.6435
0.2	0.6579	0.6695	0.6761	
0.4	0.6690	0.6971	0.7152	0.7298
0.5				0.7557
0.6	0.6774	0.7236	0.7525	0.7835
0.7	0.6795	0.7324	0.7714	0.8150
0.75				0.8270
0.8	0.6749	0.7315	0.7769	0.7948
0.9	0.6650	0.6985	0.7111	
0.95	0.6558	0.6690		
1	0.6435	0.6435	0.6435	0.6435

The simulation results for binary mixtures are shown in Table I and in Fig. 6, together with the theoretical prediction.The theoretical prediction as shown in Figure 3.9 . The big particles have diameter D_1=1, and the small particle diameters are D_2=0.5, 0.3, 0.2,and 0.1.(R= D_2/D_1)

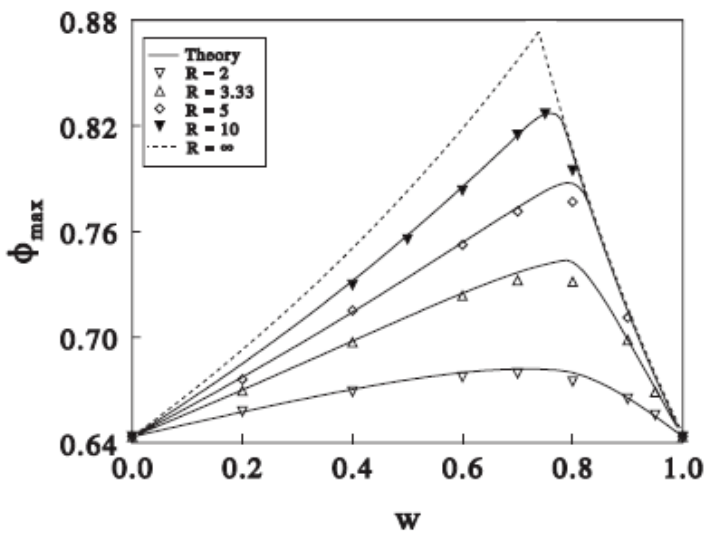

Figure 3.9. Maximum packing fraction for bidisperse spheres of different size. R is the size ratio and $w = \phi_{large} (\phi_{large} + \phi_{small})$ is the relative volume fraction of the large spheres. Symbols are simulation results, and solid lines are theoretical predictions, based on 20 000 rods. The dashed curves give the upper limit for infinite size ratio, Equation 3.1

CHAPTER IV

EXPERIMENTS

4.1 Materials and Chemicals

1. 4,4´-Oxydianiline (ODA) purchased from Fluka Company, Inc.
2. Pyromellitic dianhydride (PMDA) purchased from Aldrich Chemical Company, Inc.
3. N-Methyl-2-pyrrolidinone (NMP) purchased from Merck KGaA Germany.
4. Silicon nitride particles with particle sizes of < 10 μm, <1 μm and <50 nm were purchased from Aldrich Chemical Company, Inc.
5. 3-aminopropyltrimethoxysilane (APTS) purchased from Louis T. Leonowens (Thailand) Ltd.
6. 3-(2-aminoethylamino)propyltrimethoxysilane (AEPTS) purchased from Koventure Co., Ltd.
7. 3-[2-(2-aminoethylamino)ethylamino]propyl-trimethoxysilane(AEEPTS) purchased from Aldrich Chemical Company, Inc.
8. Ethanol (Commercial grade) was purchased from SR lab.
9. Acetic acid purchased from Aldrich Chemical Company, Inc.
10. Argon gas (Ultra high purity grade, 99.999%) was purchased from Thai Industrial Gas Co.,Ltd. (TIG) and further purified by passing through columns packed with copper catalyst.

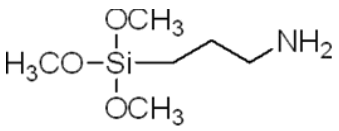

APTS

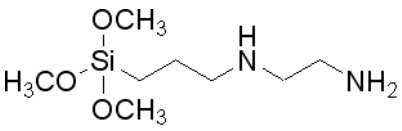

AEPTS

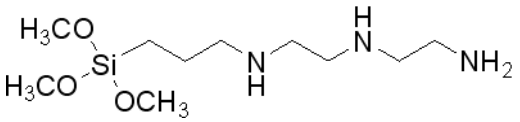

AEEPTS

Figure 4.1 Structure of three type of coupling agents

4.2 Equipments

4.2.1 Poly(amic acid) synthesis part

Since most of the reagents were very sensitive to the oxygen and moisture therefore the special techniques were undertaken during the handling of reagents and the loading of ingredient into the reactor. Such equipment utilized for this purpose are listed as follows:

(a) Glove box

Glove box (Argon Atmospheres) with oxygen and moisture analyzer designed for handling solid reagents under inert atmosphere and for storing air-sensitive reagents. Inside the glove box, oxygen and moisture levels are normally controlled to below 0.1 ppm. The glove box is shown in Figure 4.2.

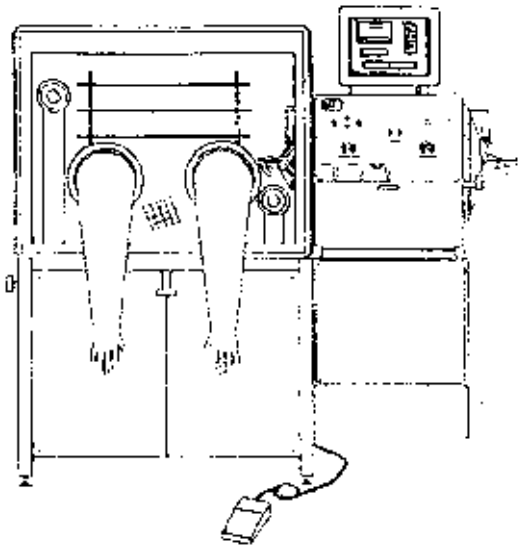

Figure 4.2 Glove box

(b) Magnetic stirrer and Hot plate

The magnetic stirrer and hot plate model RCT basic from IKA Labortechnik were used. The magnetic stirrer and hot plate are shown in Figure 4.3.

Figure 4.3 Magnetic stirrer and Hot plat

(c) Syringe and Needle

The syringe had a volume of 10 ml was used in this work and the needles were No. 17 and 20.

4.2.2 Preparation of modified Si_3N_4 fillers part

(a) Cooling System

The cooling system is importance in the solvent distillation that in order to condense the freshly evaporated solvent from the reactor during the synthesis.

(b) Ultrasonic

Ultrasonic (VGT-1860QTD) dispersing helps to improving the dispersion quality of the fillers.

Figure 4.4 Ultrasonic

4.2.3 Preparation of polyimide/silicon nitride composite films part

(a) Vacuum oven

A Cole-Parmer vacuum oven model 282A was used for removing solvent from freshly cast films. This vacuum oven can be programmed. All functions can be set from digital panel and display their status on LCD. The temperature, pressure and time are controllable variables. The vacuum oven is shown in Figure 4.5.

Figure 4.5 Vacuum oven

(b) Temperature controlled oven

A Carbolite LHT5/30 (201) Temperature controlled oven was utilized in these experiments. The maximum working temperature of this machine is 400°C. The equipment was used for conversed poly(amic aid) film to polyimide film.

Figure 4.6 Temperature controlled oven

4.3 Preparation of the silane treated Si_3N_4 particles

Before usage, the commercially Si_3N_4 particles were dried at certain temperature in vacuum oven for 24 hours. First step, started by preparing deionized water (5%w) and ethanol (95%w) solution and adjusting its pH to around 4-5 by acetic acid. Next step, an appropriate amount of silane coupling agent was added into the mixture and stirred for full hydrolysis and formation of silanol. Then, Si_3N_4 particles was added into the mixture and dispersed by ultrasonic. The mixture was heated at certain temperature with refluxing and stirring for 4 hours and, after that, the mixture was cooled down to room temperature. The mixture was rinsed with ethanol by filtration at least three times and the samples were dried in vacuum oven and then cool the silane treated Si_3N_4 fillers down to room temperature. Last step, the fillers were grinded by mortar and pestle. The same procedure was applied to all sizes of silicon nitride.

The calculation of amount of silane coupling agent

The silane coupling agent molecule is expected to attach to the surface of the fillers as a primer to form a mono-layer coating, so the calculation of amount of silane was important. The amount of silane used for surface treatment depends on the surface area of the fillers or silane treatment process. The calculation of amount of silane coupling agent can be calculated as follows: [26]

$$\text{Amount of silane (g)} = \frac{\text{amount of filler (g)} \times \text{specific surface area of filler (m}^2\text{/g)}}{\text{wetting surface of silane (m}^2\text{/g)}}$$

4.4 Preparation of polyimide/silicon nitride composite films

4.4.1 Preparation of poly(amic acid) solution

To synthesize poly(amic acid) solution by using two-step polymerization method. Firstly, an equimolar amounts of 4,4'-oxydianiline (ODA) and pyromellitic dianhydride (PMDA) were added in NMP solvent. The sample was stirred for homogenous by magnetic stirrer at the room temperature to obtain to homogeneous poly(amic acid).

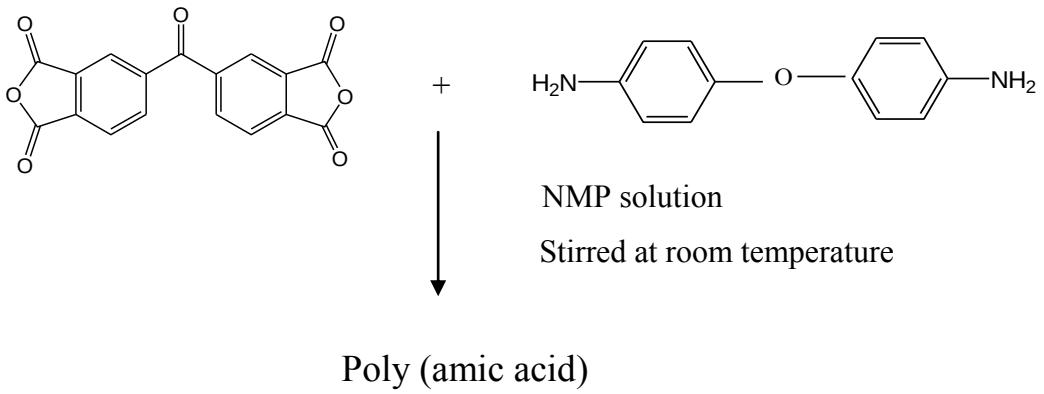

Figure 4.7 Preparation of the Poly (amic acid) solution

4.4.2 Preparation of polyimide/silicon nitride composite films

An appropriate amount of the silane treated Si_3N_4 particles were added in 1 ml. of NMP solvent and stirred for homogeneously. Next step, added the mixture in poly(amic acid) with stirring. Next step, the sample was dispersed by ultrasonic and the mixture was added into the poly(amic acid) solution and stirred by magnetic stirrer and for a long time by ultrasonic, respectively. The PI/Si_3N_4 composite films were cast on the glass plates and then dried in vacuum oven at 60°C for 6 hours to obtain the poly(amic acid) films. The composite films were cured at 100 °C, 150 °C, and then 250 °C for one hour each. The same procedure was applied to all of the samples.

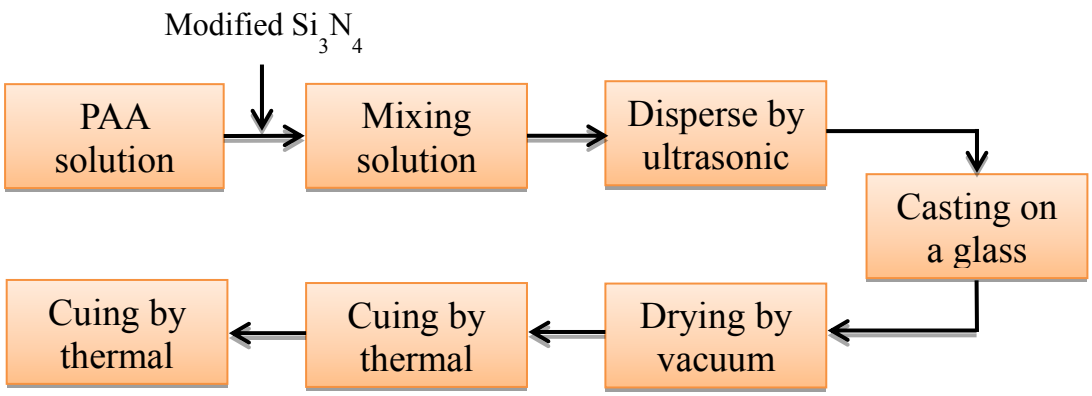

Figure 4.8 Scheme of preparation for PI/Si_3N_4 composite films

4.5 Characterization Instruments

4.5.1 Infrared Spectroscopy (FTIR)

Infrared spectra were recorded with Nicolet 6700 FTIR spectrometer. The scanning frequency ranged from 400 to 4000 cm^{-1} with 64 times scanning. The functional groups of the composite films (1.5×1.5 cm^2) were identified.

Figure 4.9 Fourier transform infrared spectroscopy (FTIR) Equipment.

4.5.2 LCR meter

The dielectric constant of polyimide films were investigated by LCR meter at 1 MHz.

Figure 4.10 LCR meter equipment.

4.5.3 Scanning electron microscope (SEM)

The morphology of the received particle size of Si_3N_4 particle, silane treated Si_3N_4 and PI/Si_3N_4 composite films were investigated by SEM. (Hitachi model S-3400N). The composite films for SEM analysis were coated with platinum.

Figure 4.11 Scanning electron microscopy (SEM) equipment.

4.4.4 Transmission electron microscopy (TEM)

The morphology of an individual grain in the samples was observed by a JEOL JEM-2100 Analytical Transmission Electron Microscope, operated at 80-200 keV at the Scientific and Technological Research Equipment Center (STREC), Chulalongkorn University. The crystallographic information was also obtained from the selected area by electron diffraction (SAED) analysis performed in the same instrument.

4.5.5 Laser flash

Thermal diffusivity (α) was measured by laser flash method. (NETZSCH, LFA 1000 Laser Flash, Germany) Laser flash method is the most useful technique to measure thermal diffusivity (α) of various kinds of solid and liquid samples at various temperatures. The laser flash measurement was operated by heating on one side of plan-parallel sample and measuring temperature rise on the opposite side that is measured versus time by IR detector as display in Figure 4.12.

Thermal conductivity was calculated as shown in the following equation:

$$k = \alpha \rho C_p$$

Thermal conductivity (k, W/mK) was the product of thermal diffusivity (α), specific heat capacity (C_p, J/gK) and bulk density (ρ, g/cm^3) of the samples. Specific heat capacity (C_p) was measure by DSC (Perkin Elmer, Pyris Diamond Differentia Scanning Calorimeter, USA). The composite films were casted on the aluminium plates. Size of a rectangular aluminium plate is 10x10x2 mm^3 and thickness of the composite films is around 0.04-0.08 mm.

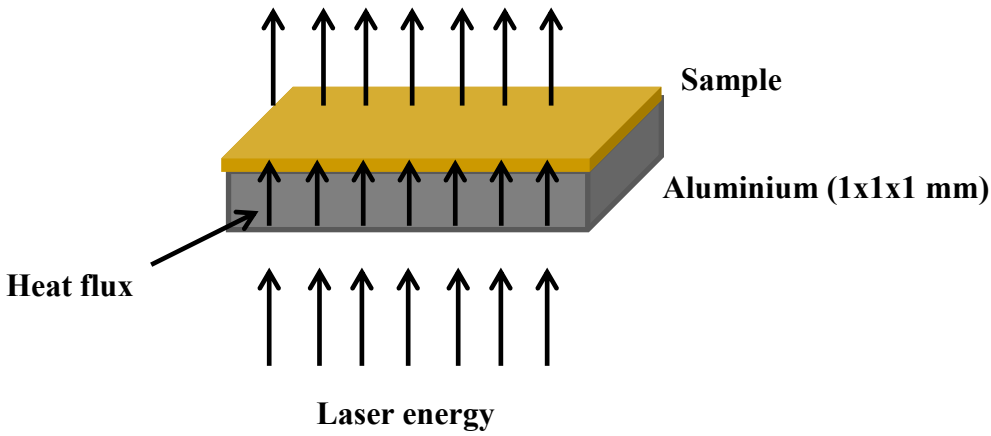

Figure 4.12 A simple schematic of a thermal diffusivity measurement

4.5.6 Universal testing machine

Tensile strength properties were characterized by INSTRON 2712-003 Universal testing machine with a test speed of 5 mm/min. (Sample size 2 x 5 cm^2). The tests were conducted according to ASTM D 882-02. The maximum pressure is 6 bar and the maximum load is 1 kN.

4.5.7 Thermogravimetric Analysis (TGA)

The weight lost with temperature ramp were investigated by TGA. The temperature ranged from ambient to 1000 ^oC and the scan rate 0.01-100 ^oC/min.

CHAPTER V

RESULTS AND DISCUSSION

The Si_3N_4 particles were chosen to include in the polyimide matrix in order to improve thermal properties of polyimide. The properties of ceramic particles filled polymer composite dependence on size, distribution of fillers in the polymer matrix and adhesion of interfacial surface. The effects of three types of silane for surface modification of Si_3N_4 particle, micron, submicron and nano size, were investigated. Effects of single size and hybrid sizes of Si_3N_4 particle on thermal and mechanical properties were illustrated as follows.

5.1 Effect of surface modification of Si_3N_4 particle on polyimide composite films properties

5.1.1 Characterization of as received Si_3N_4 particles

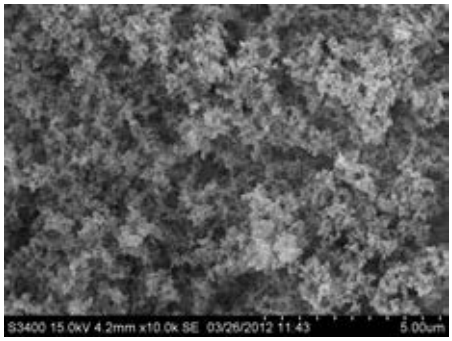

(a) Nano sized Si_3N_4 as received

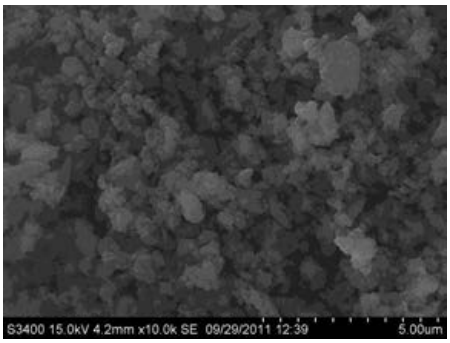

(b) Submicron sized Si_3N_4 as received

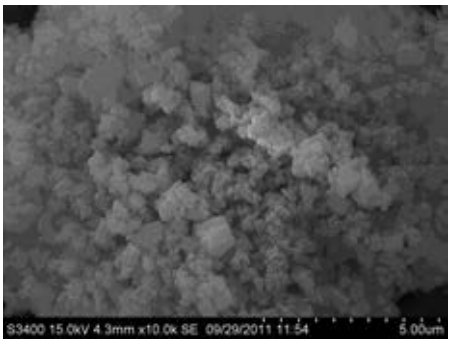

(c) Micron sized Si_3N_4 as receive

Figure 5.1 Morphology of the as received Si_3N_4 particles

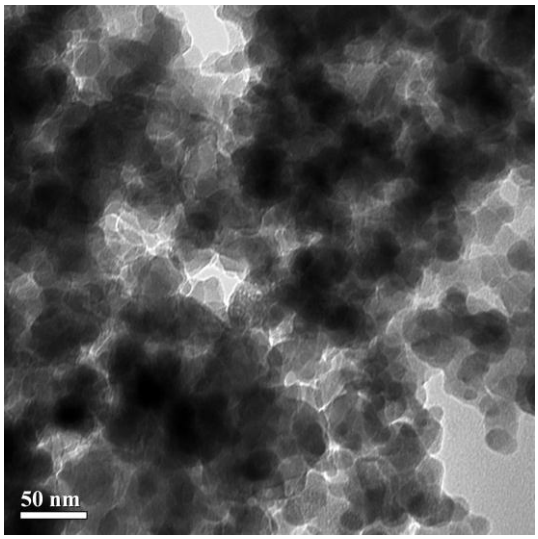

(a) Nano sized Si_3N_4 as received

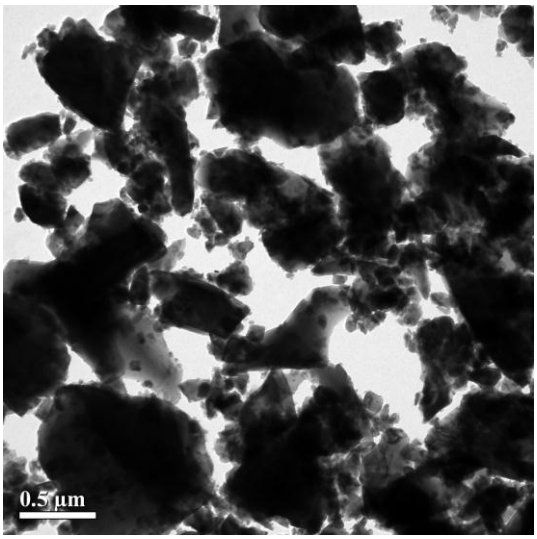

(b) Submicron sized Si_3N_4 as received

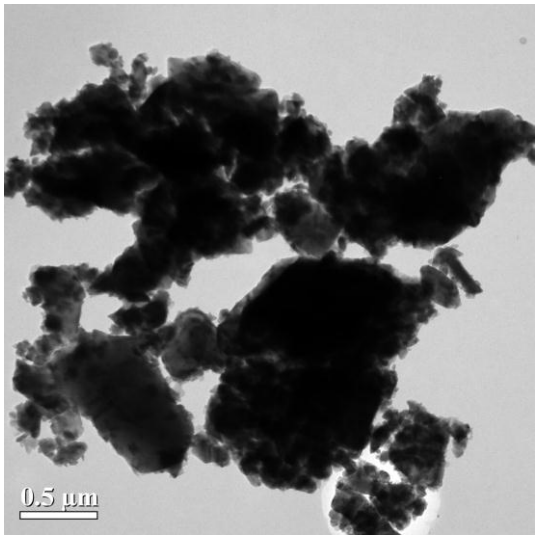

(c) Micron sized Si_3N_4 as receive

Figure 5.2 TEM images of the as received Si_3N_4 particles

The morphologies of as received Si_3N_4 particles were investigated by Scanning electron microscope (SEM) and Transmission electron microscopy (TEM) as shown in Figure 5.1 and 5.2, respectively. These figures demonstrated shape, mean size, specific surface area of Si_3N_4 particles as received. The Si_3N_4 particles used were not spherical shape, mostly irregular shapes and some particles were agglomerated together.

5.1.2 Characterization of silane treated Si_3N_4 particles

5.1.2.1 Functional groups of silane treated Si_3N_4 particles

In this research, Si_3N_4 particles were treated with three types of silane. There are 3-aminopropyltrimethoxysilane (APTS), 3-(2-aminoethylamino)propyltrimethoxy silane (AEPTS) and 3-[2-(2-aminoethylamino)ethylamino]propyl-trimethoxy Silane (AEEPTS). The silane coupling agent was hydrolyzed to form the silanol groups (Si-OH). The silanol groups (Si-OH) of silane were reacted with the hydroxyl groups on the surface of Si_3N_4 particles to form (Si-O-Si) groups linkage as displayed in Figure 5.3. The chemical structure of silane treated Si_3N_4 particles were characterized by Fourier transform infrared spectroscopy (FT-IR) as shown in Figure 5.4.

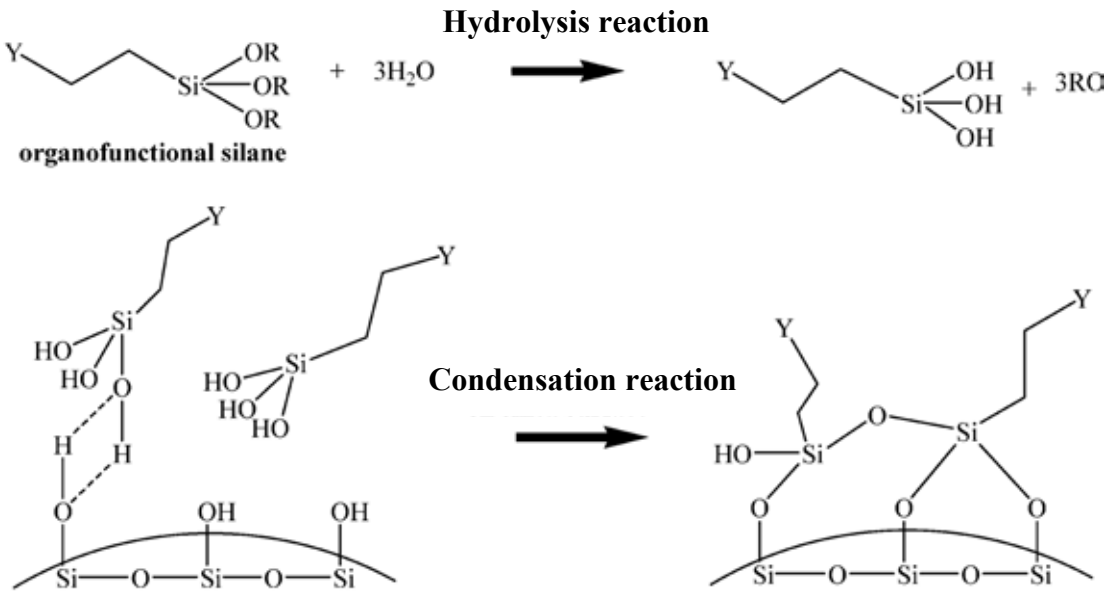

Figure 5.3 The scheme of reaction mechanism of silane treatment on Si_3N_4 surface.[27]

The FT-IR spectra of silane treated Si_3N_4 particles using the different types of silane, as shown in Figure 5.4, can identified the main absorption band at approximately 800 -1100 cm^{-1} of the stretching vibration of Si-N. The center of Si-N asymmetric bond stretching vibration was at apprximately 840 cm^{-1}. The presence of

silane grafted on the Si_3N_4 particle surface, represented by the peak at 1000 – 1200 cm^{-1} of the strong peak of Si-O-Si stretching vibration, was difficult to identify because of the very strong peak of Si-N (700-1100). Moreover, the N-H vibrations at 1500-1700 and 3300-3500 cm-^{1} are difficult to identify because of these peaks were broad and overlapped by other strong peaks. However, the characteristic of C-H vibration of propyl chains a weak band at 2900-3000 cm^{-1}, indicates that silanes are coupled on the surface of Si_3N_4 particles The strange peaks were appeared at around 1800-2200 represented carbondioxide groups that occured during the characterizing process.

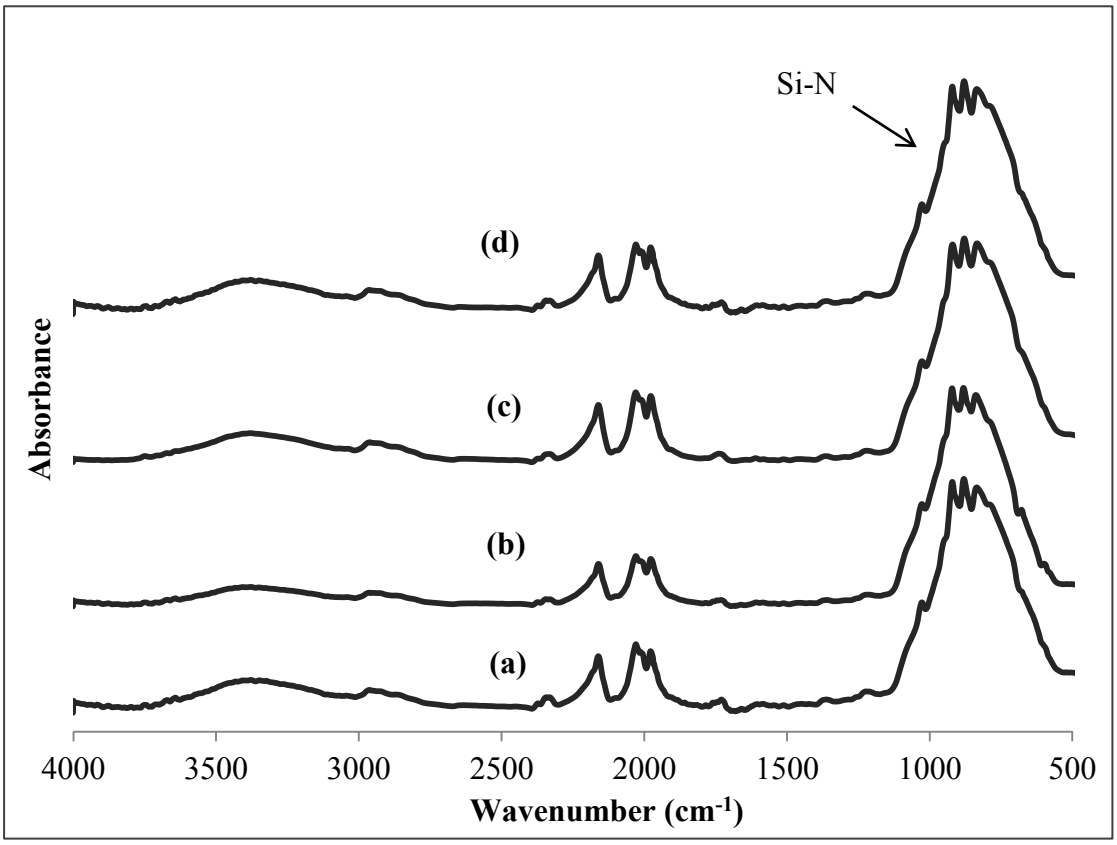

Figure 5.4 The FTIR spectra of silane treated Si_3N_4 particles ; (a) Untreated Si_3N_4, (b) APTS treated Si_3N_4, (c) AEPTS treated Si_3N_4 and (c) AEEPTS treated Si_3N_4.

5.1.2.2 Morphology of silane treated Si_3N_4 particles

The morphology of Si_3N_4 particles, between unmodified and modified with three types of silane coupling agent, were characterized by using SEM observation as shown in Figure 5.5. The average sizes of three types of silane treated particles were similar to the untreated particles. Therefore, the surface treatments of Si_3N_4 particles were not significantly changed the size of particles from as received size of particles. However, the surface treatments of particles could induce the effect of the agglomeration of filler particles and finally influence the dispersion ability of particles.

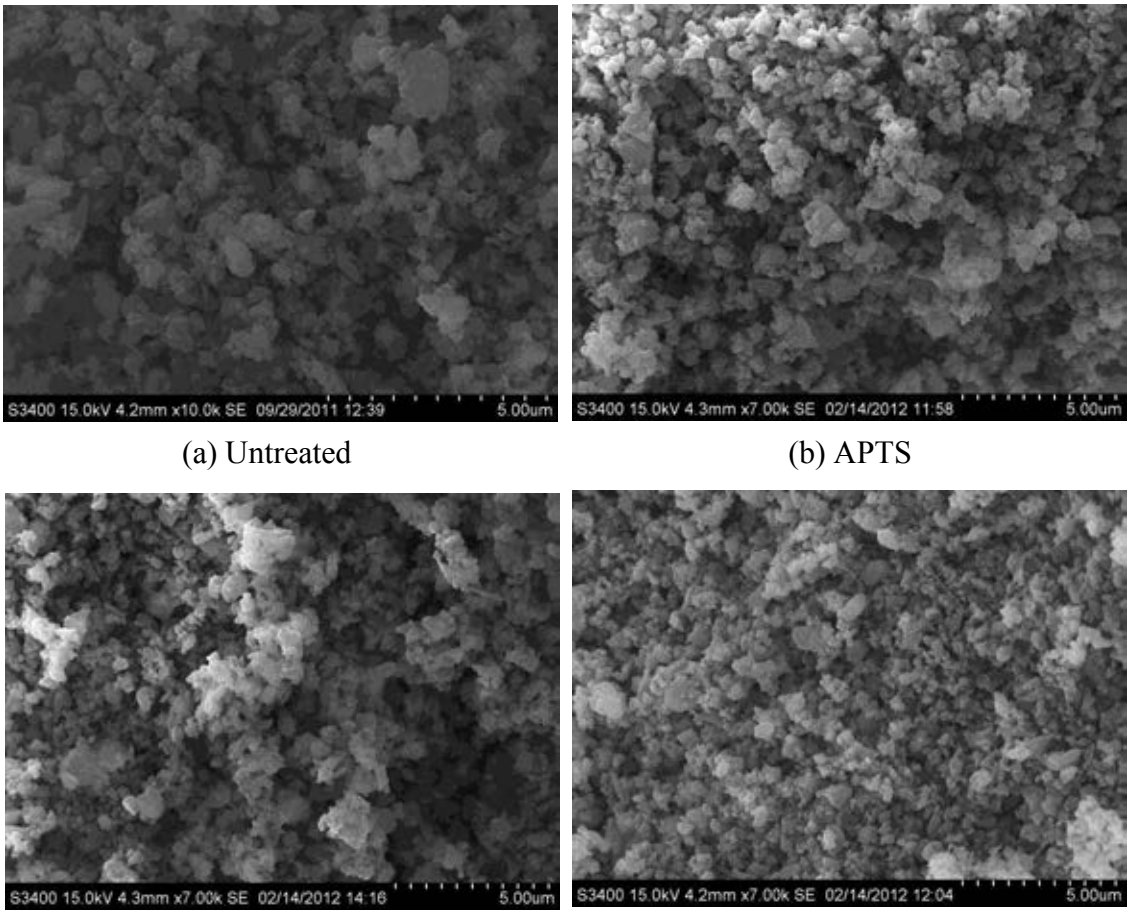

(a) Untreated (b) APTS

(c) AEPTS (d) AEEPTS

Figure 5.5 Morphology of the submicron sized Si_3N_4 particles with different silane coupling agent

5.1.3 Characterization of silane treated Si_3N_4/PI composite films

5.1.3.1 Functional groups of silane treated Si_3N_4/PI composite films

The FT-IR spectra of silane treated Si_3N_4/PI composites using the different types of silane, as shown in Figure 5.6, can identify the imide absorption bands at near 1780 cm^{-1} (C=O asymmetrical stretching), 1720 cm^{-1} (stretching vibration) and 1380 cm^{-1} (C–N stretching) which were the common characteristic absorption peak of the imide group [28]. The Si_3N_4/PI composite films using untreated and treated silane were identified by the main absorption band at approximately 800 -1100 cm^{-1}, which was the stretching vibration of Si-N. The center of Si-N asymmetric bond stretching vibration was shown approximately at 840 cm^{-1}. The peak at 1000 – 1200 cm^{-1} of the strong peak of Si-O-Si stretching vibration was difficult to identified and the N-H vibrations at 1500-1700 and 3300-3500 cm-^{1} were difficult to identify because of the overlapping by other strong peaks.

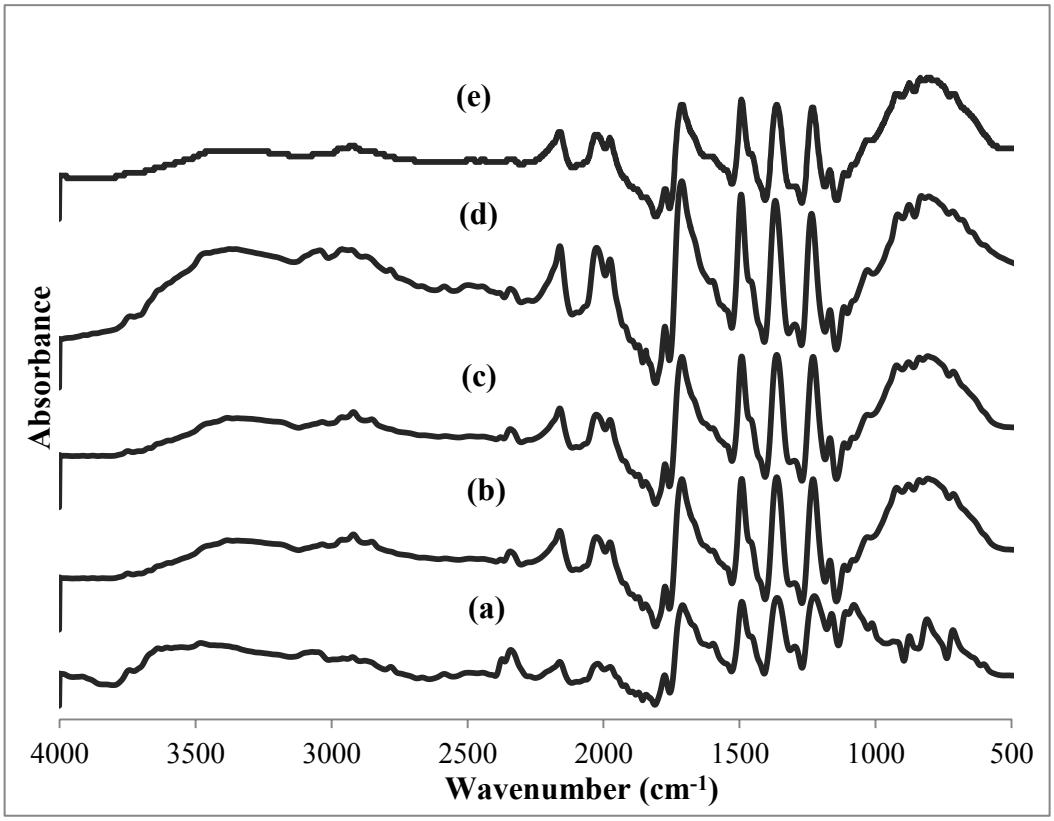

Figure 5.6 The FTIR spectra of (a) polyimide, (b) untreated Si_3N_4/PI, (c) APTS treated Si_3N_4/PI, (d) AEPTS treated Si_3N_4/PI and (e) AEEPTS treated Si_3N_4/PI

5.1.3.2 Morphology of Si_3N_4/PI composite films

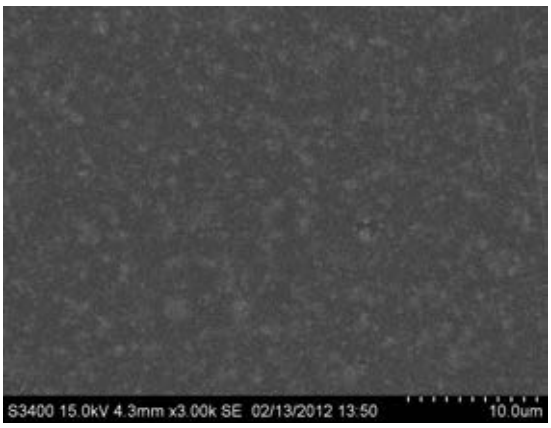

(a) Untreated

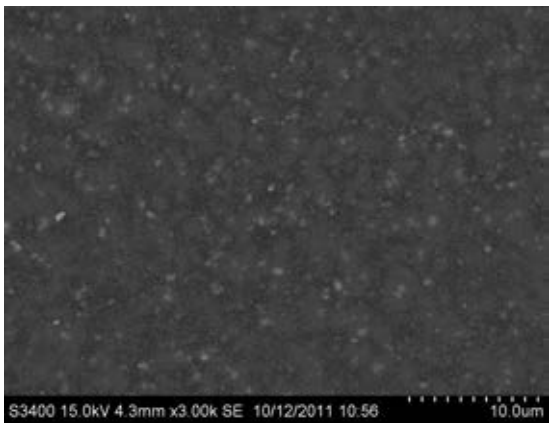

(b) APTS

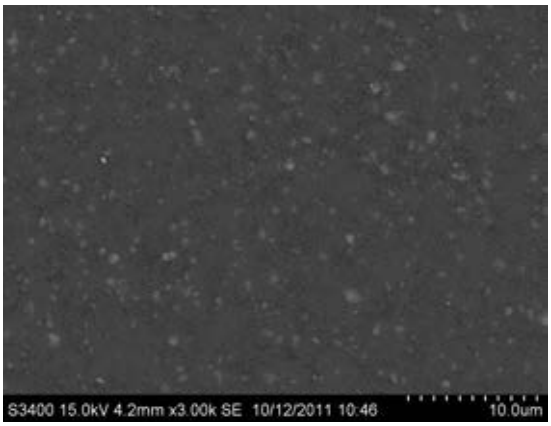

(c) AEPTS

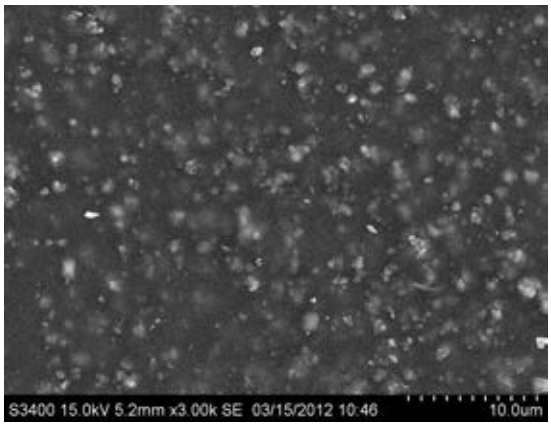

(d) AEEPTS

Figure 5.7 Morphology of 15%wt submicron Si_3N_4/PI composite films; (a) Untreated (b) APTS, (c) AEPTS and (d) AEEPTS of Si_3N_4 particles.

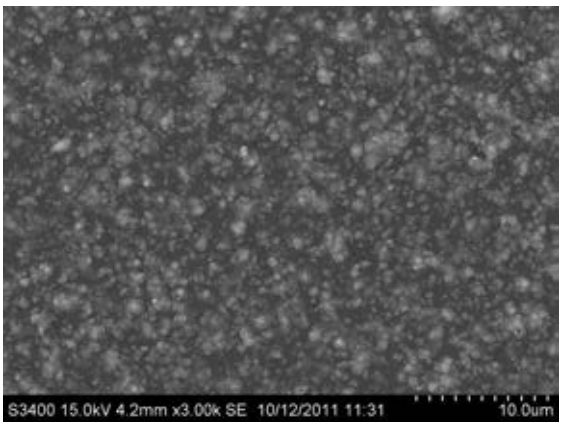

(a) Untreated

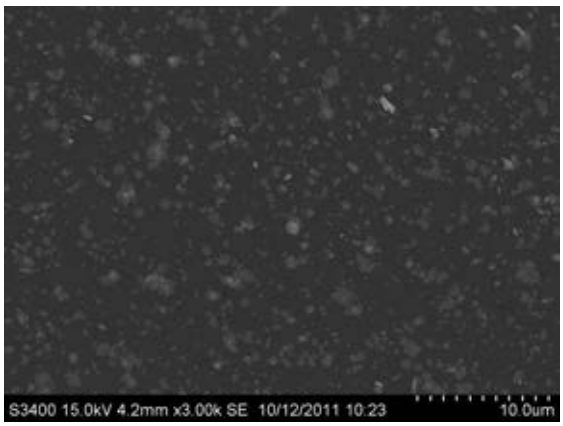

(b) APTS

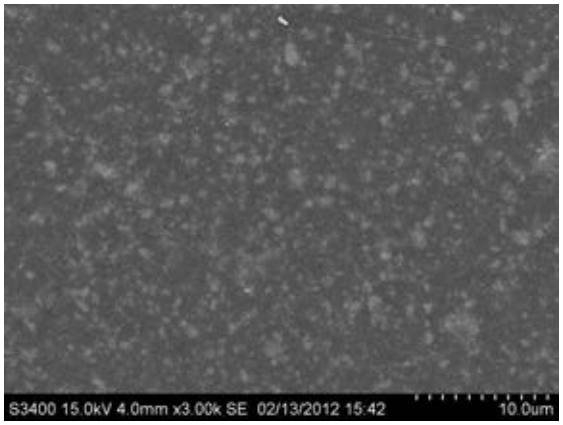

(c) AEPTS

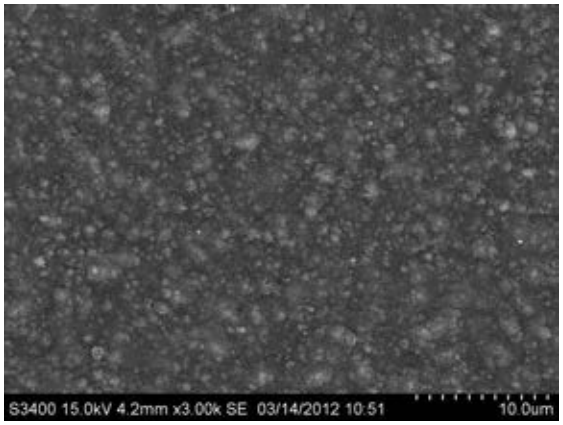

(d) AEEPTS

Figure 5.8 Morphology of 25%wt submicron Si_3N_4/PI composite films; (a) Untreated (b) APTS, (c) AEPTS and (d) AEEPTS of Si_3N_4 particles.

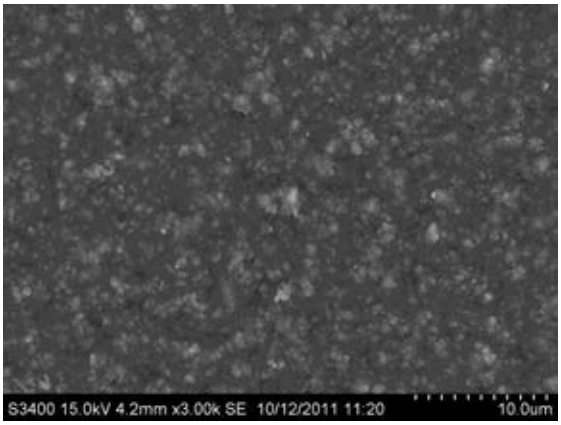

(a) Untreated

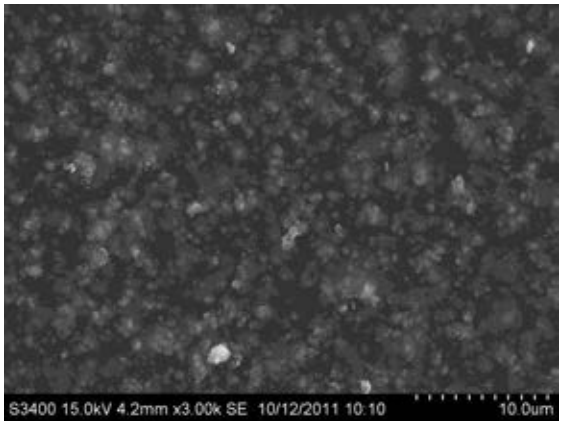

(b) APTS

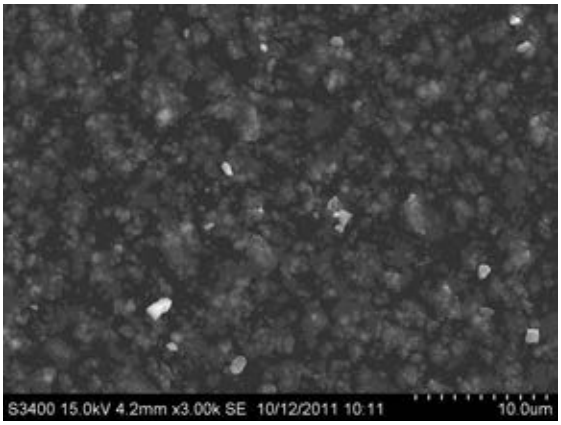

(c) AEPTS

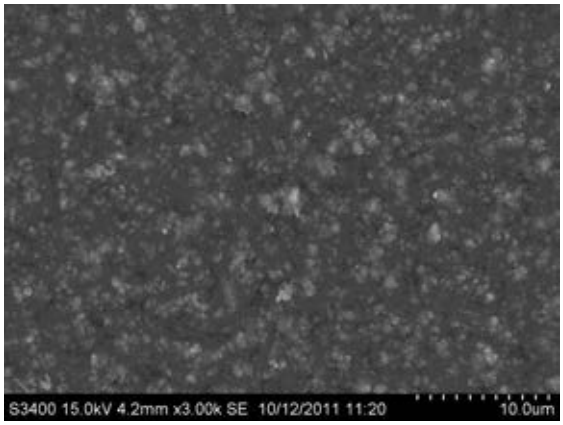

(d) AEEPTS

Figure 5.9 Morphology of 35%wt submicron Si_3N_4/PI composite films; (a) Untreated (b) APTS, (c) AEPTS and (d) AEEPTS of Si_3N_4 particles.

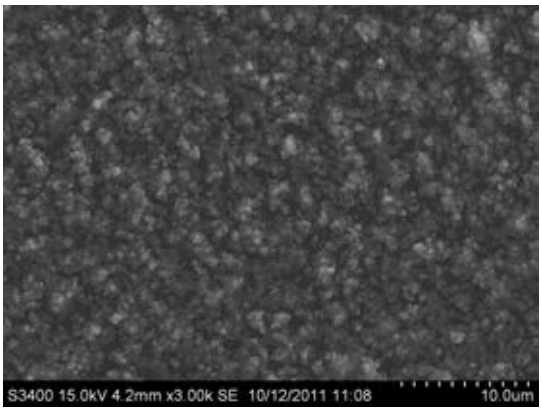

(a) Untreated

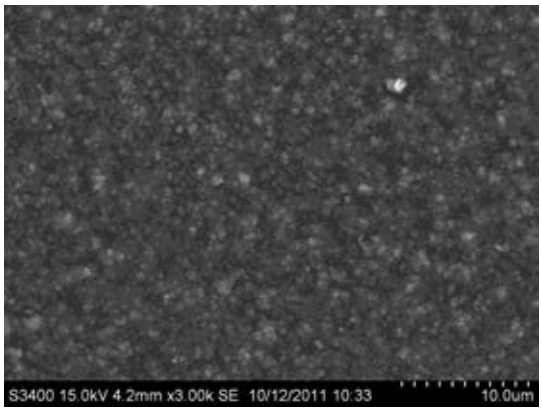

(b) APTS

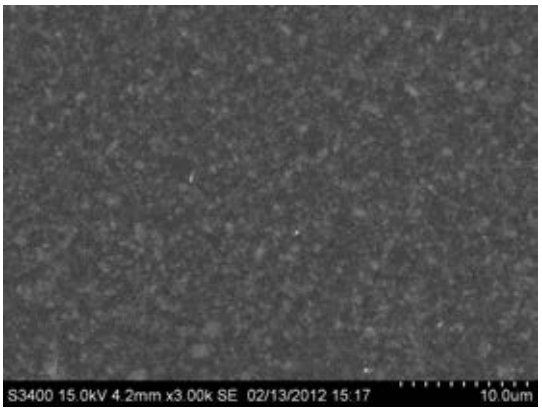

(c) AEPTS

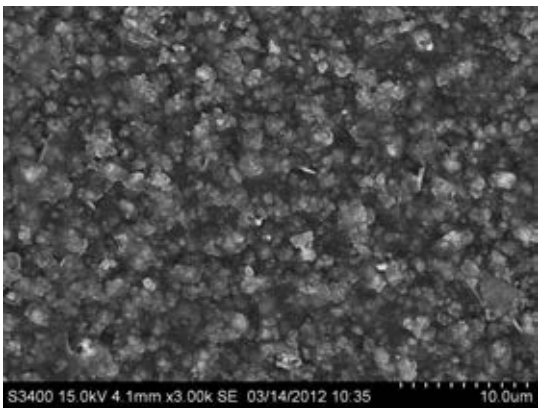

(d) AEEPTS

Figure 5.10 Morphology of 45%wt submicron Si_3N_4/PI composite films; (a) Untreated (b) APTS, (c) AEPTS and (d) AEEPTS of Si_3N_4 particles.

The observations by SEM micrographs for Si_3N_4/PI composite films are illustrated in Figure 5.7-5.10 that show the distribution of Si_3N_4 particles in polyimide matrix at different types of silane and submicron Si_3N_4 content. The SEM micrographs of different content of Si_3N_4 indicated the increase in agglomeration between Si_3N_4 when increasing contents. Compared silane treated with untreated particle showed that silane treated particles could reduce the agglomeration of fillers in the matrix due to the enhances adhesion of interfacial surfaces between filler and polymer matrix by silane coupling. However, it was surprising that the agglomeration observed by SEM of AEEPTS composite seemed to be worst even more than others silane composite. This might be because the length of the amine induced the crosslink

and entanglement of filler that covered by AEEPTS more than others silanes and even more than the limit of dispersion of particle (particles could not escape before dispersion begin), so the filler come close together by agglomeration and could not create the thermal diffusivity path through the composite.

In addition, compared the usage of different types of silane showed that APTS and AEPTS could improve the agglomerations of fillers better than AEEPTS. Figure 5.10 (45%wt Si_3N_4) obviously showed that the usage of AEEPTS was created the worse dispersion effects more other one. We can confirm the dispersion of Si_3N_4 particle in PI matrix by TEM images of cross sectin of PI/ Si_3N_4 composite films as shown in Appendix G (Figure G.1).

5.1.3.3 Mechanical properties of Si_3N_4/PI composite films

The mechanical properties of the Si_3N_4/PI composite films were analyzed by universal tensile testing machine as shown in Figure 5.11-5.13. The tensile strength, tensile modulus and elongation at break (%) of the pristine PI film under ambient conditions are 120 MPa, 3.2 GPa and 12 %, respectively. Figure 5.11 show that the tensile strength of composite films decreased with increasing the contents of Si_3N_4 fillers because of the stress concentration caused by the rigidity of Si_3N_4 fillers. Elongation at break (%) of PI composite films' results corresponded to the tensile strength of composite films that were decreased when the filler content increased, as shown in Figure 5.13. However, because of the rigidity of Si_3N_4 fillers, the modulus of PI composite films were higher than pristine PI at high content of Si_3N_4 fillers as shown in Figure 5.12.

. When compared the untreated and treated with silane of submicron Si_3N_4 filled in PI matrix, the tensile strength, tensile modulus and elongation (%) of composite films with silane treated Si_3N_4 was higher than untreated Si_3N_4, as shown in Figure 5.11-5.13. In addition, these results indicated that AEEPTS treated Si_3N_4 show higher Mechanical strength than AEPTS and APTS, respectively. Because AEEPTS has tri-amino groups (APTS mono amino and AEPTS di-amino), so more interactions between polyimide matrix and fillers were attained than other ones.

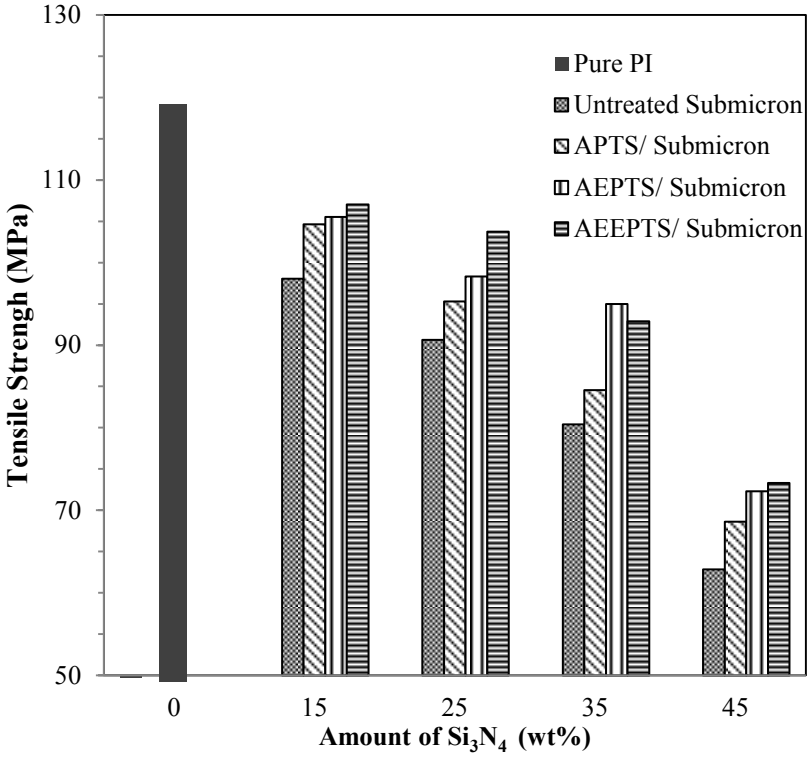

Figure 5.11 Tensile strengh of polyimide filled the silane treated Si_3N_4 fillers with different types of silane.

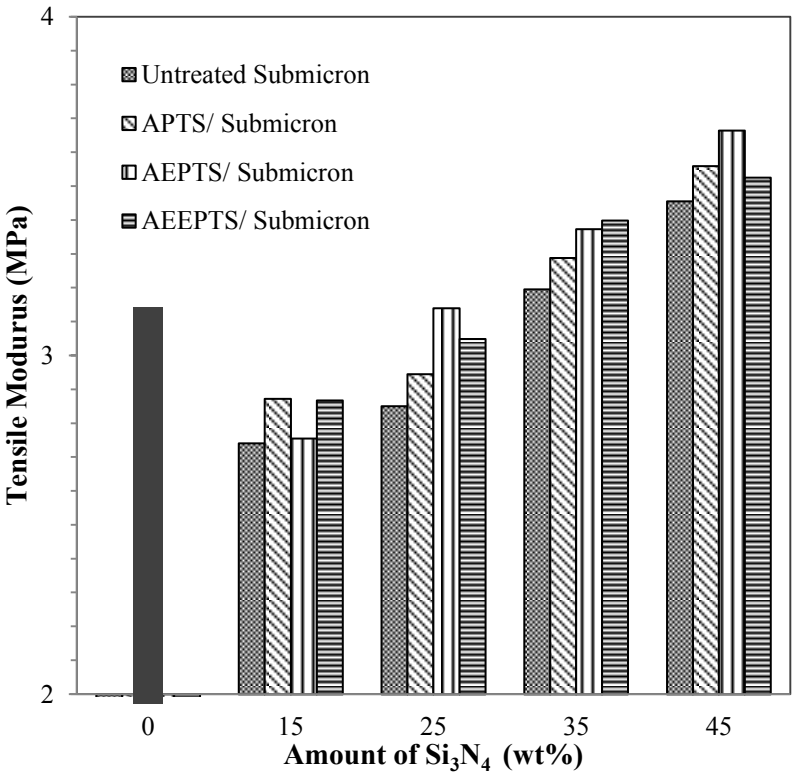

Figure 5.12 Tensile modulus of polyimide filled the silane treated Si_3N_4 fillers with different types of silane.

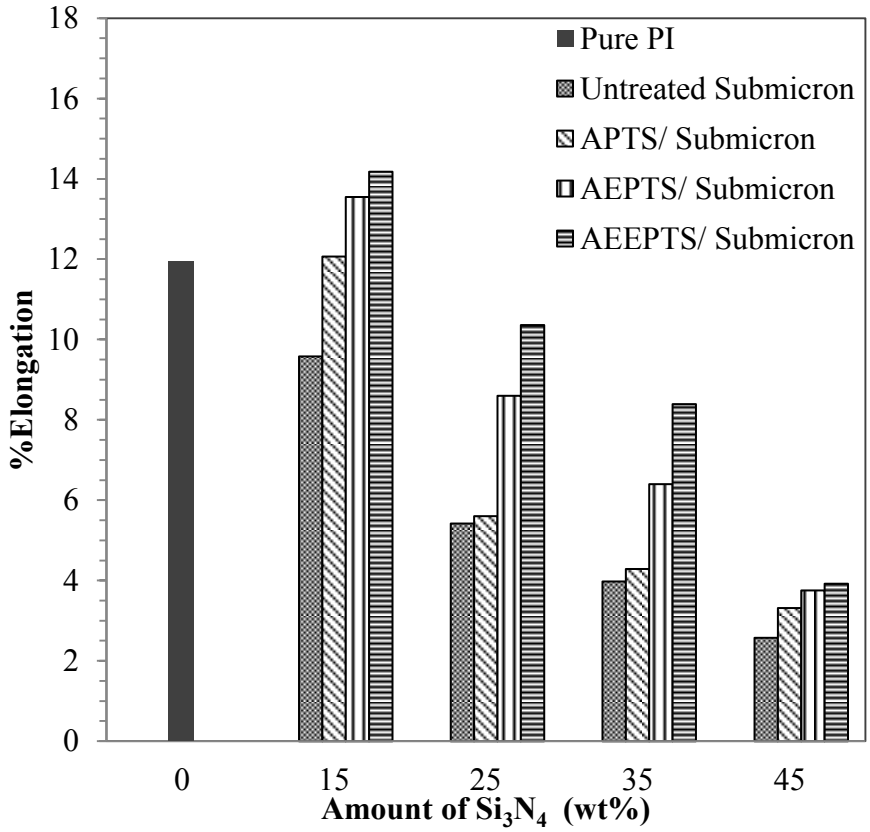

Figure 5.13 Elongation at break (%) of polyimide filled the silane treated Si_3N_4 fillers with different types of silane.

5.1.3.4 Thermal stabilities of Si_3N_4/PI composite films

The thermal stabilities of pure PI film, polyimide filled 45wt% submicron sized Si_3N_4 untreated and treated with APTS, AEPTS and AEEPTS were investigated by TGA analysis as shown in Figure 5.14. Thermal stabilities of all PI films filled with Si_3N_4 were higher than pure PI, this indicated that the incorporation of fillers into polyimide matrix improved the 5% weight loss (T_d5%) and Char yield of composite due to the inorganic fillers and silane coupling agent. The reasons for the improvement of the thermal stability were the introduction of the highly thermal stable Si_3N_4 into the polymide matrix [8, 37]. The other results agreed with these trends, observed by Li-Juan Fan [37] who investigated the preparation of nonwoven polyimide/silica hybrid nanofiberous fabrics by combining electrospinning and controlled in situ sol–gel techniques and this results agreed with the trends observed Steve Lien-Chung HsuEt al. [8] who investigated the enhanced in thermal conductivity of polyimide films via a Hybrid of Micro- and Nano-Sized boron nitride.

Moreover, more evidences supported to our investigation had found. The temperature for 5% weight loss (T_d5%) and Char yield were listed in Table 5.1. Thermal stabilities of PI filled Si_3N_4 treated with AEPTS and AEEPTS were almost similar, and both the 5% weight loss (T_d5%) and Char yield of AEPTS and AEEPTS samples were higher than APTS and untreated Si_3N_4, respectively. Because AEPTS and AEEPTS have larger number of molecules and amino groups than ATPS and untreated, the interaction between silane and filler is stonger in case of AEPTS or AEEPTS than ATPS and untreated samples, so the char yield were higher in case of AEPTS and AEEPTS. However, T_d5% of AEPTS and AEEPTS are in the same vicinity due to similar structure of silane regardless of the number of amine group.

In the case of char yield at 1000 ^oC of silane treated Si_3N_4/PI (all three types of silane), the higher char yields were observed than that one of untreated Si_3N_4, this indicated that the usage of silane improved the interaction between matrix and filler [37]. AEEPTS has longer structure and more amino groups than the other ones, then its Char yield was highest that it could affect the thermal contact resistance between matrix and filler. The interaction between matrix and filler with silane coupling were higher for AEEPTS, AEPTS, APTS and untreated respectively, as confirmed by char

yield at 1000°C and the Mechanical properties of the composite. However, when compare AEPTS and AEEPTS, AEEPTS has slightly higher char yield than AEPTS, because of the more amount of amine group. However, the contribution with amine cannot be completely active, so expected that some amine in AEEPTS is free from polyimide, so the char yield is quite near each other.

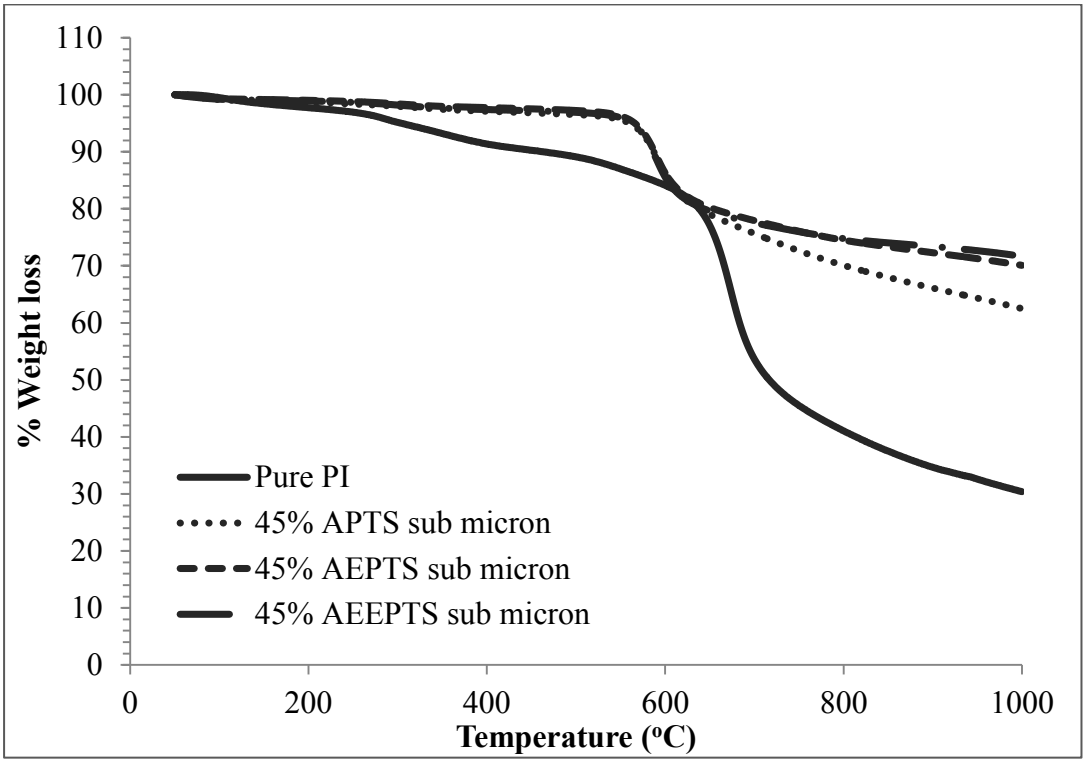

Figure 5.14 Thermogram of pure PI, PI composite films filled 45wt% APTS, AEPTS and AEEPTS treated submicron sized Si_3N_4 under N_2 atmosphere.

Table 5.1 Thermal stabilities of submicron sized Si_3N_4/PI with different types of silane coupling agents.

Material	T_d5% (C°)[a]	Char yield (%)[b]
Pure PI	303.5	30.39
45wt% of APTS treated Si_3N_4/PI	560	62.49
45wt% of AEPTS treated Si_3N_4/PI	565.83	70.08
45wt% of AEEPTS treated Si_3N_4/PI	563.17	71.65

[a] 5% Mass loss temperature under nitrogen
[b] Char yield at 1000 °C under nitrogen

5.1.3.5 Thermal conductivity of Si_3N_4/PI composite films

Thermal conductivity was calculated as shown in the following equation:

$$k = \alpha \rho C_p \qquad (5.1)$$

Thermal conductivity (k, W/mK) was the product of thermal diffusivity (α), specific heat capacity (C_p, J/gK) and bulk density (ρ, g/cm^3) of the samples.

Thermal diffusivity (α) was measured by laser flash method that the detail of the results can be shown in Appendix D (Table D.1) The results showed the increase in thermal diffusivity with increasing Si_3N_4 filler content and decrease with increasing temperature. When thermal diffusivity of composite films was increased, the thermal conductivity were also increased too.

Specific heat capacity (C_p) was measure by DSC (Differential Scanning Calorimeter) that illustrated in Appendix D (Table D.4). The results indicated the similar trend of all samples as the thermal diffusivity that the increase in specific heat capacity was observed when the Si_3N_4 filler content and temperature were increased.

The bulk density values of Si_3N_4/PI composite films increased with increasing the amount of fillers that were illustrated in Appendix D (Table D.4) because the higher density of Si_3N_4.

In Figure 5.15 shows thermal conductivity of submicron sized Si_3N_4 /PI composite films with different silane coupling agents. The results indicated that the thermal conductivity of composite films enhanced with increase in filler content. Because Si_3N_4 particles induced thermally conductive pathway in polymer matrix, conducted between adjacent fillers, therefore, thermal conductivity increased with increasing thermally conductive pathway, induced by Si_3N_4 particles.

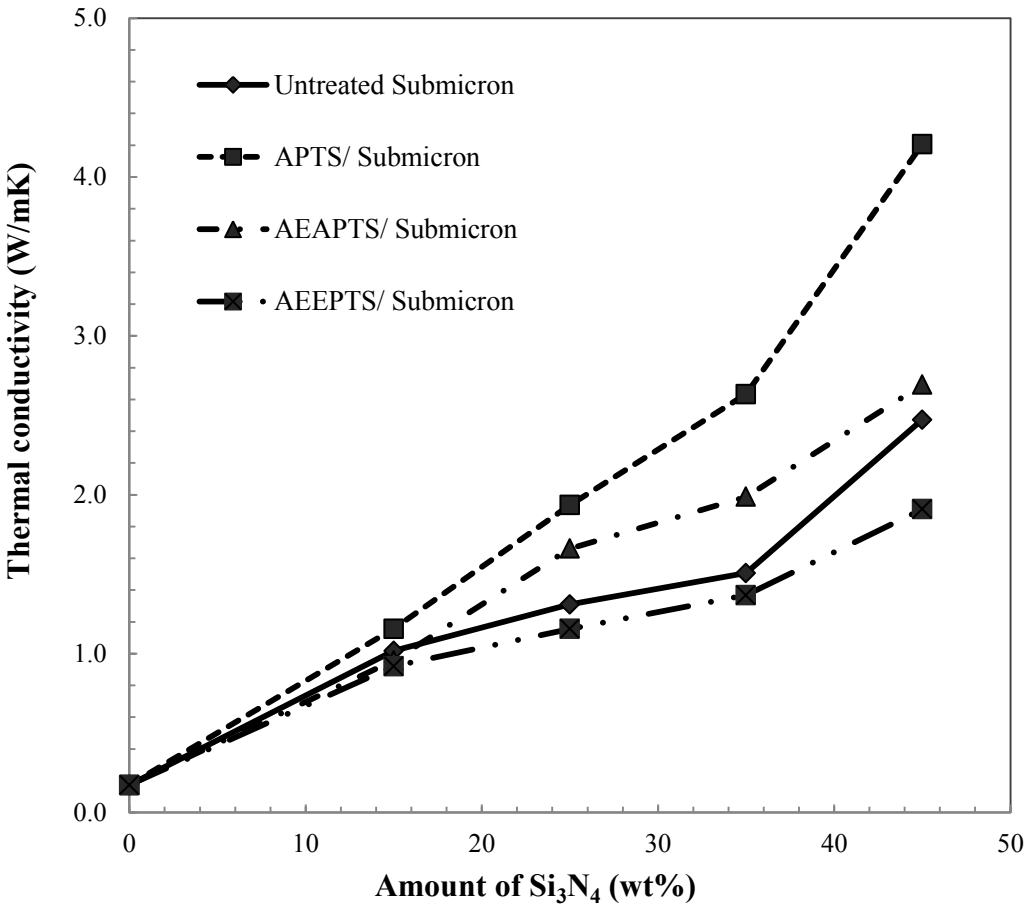

Figure 5.15 Thermal conductivity of submicron sized Si_3N_4 /PI composite films with different silane coupling agents.

In addition, to compare untreated and treated with three types of silanes, the results indicated that the PI filled Si_3N_4 treated with APTS shows higher thermal conductivity than that of AEPTS, untreated and AEEPTS, respectively. The silane surface treatment of the Si_3N_4 filler improved the interfacial bonding between filler and polymer matrix, so this improved the dispersion of filler and the interfacial thermal contact in matrix and finally enhanced the thermal conductivity. However, the increase of thermal resistance due to the interaction and coverage by silane and polyimide especially AEEPTS on particle of conductive Si_3N_4 created the adverse effects to thermal conductivity. The SEM observations, as in Figure 5.4-5.7, confirmed that the dispersion of APTS treated Si_3N_4 particles filled in matrix was better than others and untreated Si_3N_4 particles dispersion was the worst. This seemed to indicate that the best conductivity was the APTS treated composite and the worst

conductivity was the untreated Si_3N_4 composite. However, in the case of AEEPTS treated Si_3N_4/PI, the thermal conductivity was lowers than untreated Si_3N_4/PI because of the effects from resistance due to interaction and coverage of AEEPTS. Due to the longer structure and more amino groups of AEEPTS, the resistance and coverage were highest among all silane, this could act as the thermal insulate cover the surface of Si_3N_4 filler more than other silane and untreated composite, as confirm by thermal stabilities in Figure 5.14 and Table 5.1 and the mechanical properties of the AEEPTS composite. Moreover, the AEPTS seemed to give the best dispersion as SEM picture, but because of the more coverage and interaction between filler and polyimide molecules than APTS composite, the thermal conductivity of AEPTS composites were lower than APTS composites.

5.1.3.6 Dielectric properties of Si_3N_4/PI composite films

The dielectric constants can be calculated from the equation below:

$$k = \frac{Ct}{\varepsilon_0 A} \tag{5.2}$$

where C is the measured capacitance, t is the thickness of the sample, A is the area of the film and ε_0 is the permittivity of the free space (8.854×10^{-12} MKS unit).

Dielectric properties of Si_3N_4/PI composite films were investigated by LCR method and the results can be shown as in Figure 5.16 and 5.17. The dielectric constant of the pristine PI film was about 3.45 under ambient conditions. The dielectric constant of Si_3N_4/PI composite films depended on intrinsic dielectric constant of the polyimide matrix and Si_3N_4 fillers. The results showed the incorporation of Si_3N_4 filler enhanced dielectric constant and dielectric loss with increasing filler content. Compared the results of dielectric properties between PI with using untreated and PI with silane treated Si_3N_4 fillers that indicated dielectric constant and dielectric loss of untreated Si_3N_4 fillers were higher than silane treated Si_3N_4 fillers. PI composite film with using the Si_3N_4 fillers that treated with three types of silane have the nearly trends and nearly coincide.

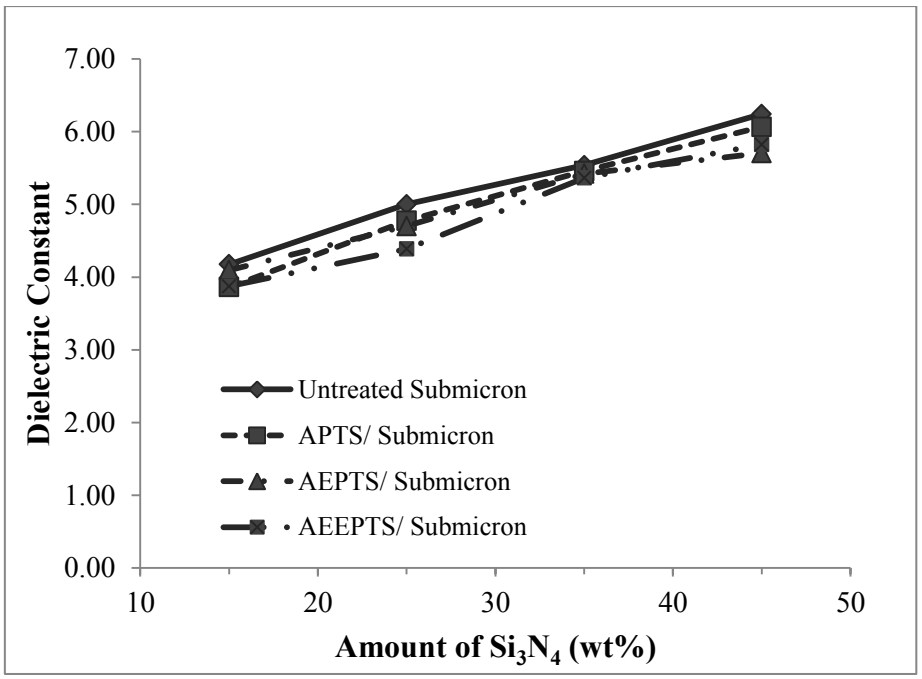

Figure 5.16 Dielectric constants of Si_3N_4/PI composite films

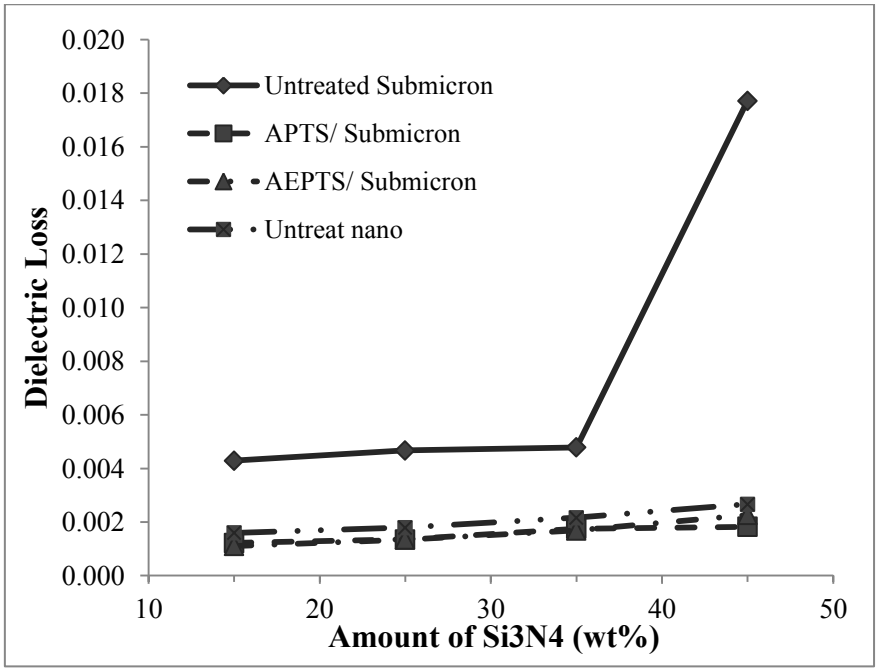

Figure 5.17 Dielectric Loss of Si_3N_4/PI composite films

5.2 Effect of particle sizes of Si_3N_4 particle on polyimide composite films properties

5.2.1 Morphology of APTS treated Si_3N_4 particles with different sizes of filler.

The morphology of APTS treated Si_3N_4 particles with different sizes of filler were characterized by using SEM method as shown in Figure 5.18. The average size of all treated particles was similar to that of the untreated particles, indicated that the surface treatments of particles did not induce a significant change in primary size of particle. However, surface treatments of particle could affect the dispersion state of particles.

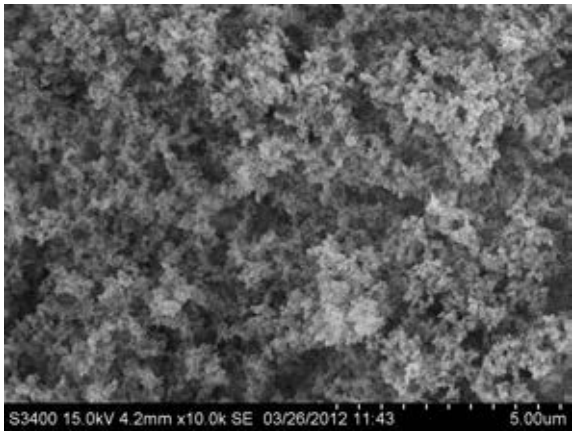

(a) APTS-nano sized Si_3N_4

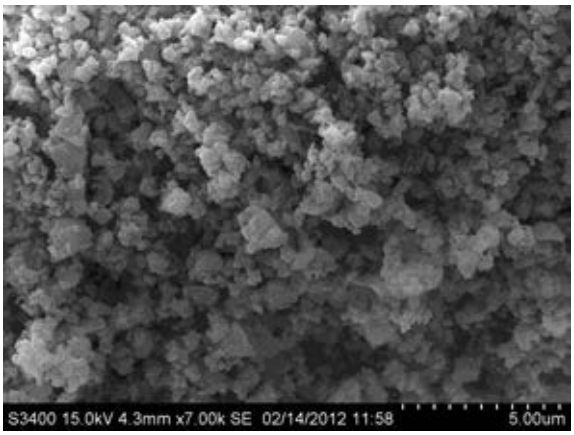

(b) APTS-submicron sized Si_3N_4

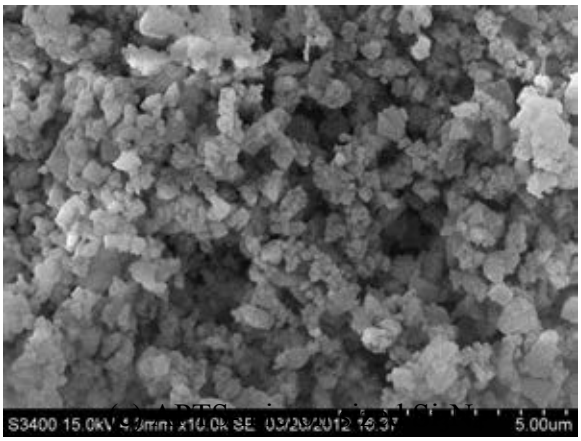

Figure 5.18 The morphology of APTS treated Si_3N_4 with different sizes of Si_3N_4 particles.

Figure 5.18 show the morphological characteristics of different size particles that have an important effect on the composite films properties. The relative number of particles, size and specific surface area as shown in these figure exhibited obviously that nanoparticles have much higher interfacial area than the larger particles. Thus, when the increase in interfacial area might significantly affect and could determine the composite films properties.

5.2.2 Characterization of Si_3N_4/PI composite films with different sizes of Si_3N_4 particles

The morphology of Si_3N_4/PI composite films with different sizes of Si_3N_4 particles were characterized by SEM observation. Three different sizes of Si_3N_4 particles were filled in PI matrix that those sizes are micron (as displayed in Figure 5.19-20), submicron (as displayed in Figure 5.7-5.10), and nano (as displayed in Figure 5.21-22).

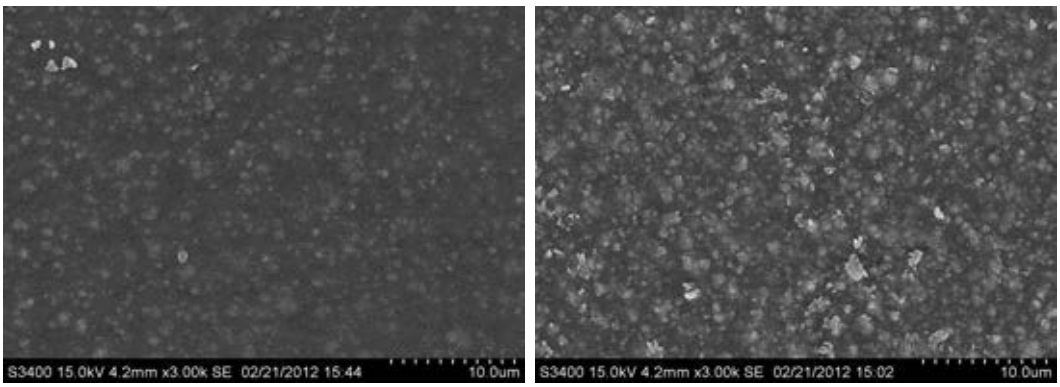

(a) 20wt% (b) 30wt%

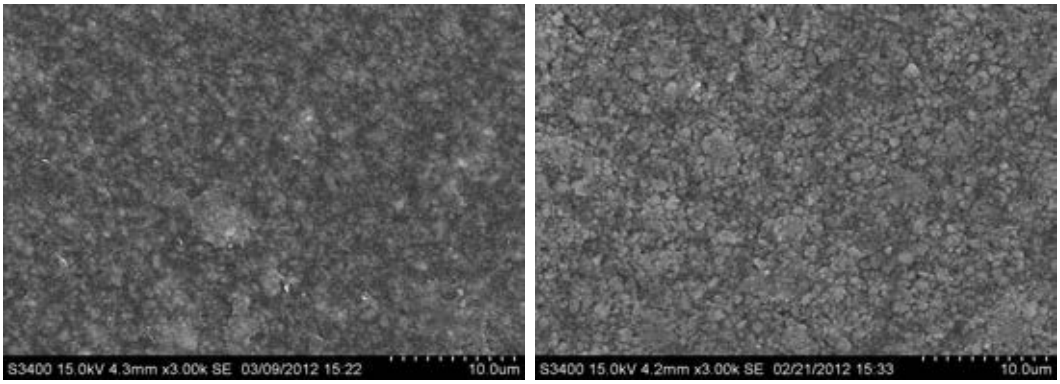

(c) 40 wt% (d) 50wt%

Figure 5.19 The morphology of untreated micron sized Si_3N_4/PI composite films with different Si_3N_4 content.

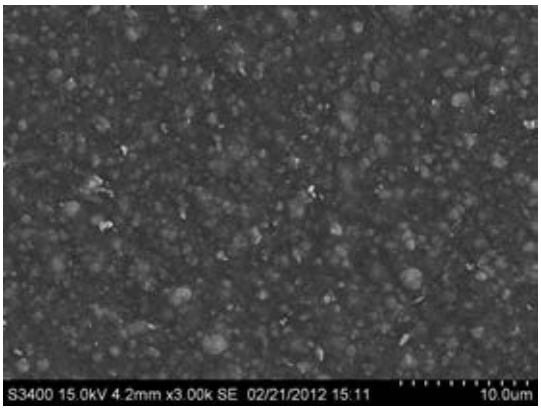

(a) 20wt%

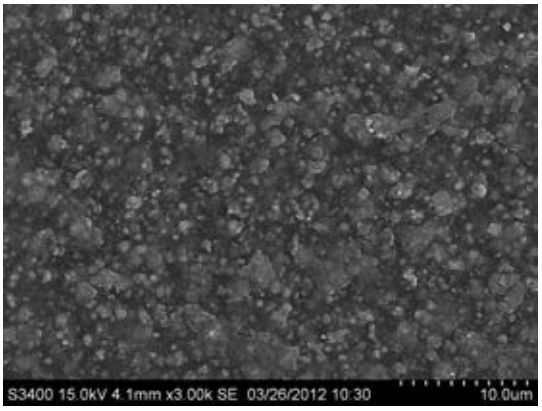

(b) 30wt%

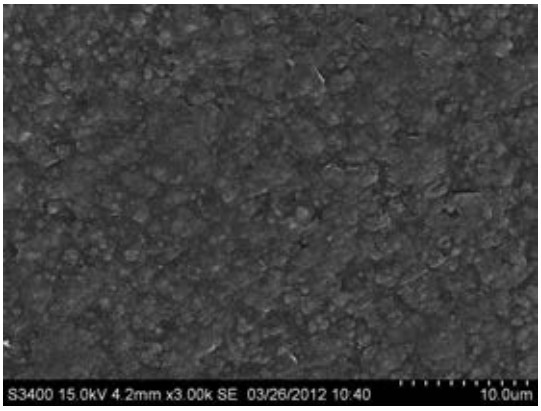

(c) 40 wt%

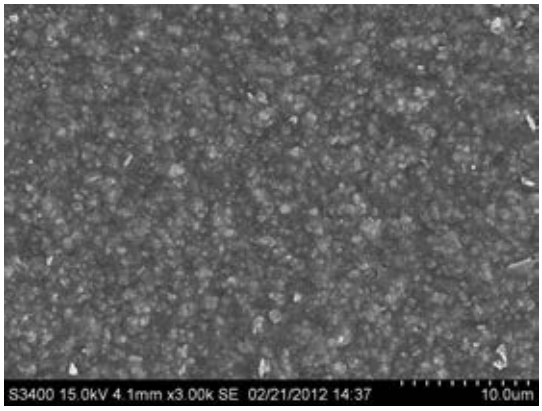

(d) 50wt%

Figure 5.20 The morphology of APTS treated micron sized Si_3N_4/PI composite films with different Si_3N_4 content

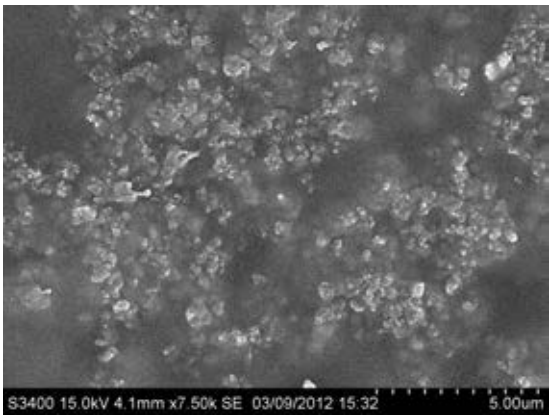

(a) 15 wt%

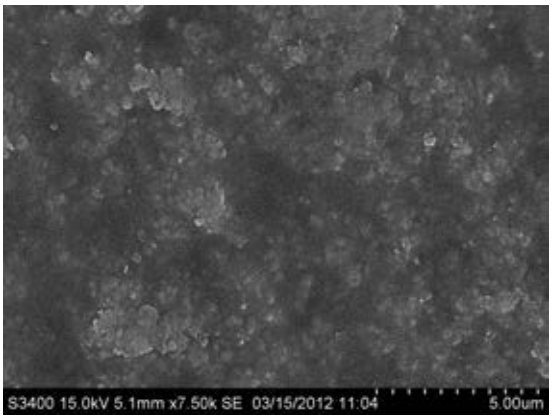

(b) 20wt%

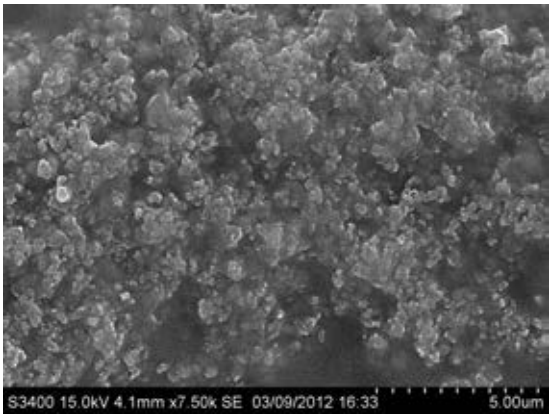

(c) 25 wt%

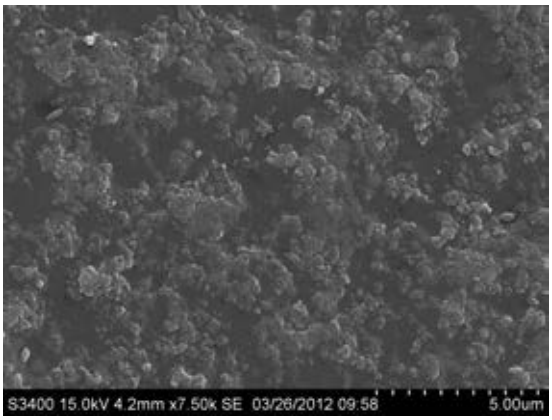

(d) 30 wt%

Figure 5.21 The morphology of untreated nano sized Si_3N_4/PI composite films with different Si_3N_4 content.

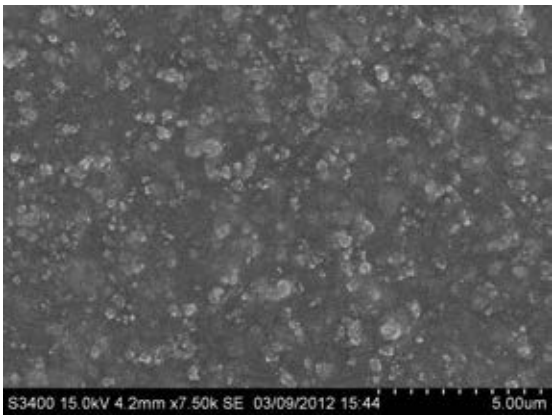

(a) 15 wt%

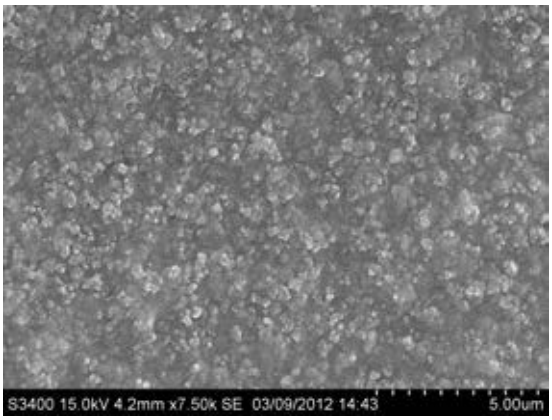

(b) 20 %wt

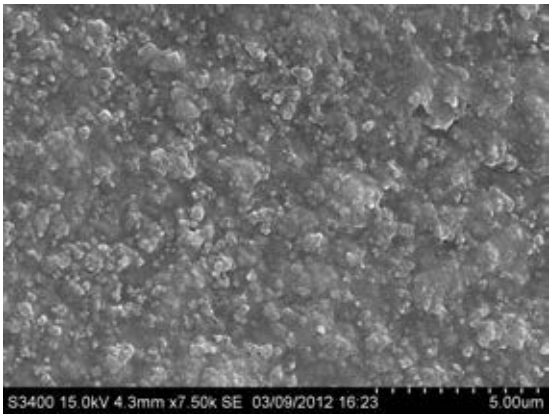

(c) 25 wt%

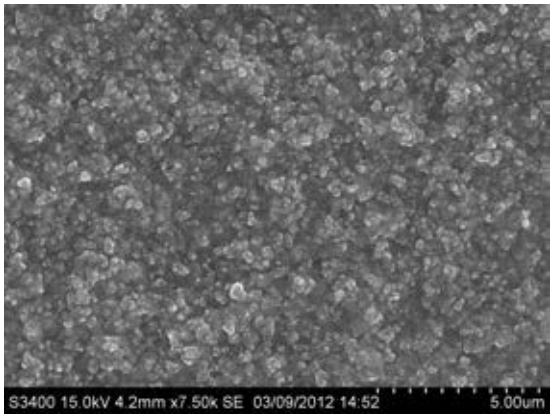

(d) 30 %wt

Figure 5.22 The morphology of APTS treated nano sized Si_3N_4/PI composite films with different Si_3N_4 content.

5.2.3 Mechanical properties of Si_3N_4/PI composite films with different sizes of Si_3N_4 fillers

Mechanical properties of Si_3N_4/PI composite films with different sizes of Si_3N_4 fillers were shown in Figure 5.23-25. The figures show the similar trend as in previous section, tensile strengh and Elongation at break decreased and Modulus increased when increasing Si_3N_4 filler with similar trend to all of the samples.

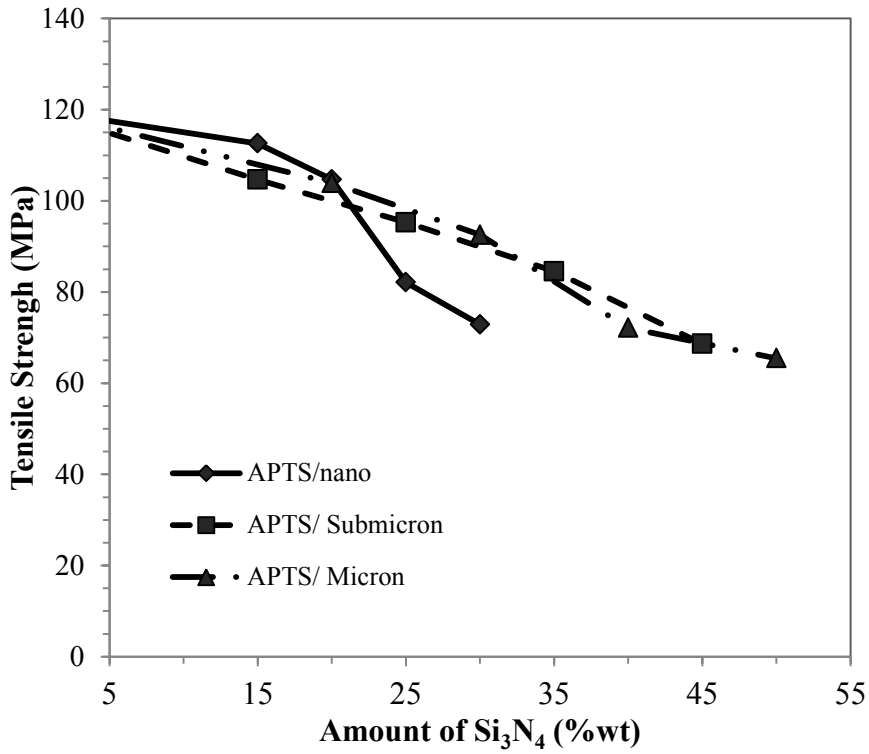

Figure 5.23 Tensile strength of polyimide filled the APTS treated Si_3N_4 fillers with different sizes of Si_3N_4 fillers at the various contents.

From mechanical strength data, it can be seen that Si_3N_4 particles had a significantly effect on the PI matrix because interfacial interaction between particles and the molecular chains (matrix) has an important effect on the mechanical properties of composite films. In comparison with the deferent particle size and different amount of Si_3N_4 is shown in Figure 5.23-5.25. These figures indicate nano sized Si_3N_4/PI composite films have the lower tensile strengh and Elongation at break

at high concentration than larger sizes due to the nanoparticles have higher surface area than the submicron and micron-sized particles. Moreover, obviously at low content of nano particles size, the tensile strength and the elongation was better than the larger size particle, because at low concentration, nano particle allowed polyimide to have more linkage between each other than the larger size particle, so reinforcement was higher at low concentration. However, the efficiency of reinforcement of nanoparticles was lower at high filler content obviously at 30wt% of Si_3N_4 due to the poor dispersion of particles in the composites film as confirmed by SEM figures.

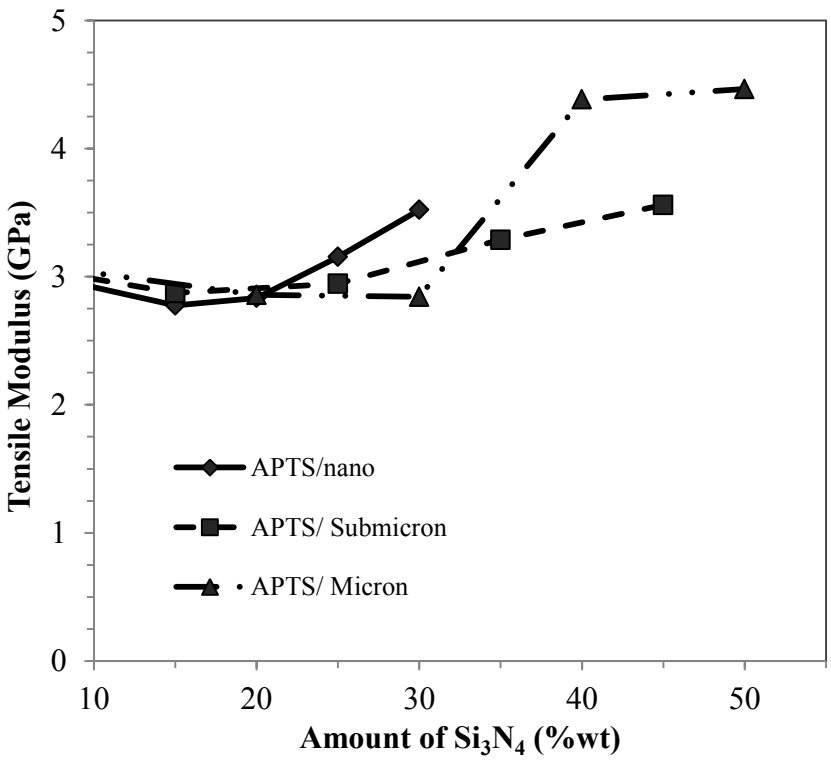

Figure 5.24 Tensile Modulus of polyimide filled the APTS treated Si_3N_4 fillers with different sizes of Si_3N_4 fillers at the various contents.

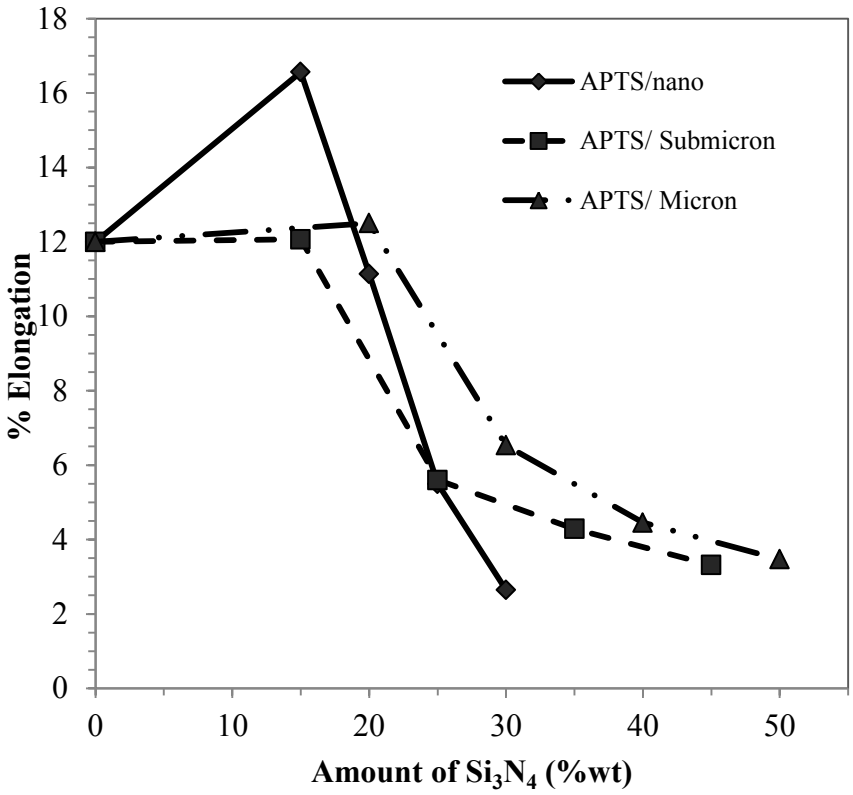

Figure 5.25 Elongation at break (%) of polyimide filled the APTS treated Si_3N_4 fillers with different sizes of Si_3N_4 fillers at the various contents.

5.2.4 Thermal stabilities of Si_3N_4/PI composite films

. The temperature for 5% weight loss (T_d5%) and Char yield were listed in Table 5.2. The decomposition temperature increased with the increasing of Si_3N_4 content incorporated into PI matrix because the integrated of Si_3N_4 fillers controled the movement of PI main chain and limited the segmental movements in PI matrix, so it reduced the decomposition rate. [29]

Table 5.2 Thermal stabilities of Si_3N_4/PI with different sizes Si_3N_4 fillers

Material	T_d5% (C^o)[a]	Char yield (%)[b]
30 wt% of untreated nano Si_3N_4/PI	515.17	62.5
30 wt% of APTS treated nano Si_3N_4/PI	528.5	62.85
50 wt% of untreated micron Si_3N_4/PI	571	72.58
50 wt% of APTS micron Si_3N_4/PI	573.5	72.63

[a] 5% Mass loss temperature under nitrogen
[b] Char yield at 1000 ^oC under nitrogen

5.2.5 Thermal conductivity of Si_3N_4/PI composite films

In Figure 5.26 show the thermal conductivity of Si_3N_4/PI composite films as a function of Si_3N_4 content with different particle size. By this figure, it can be seen that the thermal conductivity tended to increase with increasing of Si_3N_4 content for all samples. Compared different particle sizes, the results indicated that the composite filled with smaller Si_3N_4 particles showed higher thermal conductivity than the larger filler particles at the same filler content especially at higher concentration. Because of the smaller particles has higher interaction between particle and matrix and more path way of heat can create in smaller particle size. At the same particle content, the PI composite film fill 30%wt of nano sized Si_3N_4 show obviously higher thermal conductivity than other sizes. This is more than 2 times of micron size particle and about 2 times of submicron particle. The mainly reasons of that were the nano sized of Si_3N_4 particles affected higher interfacial contact area that act as thermally conductive network between particles. The other results agreed with these trends, observed by G. Xu. Et al. [11] who investigated the effect of Alumina size on thermal conductivity of

polyurethane composite. Moreover, more supported to our investigation had found from Zhou et al. [30] who also investigated the effect of Si_3N_4 size on thermal conductivity of polyethylene composite. These results can confirm the decrease in particle size resulted in the increase of number of filler particles at the same volume fraction. Therefore, the larger amount of numbers of filler particles were observed in the matrix by SEM.

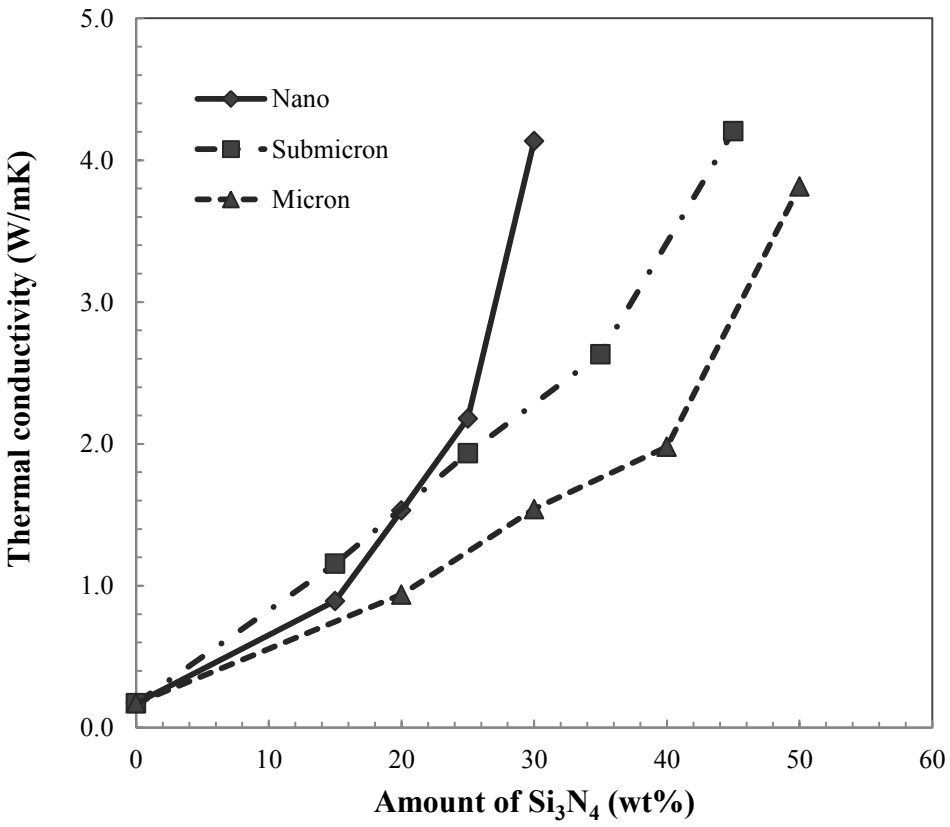

Figure 5.26 Thermal conductivity of Si_3N_4/PI composite films as a function of Si3N4 content with different particle size

5.2.6 Thermal conductivity model

In this research, three models were used to determine the thermal conductivity of Si_3N_4/PI composite films. Maxwel model, Effective medium theory (EMT model) were selected because their simplicity and Agari and Uno model was selected because the good fitting of the results found in previous literature. [31,34] The equations based on Maxwell, Effective medium theory (EMT model) and Agari and Uno model can be use for calculation of thermal conductivity based on properties of two components as shown below:

Maxwell model [31,32]

$$k_c = k_m \frac{k_f + 2k_m + 2V_f(k_f - k_m)}{k_f + 2k_m - V_f(k_f - k_m)} \tag{5.2}$$

EMT model [33]

$$V_m\left(\frac{k_{,m} - k_c}{k_{,m} + 2k_c}\right) + V_f\left(\frac{k_f - k_c}{k_f + 2k_c}\right) = 0 \tag{5.3}$$

Where k_c , k_m and k_f are the thermal conductivity of the composites, matrix and filler particles, respectively. V_f and V_m is the volume fraction of matrix and filler particles, respectively.

Agari and Uno model [32,34]

$$\log kc = V_f C_2 \log k_f + (1 - V_f)\log(C_1 k_m)$$

$$= (C_2 \log k_f - \log(C_1 k_m))V_f + \log(C_1 k_m) \tag{5.4}$$

According to the Agari and Uno model as shown in equation 5.4, The value of C_1 and C_2 were determined by plot $\log k_c$ vesus V_f that obtain from experimental data as plotted in Appendix B (Figure B.1) obtain C_1 and C_2, slope is [C_2.log k_f - log

($C_1.k_m$)] and interception is log (C_1 km). The values of C_1 and C_2 were shown in Appendix B (Table B.2).

The comparison of the experimental data and selected theoretical model to predict the thermal conductivity values can be shown in Figure 5.27. From the results, thermal conductivity of composite films is plotted compare with the volume fraction of Si_3N_4 filler. The thermal conductivity, determined from the values of Maxwell and EMT models, cannot give the good prediction because these models were only unsuitable to determine the effect of interfacial thermal barrier resistance and interaction of the Si_3N_4 fillers. In addition, Maxwell model was suitable to determine the effective thermal conductivity of composites that in the case of well dispersed particle. The thermal conductivity of Agari and Uno model was the nearest to the real experimental data even better than other models due to this model was determined by the C_1 and C_2 constants that calculated firstly from experimental data. C_1 indicated the filler effects resulted on the secondary structure of the polymer matrix and C_2 is a factor corresponding to easy forming the conductive chains of the fillers.

Therefore Agari and Uno model could predict the thermal conductivity better than any other theoretical models. Moreover, all of the results showed that Maxwell and EMT Modle could not predict the thermal conductivity of PI composite films.

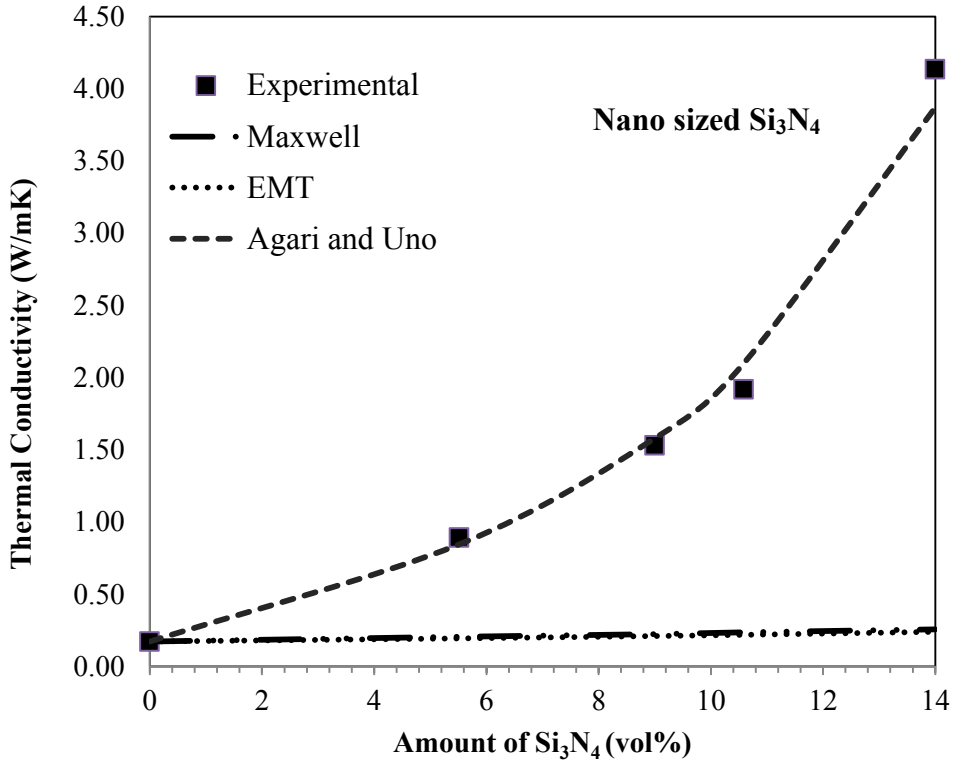

(a) Nano sized Si_3N_4

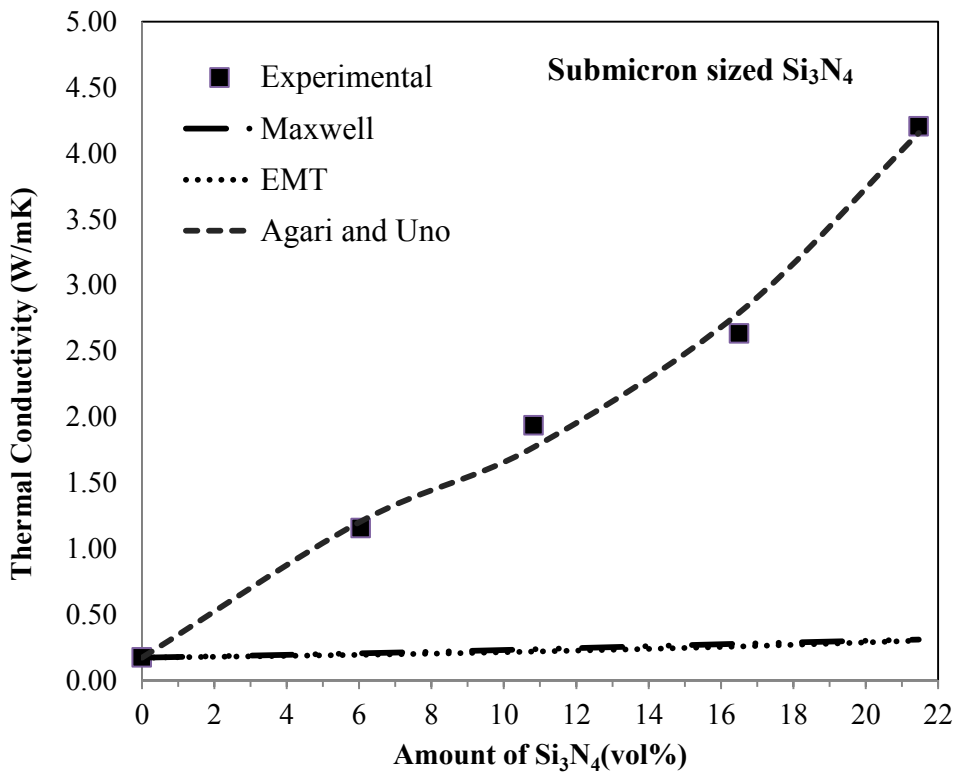

(b) Sub micron sized Si_3N_4

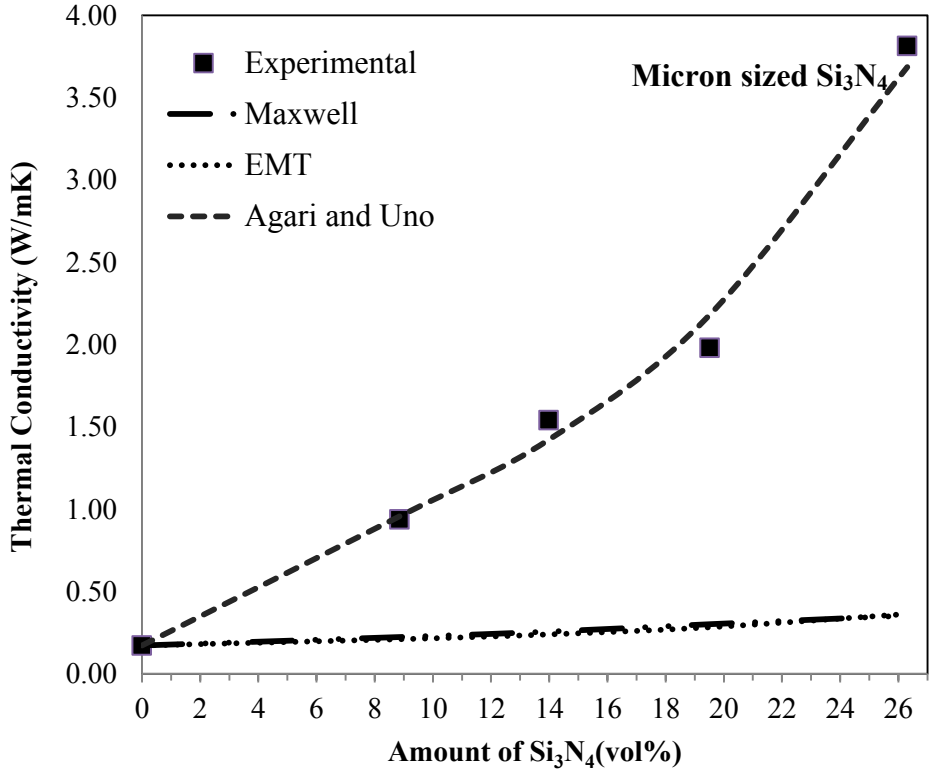

(c) Micron sized Si_3N_4

Figure 5.27 Comparison between the experimental data and theoretical models

5.2.7 Hybridization of different Si_3N_4 particle sizes/PI composite films

In this study, PI composite films were incorporated with different proportions of a maximum packing weight ratio (as shown in Table 5.3) of submicron sized with nanosized and micron sized with submicron sized Si_3N_4 particles. The morphology of APTS treated Si_3N_4 /PI composite films with hybrid different sized of Si_3N_4 particles as shown in Appendix F (Figure F.2).

Table 5.3 The maximum weight ratio of submicron sized with nanosized and micron sized with submicron sized Si_3N_4 particles. [25]

Samples	Diameter (μm)		$R=D_1/D_2$	Equilibrium Close Packing	wt%	w (g)	
	Big (D_1)	Small (D_2)				Big	Small
Micron/submicron	3.736	1.182	3.16	0.7900	50	0.593	0.158
Submicron/nano	1.182	0.025	47	0.7353	45	0.451	0.162

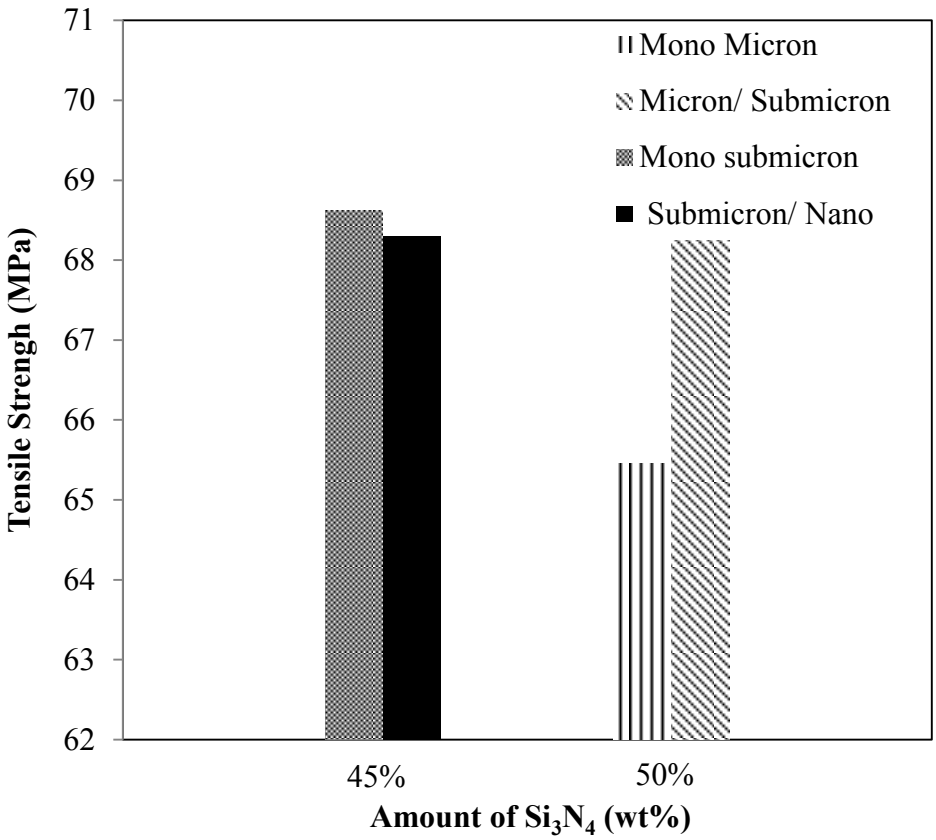

Figure 5.28 Tensile strength of APTS treated Si_3N_4 /PI composite films with hybrid different sized of Si_3N_4 particles.

Figure 5.28 showed the tensile strength of APTS treated Si_3N_4 /PI composite films with hybrid different sized compared with mono sized of Si_3N_4 particles. The tensile strengh values of 45wt% submicron/nano and 45w%t submicron mono-sized Si_3N_4/PI composite films exhibited similar strength. However, the case of 50% micron/submicron, the tensile strength of the composite was fair higher than 50% micron mono-sized Si_3N_4 /PI composite films. (%Elongation and tensile modulus as shown in Appendix E)

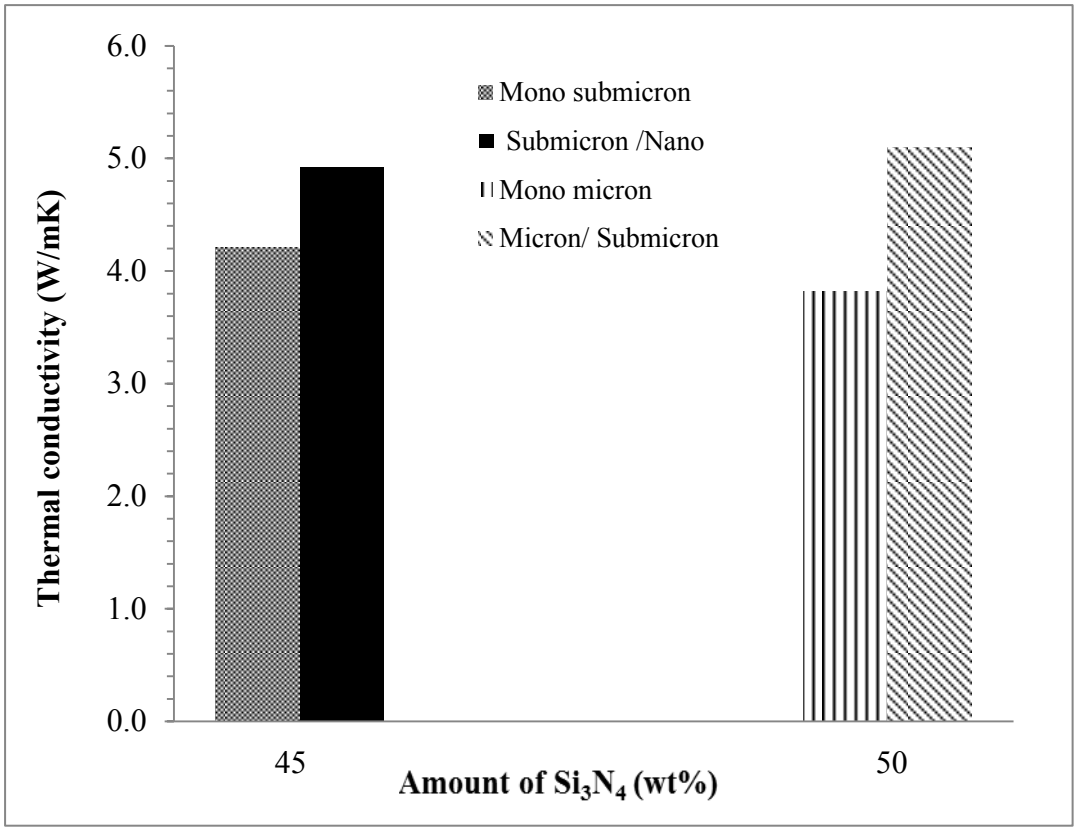

Figure 5.29 Thermal conductivity of PI/hybrid Si_3N_4 composite films with different Si_3N_4 particle sizes.

Figure 5.29 showed the results of thermal conductivity of 45%wt submicron mono-sized Si_3N_4/PI compared with 45%wt submicron/nano sized Si_3N_4/PI (weight ratio approximately 3:1) and 50%wt micron mono-sized Si_3N_4/PI compared with 50%wt submicron/nano sized Si_3N_4/PI (weight ratio approximately 3:1). Both results of PI filled with hybrid Si_3N_4 could give higher thermal conductivity than mono sizes particles due to the better packing density of the mixture by different Si_3N_4 particle sizes. This result could be explained as a better random conductive brigde or network formed by the hybrid of submicron-nano and micron-submicron Si_3N_4 particles. This results agreed with the trends observed Steve Lien-Chung HsuEt al. [8] who investigated the enhanced in thermal conductivity of polyimide films via a Hybrid of Micro- and Nano-Sized boron nitride. The higher in both thermal conductivity and tensile strength could be achieved in hybrid particle size composite and suitable for the application in microelectronics.

CHAPTER VI

CONCLUSIONS AND RECOMMENDATIONS

6.1 Conclusions

In this research, the preparation of polyimide/silicon nitride composite films was investigated in order to improve the thermal conductivity of polyimide composite films. Polyimide was prepared via two-step polymerization method of equimolar of 4,4'-oxydianiline (ODA) and pyromellitic dianhydride (PMDA). Three different sizes Si_3N_4 (nano, submicron and micron size) were used as ceramic filler and submicron Si_3N_4 were surface modified with three kinds of silane coupling agent. PI/ Si_3N_4 composite films were characterized for morphology, thermal and mechanical properties to verify the improvement in properties. The research conclusions can be summarized as follows;

6.1.1 Effect of surface modification of Si_3N_4 particle on polyimide composite films properties

Three types of silane (APTS, AEPTS and AEEPTS) were used for improvement of dispersion of Si_3N_4 fillers in polyimide matrix as confirms by SEM observations. The Si_3N_4 fillers were incorporated into polyimide matrix that could improve the thermal conductivity to about 24% more than Pure PI. The results indicated that PI composite film with using APTS treated submicron sized Si_3N_4 showed the higher thermal conductivity than that of AEPTS, untreated and AEEPTS respectively. Moreover, as confirmed by mechanical properties, the PI filled with modified Si_3N_4 fillers using each silane types were better mechanical properties than that of untreated Si_3N_4 fillers.

6.1.2 Effect of particle sizes of Si_3N_4 particle on polyimide composite films properties

Three different sizes Si_3N_4 (nano, submicron and micron size) treat APTS and untreated particles were used as ceramic fillers. The dispersion and morphology of Si_3N_4/PI composite films with different sizes of Si_3N_4 particles were confirmed by

SEM observation. Mechanical properties of PI composite films with different particle sizes show decrease in tensile strengh and Elongation at break and increase in Modulus when increasing Si_3N_4 filler with the similar trend to all of the samples. The nano sized Si_3N_4 showed obviously higher thermal conductivity than other sizes that were more than two times of micron sized particle and about two times of submicron sized particle. Nano size particles could improve properties of polyimide composite films better than larger size Si_3N_4 fillers, significant at low Si_3N_4 content. Therefore Agari and Uno model could well predict the thermal conductivity better than any other theoretical models. In addition, the incorporation of hybrid micron-submicron and submicron-nano sized Si_3N_4 into polyimide matrix at maximum packing density could give thermal conductivity higher than mono sizes of Si_3N_4 fillers at the same weight ratio of Si_3N_4 in polyimide. Due to high dielectric constant of Si_3N_4, the application of Si_3N_4 in dielectric material needs some precaution. However, the benefit of thermal conductivity should be balanced with the dielectric constant. The maximum thermal conductivity attained is 4.135 W/mK at nano particle size 30%w without significantly losing mechanical properties.

6.2 Recommendations

1. The optimum loading level of silane by varied the percent of silane cooperated should be determined to optimize the properties of composites.

2. Back titration should be performed to identify the amino group of silane on the Si_3N_4 surface.

REFERENCES

[1] Nilakshi, V. S.; Mahadeo, R. H.; alhalli, C.V. A.; and Prakash, P. W. Synthesis and characterization of new polyimides containing pendent pentadecyl chains. European Polymer Journal 45(2009): 582–589.

[2] Daisuke, Y.; and Shinji, A. Enhanced thermal diffusivity by vertical double percolation structures in polyimide blend films containing silver nano particles. Macromolecules 211(2010): 2118–2124.

[3] Jiajun, W.; and Xiao, S. Y. Preparation and the properties of PMR-type polyimide composites with aluminum nitride. Journal of Applied Polymer Science 9(2003): 3913–3917

[4] Yunsheng, X.; Chung, D. D. L.; and Cathleen, M. Thermally conducting aluminum nitride polymer-matrix composites, Composite: Part A 32(2001): 1749-1757.

[5] Shoichi, K.; Ikuko, Y.; and Koji, W., High-thermal-conductivity AlN filler for polymer/ceramics composites. The American Ceramic Society 92(2009): S153–S156.

[6] Shu, H. X.; Bao, K. Z.; Ju, B. L.; Xiu, Z. W.; and Zhi, K. X., Preparation and properties of polyimide/aluminum nitride composites. Polymer Testing 23(2004): 797–801.

[7] Hong, H.; Renli, F.; Yuan, S.; Yanchun, H.; and Xiufeng, S. Preparation and properties of Si_3N_4/PS composites used for electronic packaging. Composites Science and Technology 67(2007): 2493–2499.

[8] Tung, L. L.; and Steve, L. C. H., Enhanced thermal conductivity of polyimide films via a hybrid of micro- and nano-sized boron nitride. The Journal of Physical Chemistry B 114(2010): 6825-6829.

[9] Hatsuo, I.; and Sarawut, R. Very high thermal conductivity obtained by boron nitride-filled polybenzoxazine. Thermochimica Acta 320 (1998): 177-186.

[10] Geon, W. L.; Min, P.; Junkyung, K.; Jae, I. L.; and Ho, G. Y.Enhanced thermal conductivity of polymer composites filled with hybrid filler, Composites 37(2006): 727–734.

[11] LU, X.; and XU, G. Thermally conductive polymer composites for electronic packaging. Journal of Applied Polymer Science 65(1997): 2733–2738.

[12] Qing, Y. T. A.; Jie, C. A.; Chan, Y.C.A.; and Chung Y. Effect of carbon nanotubes and their dispersion on thermal curing of polyimide precursors Polymer Degradation and Stability 95(2010): 1672-1678

[13] Mantana, S. The effects of size and surface modification of siliconnitride on mechanical and thermal properties of epoxy composites, Mafter 's thesis, Chemical Engineering, Faculty of Engineering, Chulalongkorn University, 2010.

[14] Tamaki, R.; Tanaka, Y.; Asuncion, M.Z.; Choi, J.; and Laine, R.M. Octa(aminophenyl)silsesquioxane as a nanoconstruction site. Journal of The American Chemical Society 123(2001): 12416-7.

[15] Wikipedia [Online].2010. Available from: http://en.wikipedia.org/wiki/ polyimide [20, May 2011]

[16] Takekoshi, T. ; Ghosh, E. M.K. ;and Mittal, K.L. Polyimides- Fundamentals and Applications, Marcel Dekker, New York, 1996, Chapter 2.

[17] Debra, L. D. Synthesis and characterization of thermosetting polyimide oligomer for microelectronics packaging, Doctor's thesis, chemistry, faculty of the Virginia Polytechnic Institute, State University, (2000): 1-12

[18] He, H.; Fu, R.; Han, Y.; Shen, Y.; and Wang, *D.* High thermal conductive Si_3N_4 particle filled epoxy composites with a novel structure. Journal of Electronic Packaging 129(2007): 469-472.

[19] Dobkin, D. M. Silicon nitride: Properties and applications [Online]. (n.p.). 2009. Availablefrom:http://www.enigmaticconsulting.com/semi conductor_processing/CVD_Fundamentals/films/SiN_properties.html

[20] Power Chemical Corporation Ltd. Silane coupling agent [Online].2009 Available from :http://www.pcc.asia/library/public/Silane% 20Coupling% 20Agents.htm [26, Febuary 2012]

[21] Smits, V.; Chevalier, P.; Deheunynck, D.; and Miller, S. A new filler dispersion technology. Reinforced plastics 52(2008): 37-43.

[22] Shefali, G. S. Chemistry and applications. The Journal of Indian Prosthodontic Society 6(2006): 14-18.

[23] Lee, W. S.; Han, I. Y.; Yu, J.; Kim, S. J.; and Byun, *K. Y.* Thermal characterization of thermally conductive underfill for a flip-chip package using novel temperature sensing technique, Thermochimica Acta 455(2007): 148-155.

[24] Maity, P.; Kasisomayajula, S. V.; Parameswaran, V.; Basu, S.; and Gupta, N. Improvement in surface degradation properties of polymer composites due to pre-processed nanometric alumina fillers. IEEE Transactions on Dielectrics and Electrical Insulation 15(2008): 63-72.

[25] Robert, S. F.; and Robert, D. G. Close packing density of polydisperse hard. The journal of chemicalphysics 131(2009):244104-2-7

[26] Gelest, I. Applying a silane coupling agent [Online]. (n.p.). 2010. Available from: http://www.gelest.com/Library/09Apply.pdf [12, May 2011]

[27] Jana, R.N.; and Bhunia, H. Thermal stability and proton conductivity of silane based nanostructured composite membranes. Solid State Ionics 178(2008): 1872-1878.

[28] Morishita, S.; Sugahara, S.; and Matsumura, M. Atomic-layer chemical-vapor-deposition of silicon-nitride. Applied Surface Science 112 (1997): 198-204.

[29] Raman, C.; and Meneghetti, P. Boron nitride finds new applications in thermoplastic compounds. Plastics, Additives and Compounding 10: 26-29, 31.

[30] Zhou, W.; Wang, C.; Ai, T.; Wu, K.; Zhao, F.; and Gu, H. A novel fiber-reinforced polyethylene composite with added silicon nitride particles for enhanced thermal conductivity. Composites Part A: Applied Science and Manufacturing 40 (2009): 830-836.

[31] Woong, S.L.; Jin Y. Comparative study of thermally conductive fillers in underfill for the electronic components. Diamond and related material 14 : (2005) 1647 – 1653

[32] Shi, G.; Zhang, M. Q.; Rong, M. Z.; Wetzel, B.; and Friedrich, K. Friction and

wear of low nanometer Si3N4 filled epoxy composites. Wear 254 (2003): 784-796.

[33] He, H.; Fu, R. L.; Han, Y. H.; Shen, Y.; and Song, X. F. Thermal conductivity of ceramic particle filled polymer composites and theoretical predictions. Journal of Materials Science 42 (2007): 6749-6754

[34] Qunli, A.; Shuhua, Q.; Wenying, Z.; Thermal, electrical, and mechanical properties of Si_3N_4 filled LLDPE composite. Polymer Composite (2009): 866-871

[35] Tessler, N.; Medveder, V.; Kazes, M.; Kan, S.; and Banin U. Efficient Near-Infrared Polymer Nanocrystal Light-Emitting Diodes, Science 295(2002): 1506-1508.

[36] Choi, J.; Yee, A. F.; and Laine, R. M. Organic/inorganic hybrid composites from cubic silsesquioxanes. Epoxy resins of octa(dimethylsiloxyethyl-cyclohexylepoxide) silsesquioxane. Macromolecules 36 (2003):

5666-5682.

[37] Si, C. A.; Dezhi, S. A.; Xinsheng, Z. C.; Xingguang, T. A.; Dongying, Z. A.; Li, and J. F. Preparation of nonwoven polyimide/silica hybrid nanofiberous fabrics by combining electrospinning and controlled in situ sol–gel techniques. European Polymer Journal 45 (2009): 2767–2778.

APPENDICES

APPENDIX A

Calculation of polyimide/Si_3N_4 composite films preparation

The composition of Si_3N_4 particle preparation is illustrated in Table A.1 and Table A.2 examples of calculations are shown as follows.

Table A.1 Composition of Si_3N_4

Size	Amount of Si_3N_4 (wt%)	Amount of Si_3N_4 (vol%)	Mass of Si_3N_4 (g)
Nano	15 wt%	6	0.1324
	20 wt%	9	0.1875
	25 wt%	11	0.2500
	30 wt%	14	0.3214
Submicron	15 wt%	6	0.1324
	25 wt%	11	0.2500
	35 wt%	17	0.4038
	45 wt%	21	0.6136
Micron	20 wt%	9	0.1875
	30 wt%	14	0.3214
	40 wt%	20	0.5000
	50 wt%	26	0.7500
Micron/ Submicron	48 wt%(2.779:1)	25	0.6923
	50 wt%(2.778:1)	26	0.7500
Submicron /Nano	43 wt%(2.779:1)	20	0.5658
	45 wt%(2.778:1)	21	0.6136

APPENDIX B

Determination of thermal conductivity model

The comparison between experiment and theoretical thermal conductivity are shown in Table B.1.

Table B.1 The data of experimental and theoretical thermal conductivity of APTS treated Si_3N_4/polyimide composite films.

Samples	Amount of Si_3N_4		Experimental	Theoretical model		
	(wt%)	(vol%)		Maxwell	EMT	Agari and Uno
Pure PI	-	-	0.1728	0.1728	0.1728	0.1728
Nano	15 wt%	6	0.8932	0.2058	0.1942	0.8459
	20 wt%	9	1.5305	0.2239	0.2107	1.5793
	25 wt%	11	1.9191	0.2366	0.2191	2.0995
	30 wt%	14	4.1346	0.2569	0.2398	3.8692
Submicron	15 wt%	6	1.1560	0.2058	0.1942	1.2066
	25 wt%	11	1.9352	0.2366	0.2191	1.7698
	35 wt%	17	2.6329	0.2785	0.2577	2.7910
	45 wt%	21	4.2055	0.3100	0.3024	4.1554
Micron	20 wt%	9	0.9382	0.2239	0.2107	0.9569
	30 wt%	14	1.5406	0.2567	0.2398	1.4217
	40 wt%	20	1.9804	0.3018	0.2831	2.1798
	50 wt%	26	3.8144	0.3541	0.3640	3.6850

The thermal conductivity model of calculation for each selected model was illustrated as following:

For our example, thermal conductivity of Si_3N_4 filler (k_f) and thermal conductivity of polyimide matrix (k_m) are 150 and 0.1728 W/mK, respectively and the volume fraction (V_f) of Si_3N_4 is 0.06.

Maxwell model

Maxwell equation was shown as below:

$$k_c = k_m \quad \frac{k_f + 2k_m + 2V_f(k_f - k_m)}{k_f + 2k_m - V_f(k_f - k_m)} \qquad \text{(C.1)}$$

When the value of kf and km were substituted in equation, then kc is obtained as following:

$$k_c = 0.1728 \quad \frac{150 + 2(0.1728) + 2(0.06)(150 - 0.1728)}{150 + 2(0.1728) - (0.06)(150 - 0.1728)}$$

$$k_c = 0.2058 \text{ W/mK}$$

EMT model

EMT equation was shown as below:

$$V_m\left(\frac{k_{,m} - k_c}{k_{,m} + 2k_c}\right) + V_f\left(\frac{k_f - k_c}{k_f + 2k_c}\right) = 0 \qquad \text{(C.2)}$$

This equation can be rearrangement into equation C.3 as following

$$k_c = 2(V_f - V_m)k_c^2 + (2V_m k_m - k_f + 2V_f k_f - V_f k_m)k_c + k_m k_f \qquad \text{(C.3)}$$

When the values of k_f and k_m were substituted in equation, then k_c is obtained as following:

$k_c = 2(0.06–0.94)k_c^2 + (2(0.94)(0.1728) – 150 + 2((0.06)(150) - (0.06)(0.1728)))k_c$ $+(0.1728)(150)$

$$k_c = 0.1942 \text{ W/mK}$$

Agari and Uno model

Agari and Uno was shown as below:

$$\log kc = V_f C_2 \log k_f + (1 - V_f)\log(C_1 k_m)$$

$$= (C_2 \log k_f - \log(C_1 k_m))V_f + \log(C_1 k_m) \qquad (C.4)$$

According to the Agari and Uno model as shown in equation C.4, The value of C_1 and C_2 were determined by plot $\log k_c$ vesus V_f that obtain from experimental data as plotted in Figure C.1 obtain C_1 and C_2, slope is [C_2.log k_f - log (C_1.k_m)] and interception is log (C_1 km). The values of C_1 and C_2 were shown in Table C.2.

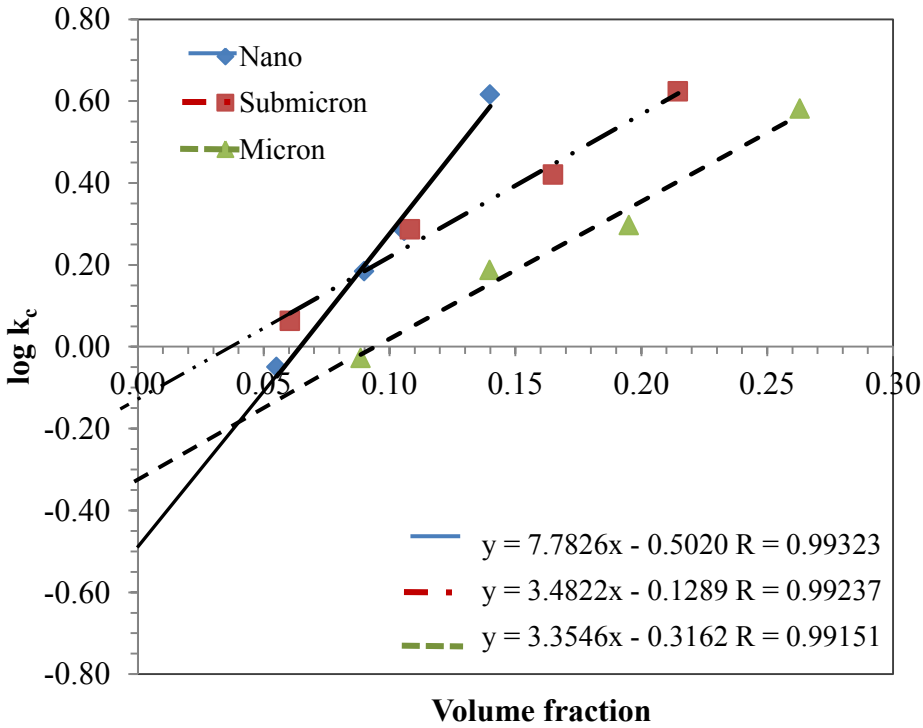

Figure B-1 Logarithm of thermal conductivity of APTS treated Si_3N_4/polyimide composite films linear fitted by Agari and Uno model

Table B.2 The values of C1 and C2 by Agari and Uno model

Systems	[C_2.logk_f - log (C_1.k_m)]	log(C_1.k_m)	C_1	C_2
Nano	7.783	-0.5020	1.8216	0.2307
Submicron	3.482	-0.1289	4.3009	0.0592
Micron	3.355	-0.3162	2.7942	0.1453

The comparison between experiment and theoretical thermal conductivity are shown in Table B.1.

APPENDIX C

Determination of thermal conductivity

Thermal conductivity was calculated as following equation:

$$k = \alpha \rho C_p$$

where k is the thermal conductivity (W/m K), α is the thermal diffusivity (mm^2/s), ρ is the bulk density (g/cm^3) and C_p is the specific heat capacity (J/g ˚C). The data of these parameters was listed in Table D.1-D.9

Table C.1 Thermal diffusivity of submicron sized Si_3N_4/PI composite films.

Samples	Amount of Si3N4 (wt%)	Temperature (°C)					
		25	50	75	100	125	150
Pure PI	-	0.356	0.565	0.691	3.157	4.657	5.810
Untreated Submicron	15 wt%	0.585	0.501	0.498	0.465	0.437	0.414
	25 wt%	0.609	0.603	0.581	0.565	0.553	0.534
	35 wt%	0.656	0.640	0.636	0.612	0.582	0.556
	45 wt%	1.008	0.934	0.918	0.825	0.735	0.659
APTS/ Submicron	15 wt%	0.585	0.552	0.515	0.479	0.438	0.412
	25 wt%	0.835	0.831	0.795	0.777	0.761	0.745
	35 wt%	1.109	1.012	0.874	0.763	0.709	0.646
	45 wt%	1.663	1.452	1.247	1.124	0.981	0.899
AEAPTS/ Submicron	15 wt%	0.577	0.547	0.508	0.478	0.448	0.415
	25 wt%	0.803	0.762	0.695	0.636	0.585	0.531
	35 wt%	0.831	0.787	0.711	0.655	0.580	0.546
	45 wt%	1.012	0.998	0.974	0.967	0.943	0.934
AEEPTS/ Submicron	15 wt%	0.541	0.496	0.454	0.410	0.369	0.346
	25 wt%	0.542	0.536	0.530	0.520	0.516	0.510
	35 wt%	0.571	0.566	0.552	0.546	0.523	0.513
	45 wt%	0.752	0.745	0.743	0.741	0.740	0.737

Table C.2 Thermal diffusivity of untreated Si_3N_4/PI composite films

Samples	Amount of Si_3N_4 (wt%)	Temperature (^oC)					
		25	50	75	100	125	150
Nano	15 wt%	0.298	0.288	0.28	0.276	0.266	0.263
	20 wt%	0.599	0.569	0.54	0.499	0.469	0.439
	25 wt%	0.725	0.669	0.599	0.537	0.49	0.444
	30 wt%	1.155	1.085	0.951	0.922	0.829	0.809
Submicron	15 wt%	0.585	0.501	0.498	0.465	0.437	0.414
	25 wt%	0.609	0.603	0.581	0.565	0.553	0.534
	35 wt%	0.656	0.64	0.636	0.612	0.582	0.556
	45 wt%	1.008	0.934	0.918	0.825	0.735	0.659
Micron	20 wt%	0.421	0.419	0.407	0.393	0.38	0.371
	30 wt%	0.574	0.532	0.49	0.463	0.428	0.389
	40 wt%	0.803	0.739	0.672	0.596	0.544	0.505
	50 wt%	1.271	1.176	1.048	0.97	0.893	0.817

Table C.3 Thermal diffusivity of APTS treated Si_3N_4/PI composite films

Size	Amount of Si3N4 (wt%)	Temperature (^oC)					
		25	50	75	100	125	150
Nano	15 wt%	0.352	0.338	0.309	0.288	0.271	0.267
	20 wt%	0.679	0.645	0.566	0.535	0.472	0.456
	25 wt%	0.991	0.837	0.718	0.683	0.582	0.456
	30 wt%	1.495	1.398	1.220	1.207	1.164	1.064
Submicron	15 wt%	0.585	0.552	0.515	0.479	0.438	0.412
	25 wt%	0.835	0.831	0.795	0.777	0.761	0.745
	35 wt%	1.109	1.012	0.874	0.763	0.709	0.646
	45 wt%	1.663	1.452	1.247	1.124	0.981	0.899
Micron	20 wt%	0.474	0.466	0.459	0.453	0.443	0.430
	30 wt%	0.729	0.673	0.608	0.546	0.503	0.462
	40 wt%	0.822	0.778	0.724	0.676	0.625	0.598
	50 wt%	1.423	1.278	1.192	1.108	0.981	0.932
Micron/ Submicron	48 wt%(2.779:1)	1.809	1.715	1.463	1.348	1.305	1.262
	50 wt%(2.778:1)	1.783	1.688	1.406	1.264	1.107	1.023
Submicron /Nano	43 wt%(2.779:1)	2.209	1.95	1.77	1.512	1.343	1.25
	45 wt%(2.778:1)	1.755	1.629	1.404	1.368	1.224	1.115

Table C.4 The specific heat of submicron sized Si_3N_4/PI composite films

Samples	Amount of Si_3N_4 (wt%)	Temperature (°C) 25	50	75	100	125	150
Pure PI	-	0.356	0.565	0.691	3.157	4.657	5.81
Untreated Submicron	15 wt%	0.710	1.446	2.154	2.979	2.786	4.154
	25 wt%	0.983	1.475	2.277	2.387	2.591	3.980
	35 wt%	1.098	1.454	2.285	2.494	2.653	4.564
	45 wt%	1.125	1.619	1.949	2.546	3.714	5.161
APTS/ Submicron	15 wt%	0.772	1.511	2.235	2.713	3.776	4.234
	25 wt%	0.977	1.564	2.594	3.212	4.021	4.821
	35 wt%	1.057	1.604	2.524	3.112	3.919	4.973
	45 wt%	1.132	1.765	2.567	3.121	4.091	4.902
AEAPTS/ Submicron	15 wt%	0.264	1.272	1.838	2.673	3.548	4.082
	25 wt%	0.920	1.472	1.952	2.682	3.682	4.784
	35 wt%	0.874	1.553	2.231	2.655	4.179	5.243
	45 wt%	0.965	1.647	2.521	3.295	3.945	4.841
AEEPTS/ Submicron	15 wt%	0.729	1.352	1.966	2.144	2.968	3.987
	25 wt%	0.562	1.475	2.118	2.581	2.986	4.075
	35 wt%	0.816	1.484	2.051	2.638	3.281	4.432
	45 wt%	1.098	1.568	2.056	2.563	3.328	4.628

Table C.5 The specific heat of untreated Si_3N_4/PI composite films

Size	Amount of Si_3N_4 (wt%)	Temperature (°C) 25	50	75	100	125	150
Nano	15 wt%	0.553	0.939	1.437	2.033	2.649	3.602
	20 wt%	0.604	1.137	1.637	2.034	2.825	3.962
	25 wt%	0.626	1.399	2.006	2.807	3.062	4.293
	30 wt%	0.705	1.526	2.328	3.400	4.100	5.781
Submicron	15 wt%	0.710	1.446	2.154	2.979	2.786	4.154
	25 wt%	0.983	1.475	2.277	2.387	2.591	3.980
	35 wt%	1.098	1.454	2.285	2.494	2.653	4.564
	45 wt%	1.125	1.619	1.949	2.546	3.714	5.161
Micron	20 wt%	0.655	0.924	1.611	1.970	2.451	3.345
	30 wt%	0.508	1.241	1.707	2.403	3.572	4.299
	40 wt%	0.629	1.215	1.540	2.345	3.598	5.106
	50 wt%	0.709	1.306	1.784	2.552	3.646	5.318

Table C.6 The specific heat of APTS treated Si_3N_4/PI composite films

Size	Amount of Si_3N_4 (wt%)	Temperature (^oC)					
		25	50	75	100	125	150
Nano	15 wt%	0.584	1.936	2.209	2.512	3.546	4.420
	20 wt%	0.627	1.632	1.932	2.666	3.849	5.078
	25 wt%	0.708	1.775	2.216	3.225	3.908	4.786
	30 wt%	1.366	1.913	2.585	3.212	3.975	4.974
Submicron	15 wt%	0.772	1.511	2.235	2.713	3.776	4.234
	25 wt%	0.977	1.564	2.594	3.212	4.021	4.821
	35 wt%	1.057	1.604	2.524	3.112	3.919	4.973
	45 wt%	1.132	1.765	2.567	3.121	4.091	4.902
Micron	20 wt%	0.564	1.322	2.09	2.132	3.311	5.034
	30 wt%	0.572	1.428	2.245	2.723	3.969	5.104
	40 wt%	0.899	1.517	1.688	3.152	4.566	5.035
	50 wt%	0.926	1.649	3.126	4.25	4.786	5.437
Micron/ Submicron	48 wt%(2.779:1)	1.200	1.473	1.891	2.016	4.586	5.982
	50 wt%(2.778:1)	0.986	1.677	2.419	3.340	4.772	6.690
Submicron /Nano	43 wt%(2.779:1)	1.132	1.658	2.513	3.257	4.973	6.435
	45 wt%(2.778:1)	1.253	1.868	2.571	3.417	5.143	7.826

Table C.7 The specific heat of APTS treated Si_3N_4/PI composite films

Size	Amount of Si3N4 (wt%)	Density (g/cm^3)	
		Untreated	APTS treated
Nano	15 wt%	1.398	1.365
	20 wt%	1.457	1.454
	25 wt%	1.469	1.467
	30 wt%	1.553	1.546
Submicron	15 wt%	1.404	1.386
	25 wt%	1.472	1.489
	35 wt%	1.619	1.622
	45 wt%	1.635	1.641
Micron	20 wt%	1.477	1.523
	30 wt%	1.619	1.603
	40 wt%	1.698	1.678
	50 wt%	1.774	1.810
Micron/ Submicron	48 wt%(2.779:1)	-	1.806
	50 wt%(2.778:1)	-	1.801
Submicron /Nano	43 wt%(2.779:1)	-	1.572
	45 wt%(2.778:1)	-	1.617

APPENDIX D

Fourier transform infrared spectroscopy (FTIR) characterization

Table D.1 Characteristics absorptions of functional groups [36]

functional group	wavenumber (cm^{-1})	vibration type [a]
Si-H	~2200	υ_s
Si-H	800 - 950	δ_s
Si-O-Si	1030 - 1100	υ_s
Si-N	840, 800-1100	υ_{as}
Si-N-Si	500-700	υ_{as}
N-H	1580 - 1650	δ_s
N-H	3400 - 3500	υ_s, υ_{as}, doublets
O-H	3200 - 3500	υ_s
C-H, aliphatic	2840 - 3000	υ_s, υ_{as}
C-H, aliphatic	1370 - 1450	δ_s
C-H, aliphatic	1150 - 1350	ω, τ
C-H, aromatic	3000 - 3100	υ_s
C-H, aromatic	675 - 900	out-of-plane bending
C-H, aromatic	1000 - 1300	in-plane bending
	1250	υ_s
	810 - 950	υ_{as}
	750 - 840	υ_s, 12 μ band
C-H in 	2990 - 3050	υ_s

[a] υ_s: symmetric vibration. υ_{as}: asymmetric vibration. δ_s: in-plane bending (scissoring). ω: out-of-plane bending (wagging). τ: out-of-plane bending (twisting).

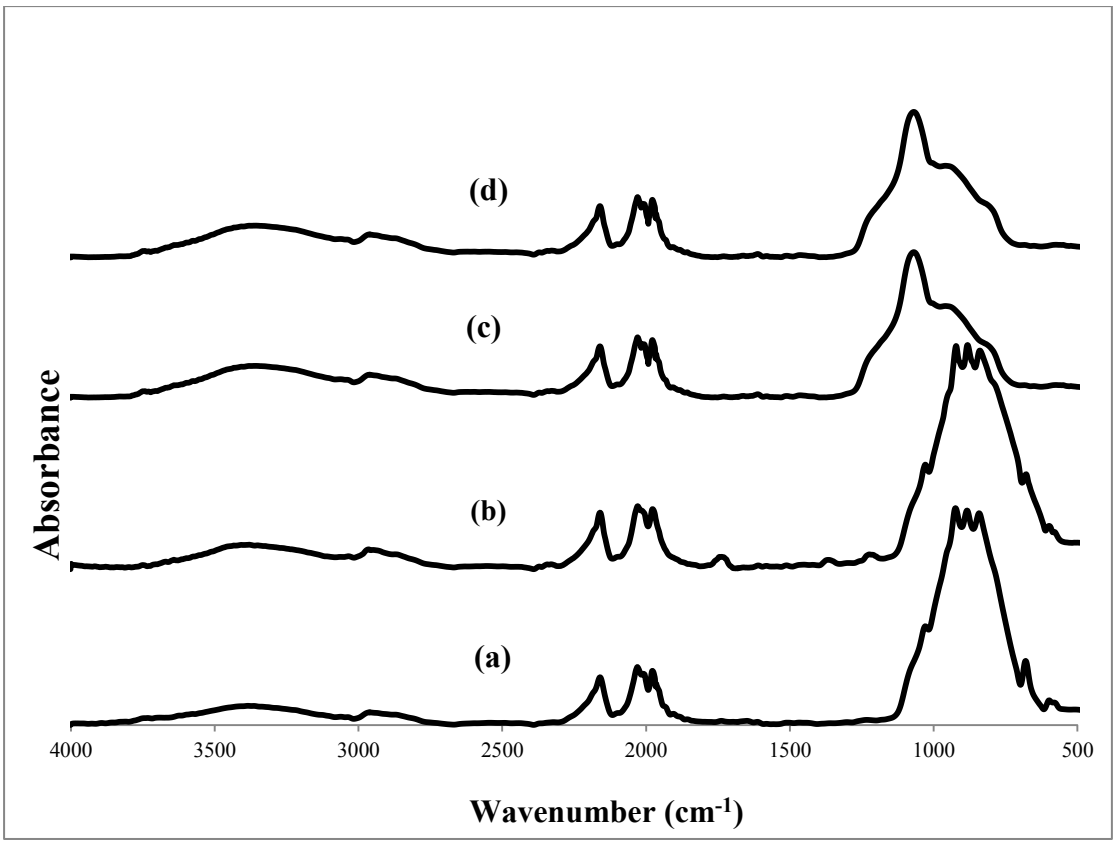

Figure D-1 The FTIR spectra of Si_3N_4 particles ; (a) Untreated micron sized Si_3N_4, (b) APTS treated micron sized Si_3N_4, (c) Untreated nano sized Si_3N_4 and (c) APTS nano sized treated Si_3N_4

APPENDIX E

Mechanical properties of PI/Si_3N_4 composite films

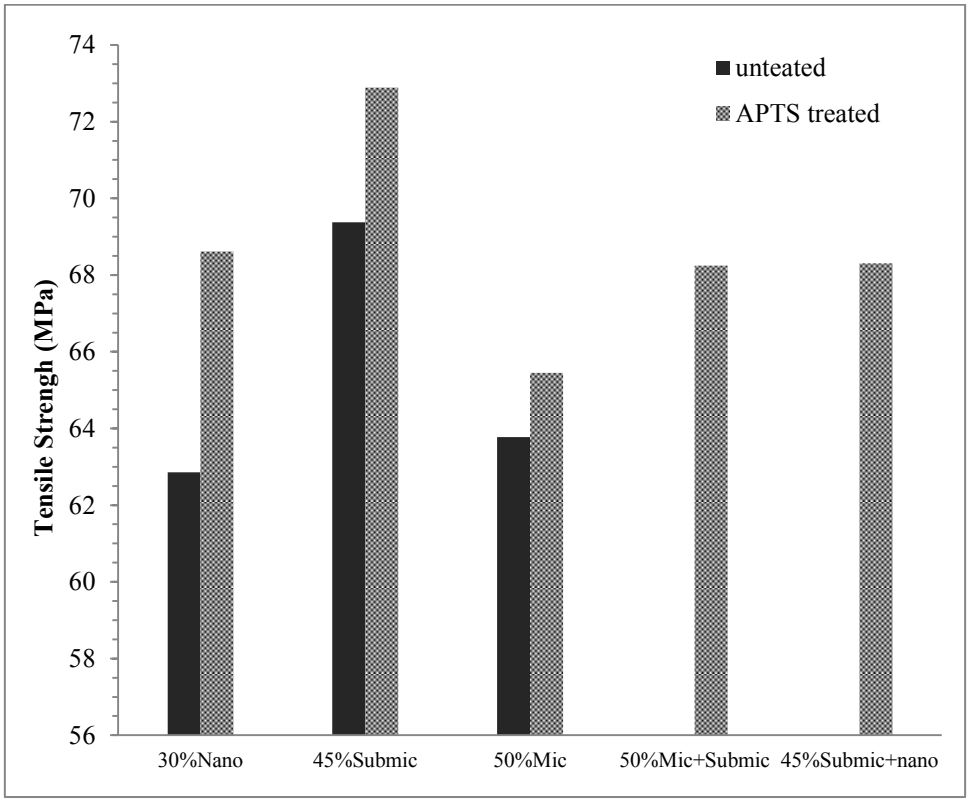

Figure E-1 Tensile strength of polyimide filled the silane treated Si_3N_4 fillers with different sizes of Si_3N_4 fillers

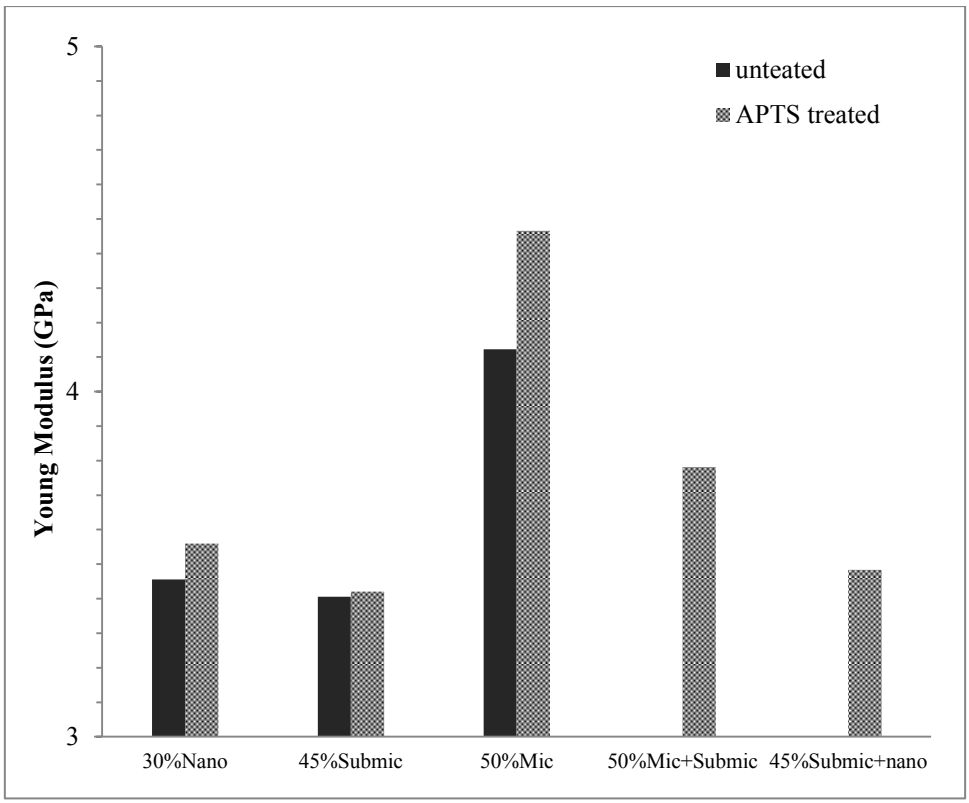

Figure E-2 Tensile Modulus of polyimide filled the silane treated Si_3N_4 fillers with different sizes of Si_3N_4 fillers

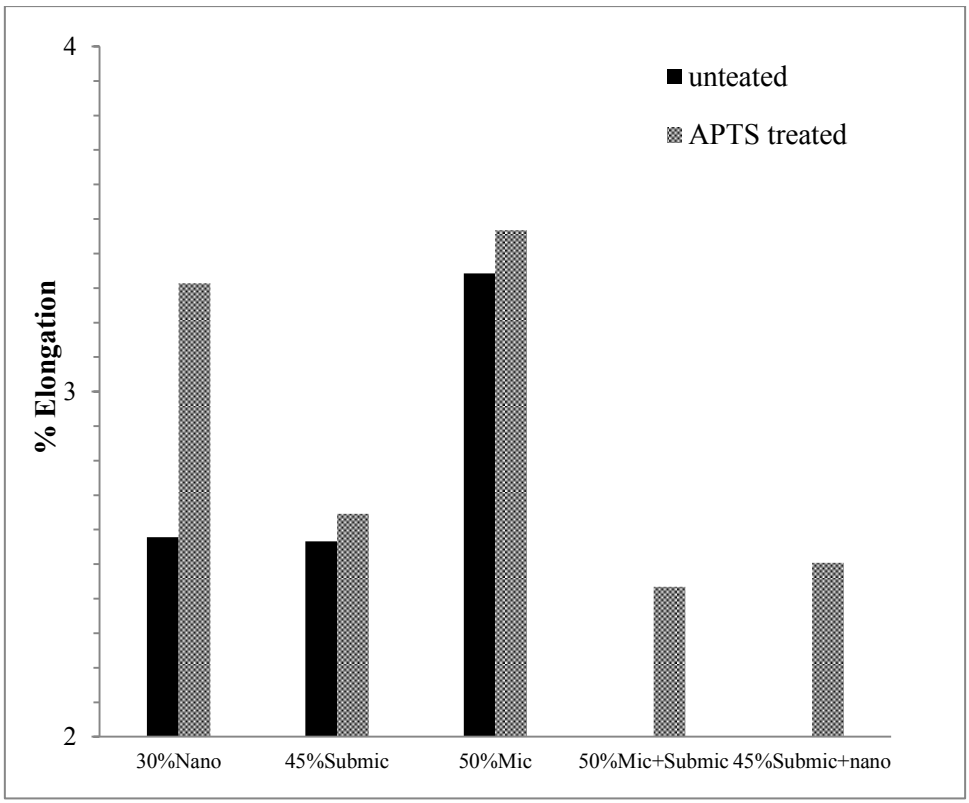

Figure E-3 Elongation at break of polyimide filled the silane treated Si_3N_4 fillers with different sizes of Si_3N_4 fillers

APPENDIX F

Morphology of PI/Si_3N_4 composite films

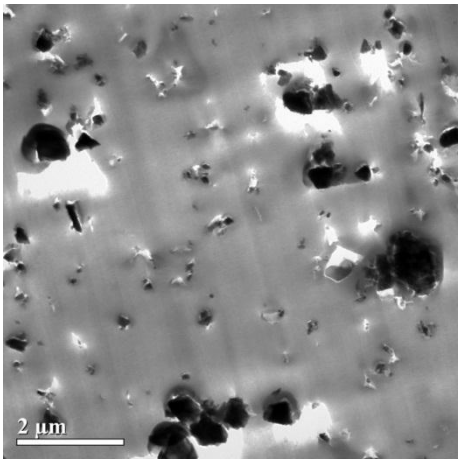

(a) 15% untreatred

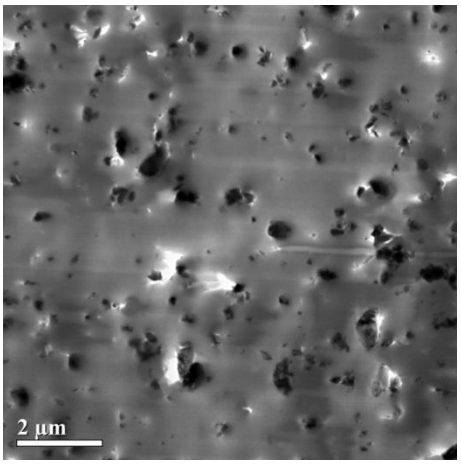

(b) 15% APTS treated

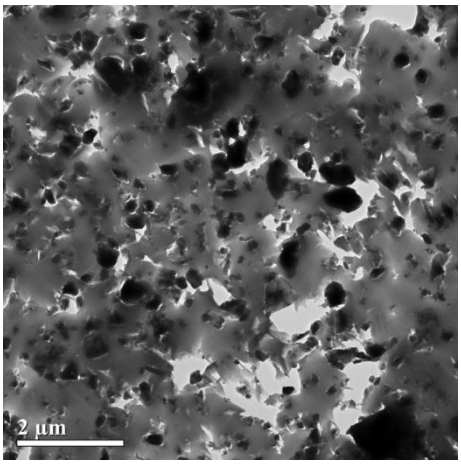

(c) 45% untreatred

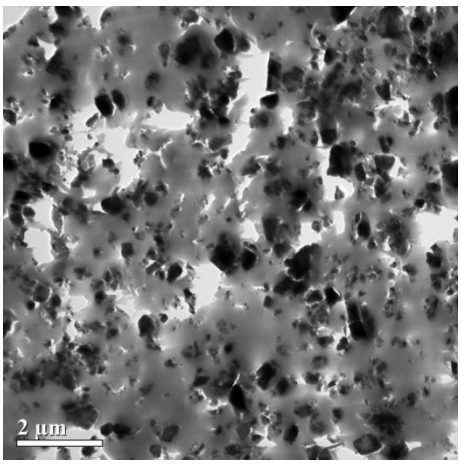

(d) 45% APTS treated

Figure F-1 TEM images of cross section of PI/ Si_3N_4 composite films

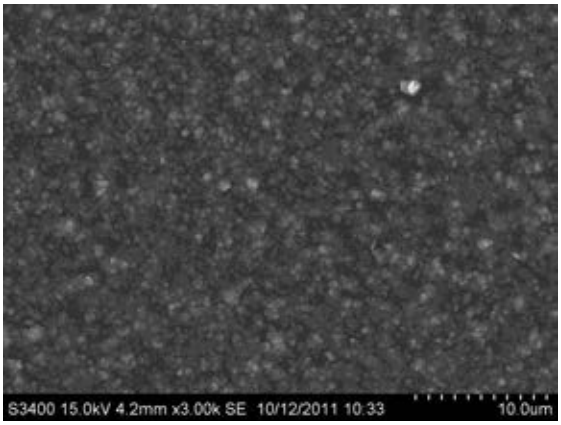

(a) 45% submicron sized

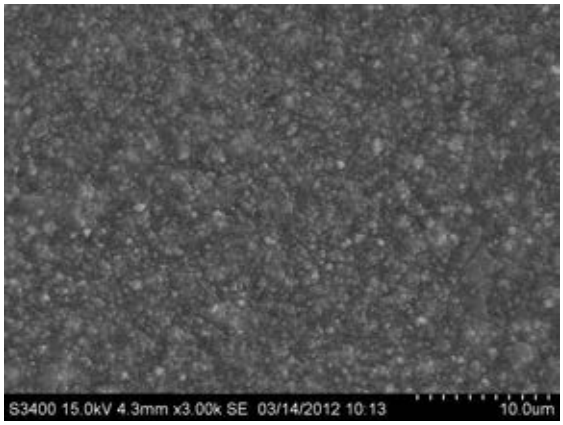

(b) 45% submicron/nano sized

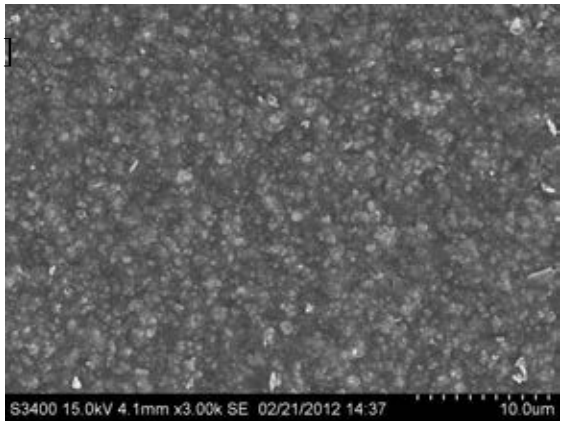

(c) 50% micron sized

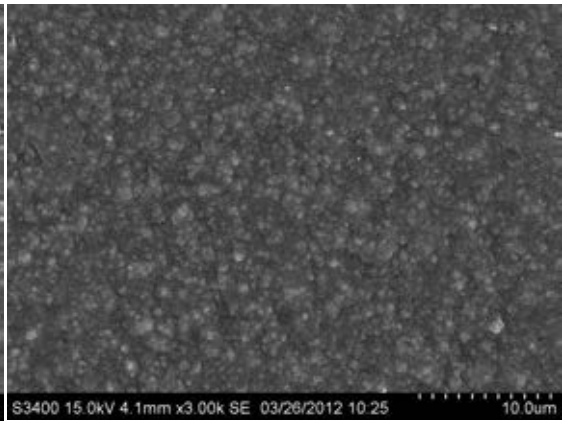

(d) 50% micron/submicron sized

Figure F-2 The morphology of hybrid different sized of APTS treated Si_3N_4 /PI composite films

APPENDIX G

The size distributions of Si_3N_4 particles

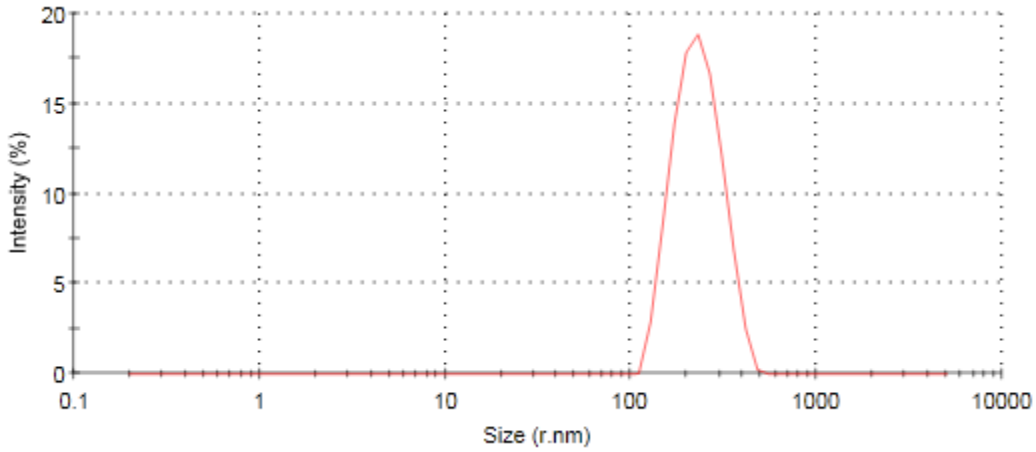

Figure G-1 Size distributions of APTS treated nano-sized Si_3N_4

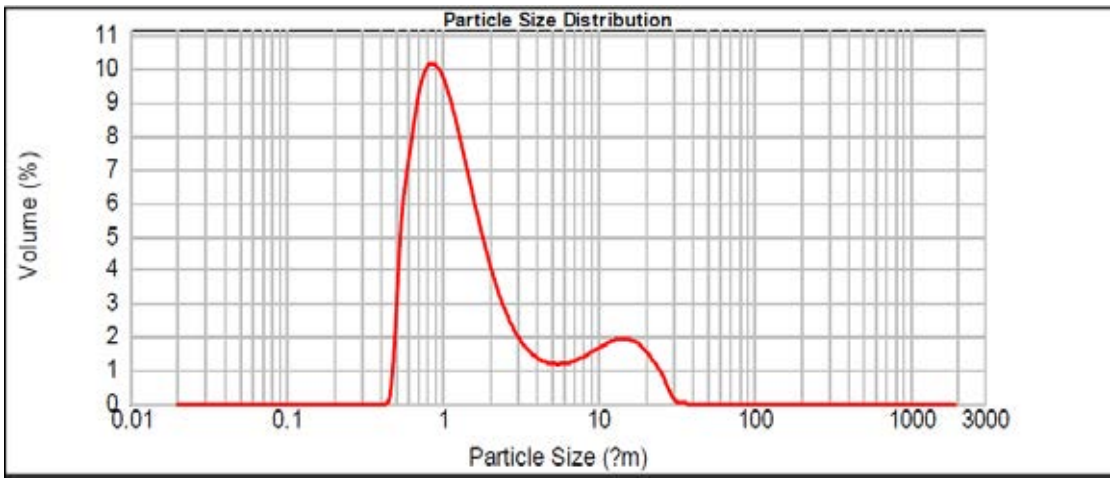

Figure G-2 Size distributions of APTS treated submicron-sized Si_3N_4

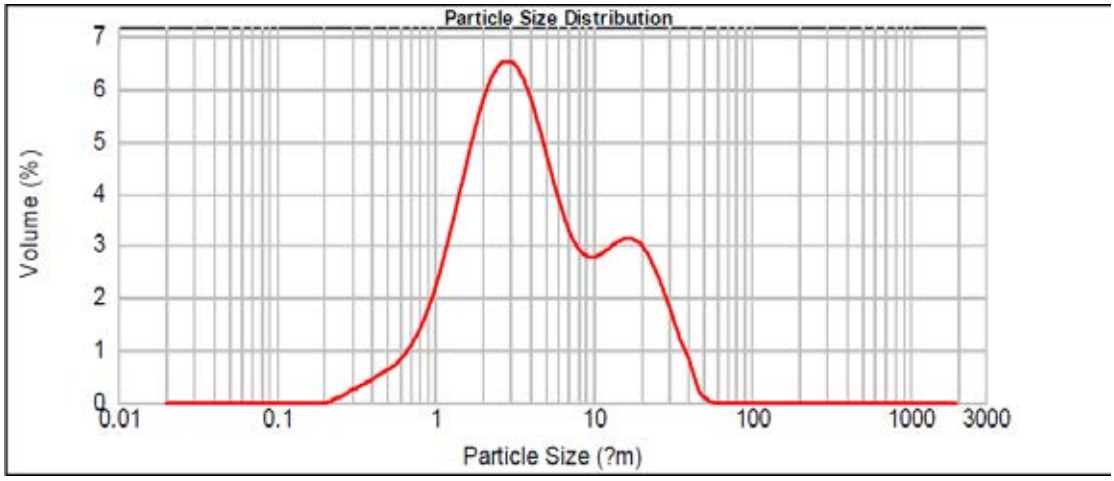

Figure G-3 Size distributions of APTS treated micron-sized Si_3N_4

VITA

Ms.Khwanjit Peeraporntam was born on November 9, 1986 in Nakhon Nayok, Thailand. She graduated the Bachelor's Degree in Chemical Engineering from Department of Chemical Technology, Faculty of Enginerring, King Mongkut University of Thechnology Thonburi in May 2009, She continued to further study in Master's Degree of Chemical Engineering in Department of Chemical Engineering, Faculty of Engineering at Chulalongkorn University in June, 2010.